University of Salford
A Greater Manchester University

Defra NANR244

Noise and vibration from building-mounted micro wind turbines

Part 2:
Results of measurements and analysis

January 2011

Prepared for by:

Andy Moorhouse[1], Andy Elliott[1], Graham Eastwick[2], Tomos Evans[1],
Andy Ryan[1], Sabine von Hunerbein[1], Valentin le Bescond[1], David Waddington[1]

1: Acoustics Research Centre, University of Salford, M5 4WT, www.acoustics.salford.ac.uk
2: Encraft Ltd, Perseus House, 3 Chapel Court, Holly Walk, Leamington Spa, CV32 4YS

DEPARTMENT OF ENERGY & CLIMATE CHANGE
Communities and Local Government
defra
Department for Environment Food and Rural Affairs

This research was commissioned by the previous government. The views and analysis expressed in this report are those of the authors and do not necessarily reflect those of the Department for Communities and Local Government, the Department of Energy and Climate Change or the Department for Environment Food and Rural Affairs.

The work was funded by the Department for Communities and Local Government, the Department of Energy and Climate Change and the Department for Environment Food and Rural Affairs.

Executive Summary

The aims of the project are to propose and test a method for the characterisation of micro wind turbines (MWTs) as sources of structure-borne sound and vibration and secondly to develop a method of predicting structure-borne sound and vibration in a wide variety of installations in the UK.

Potential causes of disturbance from MWT noise and vibration are: structure-borne sound, tactile (feelable) vibration, rattling of fixtures and fittings. A criterion for damage to buildings due to vibration is also considered.

Three separate factors influence the noise and vibration levels in the buildings due to a MWT: (a) the MWT itself which acts as the source of sound and vibration (b) the mounting system including pole, brackets, stand etc. and (c) the building. The methodology proposed allows for each of these factors to be quantified separately. These three elements are discussed in order starting with the treatment of the MWT as a vibration source.

A method has been proposed for characterisation of the MWT as a source of structure-borne sound and vibration; namely the in situ blocked force method. Vibration and sound levels in buildings are not intrinsic characteristics of the MWT. However, the in situ blocked force method allows intrinsic characteristics of the MWT, the blocked force, to be calculated from vibration levels measured in situ for example on the MWT mast.

Preliminary laboratory tests have been conducted to validate the method in principle. Since a real MWT cannot be run under controlled conditions in a laboratory, the test was conducted using a mock up MWT installation. These tests demonstrated the validity of the in situ blocked force method for independent characterisation of MWTs.

Two MWTs have been monitored at a rural/ industrial test site at Carrington, Cheshire. Vibration was continuously monitored using 11 accelerometers mounted for a period of three months for MWT1 (1.7 m diameter) and one month for MWT2 (1.1 m diameter). The rotational speed of the MWT rotor was monitored simultaneously and a sonic anemometer continuously monitored wind speed and turbulence intensity.

Since the MWT operation is not controllable or repeatable it was felt necessary to use a continuous ‘on board validation’ approach to ensure the quality of the data. Good

agreement has been obtained over a wide frequency range which includes the range of tactile vibration and structure-borne sound. When combined with the results of the laboratory tests, this leads to one of the main conclusions of the project; i.e. that it is possible to obtain reliable and independent source strength data for a MWT in realistic operation based on vibration measurements made in situ.

For purposes of prediction the MWT source strength should ideally be expressed as a function of wind speed. This has proved possible for the wind conditions encountered on the test site, but the results cannot be extrapolated to different wind conditions because of the fact that the source strength changes more or less every second. In order to produce more general results the source strength has been obtained as a function of the rotational speed of the MWT. This data can be applied to any site and any wind conditions.

The role of turbulence was also investigated. The turbulence intensity was found to correlate negatively with both wind speed and rotor speed, i.e. the highest turbulence occurs at the lowest speeds. The results suggest that turbulence will not be a dominant factor in structure-borne sound, although the standard turbulence parameters are perhaps not well suited to relate to noise and vibration. Sudden changes of wind direction were also investigated and there is no suggestion of any strong influence of turbulence on rotor speed and by inference on source strength. However, audible noise could potentially be produced if the mount system were to spring back after being loaded by a strong gust.

The above points all relate to characterisation of the MWT. A separate but related investigation was also carried out to determine how wall and roof-mounting systems influence the transmission of structure-borne sound and vibration from the MWT into the building. Laboratory and field measurements (supplemented by a simple model) were conducted on one roof mounting and two wall mounting systems, each of the latter with three different pole lengths. The transmissibility of the mounts, which quantify the attenuation, was thus obtained. The results indicate that the sound transmission through the mountings and into the building is a complex phenomenon and fairly sensitive to pole length.

Regarding the role of the building structure in transmitting structure-borne sound and vibration to the receiver room, a series of field tests has been conducted including six properties with solid brick, cavity brick and stone walls in a variety of building layouts. The aim was to quantify transfer functions for masonry buildings, i.e. the

extent to which a force excitation on an external façade is converted to sound and vibration in rooms adjacent to, and remote from, the excitation point. It was shown that higher sound levels by about 10 dB would be expected from a MWT mounted on a solid brick wall as compared with the same MWT (hypothetically) attached to a cavity brick wall. However, this situation could be subject to significant variance depending on details such as wall ties and junctions. Surprisingly little attenuation was found from the most exposed room to adjacent rooms along the same facade, particularly for cavity walls. For solid brick walls the attenuation to rooms into the building (away from the façade) would be more significant.

Results from the separate investigations into the MWT, the mountings and buildings have been combined into a prediction method. The concept of a 'reference installation' has been used to help simplify things as far as possible. Calculation of the sound levels in the reference installation requires specialist knowledge but the results can then be adjusted using a simple procedure to give sound levels in buildings with different constructions, rooms sizes and layouts. The simplified procedure applies to the MWTs and masts tested and for installation on masonry buildings. Other MWTs, masts and building types can also be handled by the more general procedure but require more detailed analysis and/ or measurement.

A series of four case studies has been conducted including installations with both MWT1 and MWT2 models. Sites included wall and roof-mounted installations, cavity and solid walls and a variety of building layouts including detached and multiple-dwelling buildings. Noise and vibration measurements were made at each site and compared with prediction. At every site there were difficulties in obtaining reliable measurements of wind speed actually incident on the MWT but rotational speed could be estimated from noise traces.

Subjectively the MWT was audible, mainly as a 'whine' of varying pitch in each of the dwellings. In the roof-mounted case there was also an audible rumble which was believed to be caused by vibration of ballast in the roof-mounting system rather than directly due to source mechanisms in the MWT itself. At three of the sites the occupants (who were owners of the MWT) reported not to be disturbed by the noise. However in the roof-mounted case study the occupant, who was not the owner, reported being 'very annoyed' by the noise and had made a complaint. No tactile (feelable) vibration was evident in any of the properties at the time of the survey and none of the residents reported feeling vibration.

Analysis of the recorded noise and vibration signals showed the spectrum of noise from MWT to be dominated by a tonal peak which was linked to the rotor speed and occurred at between about 160 Hz and 250 Hz. This would give a tone with a pitch of notes around middle C and is consistent with the description given above of a 'whining' sound. The spectrum from MWT2 also contained peaks but these were less pronounced and generally lower in level consistent with the smaller size of the unit.

The maximum $L_{Aeq\ (5\ minutes)}$ at each site varied between 29 dB and 45 dB. Although significant background noise was present at every site, care was taken to extract 'clean' periods of data for analysis, and so the above L_{Aeq} values predominantly relate to the MWT. 16 hour VDVs (vibration dose values) were calculated based on short periods of relatively clean data and were found to be in the range 0.03-0.05 $ms^{-1.75}$. An alternative measure of vibration is the weighted rms acceleration, which was typically around 0.01 mm /s^2. These levels were just below the usual threshold of perception, except during transient events presumed to be from human activity in the building, such as door closures, rather than the MWT. These results are consistent with the observation of no perceptible tactile vibration mentioned above. Peak particle velocity in the wall close to the point of attachment was well below damage thresholds at every site (assessment of potential damage due to wind loading was outside the scope of the study).

Structure-borne sound levels for MWT1 are over-predicted by around 5dB and those for MWT2 are under-predicted by a similar margin. In view of the known difficulty in predicting structure-borne sound this is considered to be a good level of agreement, particularly for such a complex problem. We therefore consider it reasonable to use the results of the project as the basis for predictions. However, many simplifications have been required in order to produce a sufficiently simple method and it will be advisable to build up confidence in the method by trials on real installations.

There are several significant differences between the noise generated by large wind turbines and the structure-borne sound from MWTs. The rotor speed of MWTs changes more or less every second leading to a 'whine' of varying pitch rather than a steady 'swish'. Furthermore, whereas noise levels from large machines increase fairly steadily with wind speed, this is not the case from MWTs due to the amplifying effect of structural resonances at particular rotational speeds.

Contents

1 Introduction

The aims of this project are to "*research the quantification of vibration from a micro turbine, and to develop a method of prediction of vibration and structure borne noise in a wide variety of installations in the UK"* (quoted from the NANR244 project specification, June 2009).

The outcomes of the project are described in three reports:
Part 1: Review and proposed methodology;
Part 2: Development of prediction method;
Part 3: Prediction method.

This report is Part 2, the aim of which is to present the results of measurements and analysis for the prediction methodology as proposed in Part 1. The purpose of the prediction method is to assist in the assessment of potential disturbance due to structure-borne sound and vibration from building-mounted micro-wind turbines (MWTs).

The background to the project is the UK Government's desire for increased use of renewable technologies. Whilst several such technologies have been classified as permitted development under the General Permitted Development Order (GPDO), to date no such rights have been granted for micro wind turbines (MWTs). Under permitted development rights, certain products may be installed without planning permission, which is underpinned by the principle that the installation will not have an impact beyond the host property. When a MWT is installed on a building there is the potential for airborne noise, structure borne noise and vibration. Prediction methods exist for airborne noise i.e. that transmitted through the air from the WT blades, but not for structure-borne noise and vibration. As a result of the uncertainty about possible impacts, building-mounted MWTs on attached dwellings have not been granted permitted development rights.

The project scope includes:

- structure-borne sound, i.e. that transmitted through the building structure from the point of attachment of the MWT, and
- vibration which could potentially be felt, cause rattling of fixtures and fittings or damage to the building.

Airborne sound is outside the scope of the project but should be taken into account in any assessment of potential disturbance.

Potential for building damage due to vibration is considered; potential damage due to (quasi static) wind loading of the MWT on the mast is not within the scope of the project but can be assessed by standard methods.

1.1 Outline of this report

Chapter 2 provides an outline of the problem and of the proposed prediction scheme. It is described how the influence of the MWT, the mounting and the building are accounted for. Criteria used to assess the acceptability of noise and vibration are also recalled from Part 1. In Chapter 3 we describe how the MWTs are characterised as potential sources of sound and vibration. The measurement method is described and example results are presented from test installations of two MWTs. The analysis of these results continues in Chapter 4 where the relationship between wind speed and MWT source strength is examined. In Chapter 5 and 06 it is described how the transmission of structure-borne sound and vibration is affected by typical MWT mountings and by typical building constructions. Field trials of existing MWT installations are described in Chapter 7 and in Chapter 7 these case studies are used as examples to illustrate the prediction method. Conclusions follow in Chapter 9.

2 Overview of prediction methodology

The aim of this chapter is to provide an overview of the proposed prediction scheme which was first presented in Part 1. The prediction methodology is to apply to both wall-mounted and roof-mounted installations, examples of which are illustrated in Figure 1.

Vibration is initially generated by the moving parts of the MWT by mechanisms similar to those found in any machine such as fans and electric motors. Structure-borne sound is then transmitted down the mounting system and into the building structure where it may or may not be at a sufficient level to be heard as structure-borne sound or felt as vibration. It must be made clear that throughout this report when referring to structure-borne sound and vibration, that measureable structure-borne sound and vibration in a building does not always mean that these effects will be perceptible by a person of average sensitivity or even a person more sensitive than average.

Figure 1: Examples of wall-mounted and roof-mounted installations (photo: Encraft Ltd.)

2.1 Overview of scheme

It is proposed to treat the installation as the combination of three different subsystems:

- Wind turbine
- Mounting
- Building.

The arrangements are schematically shown for wall- and roof-mounted systems in Figure 2. The three above elements are shown in blue, grey and orange respectively. Using this scheme the sound and vibration in the room immediately behind the attachment point, the 'most exposed room', is predicted. The prediction method also allows for prediction to rooms further from the attachments.

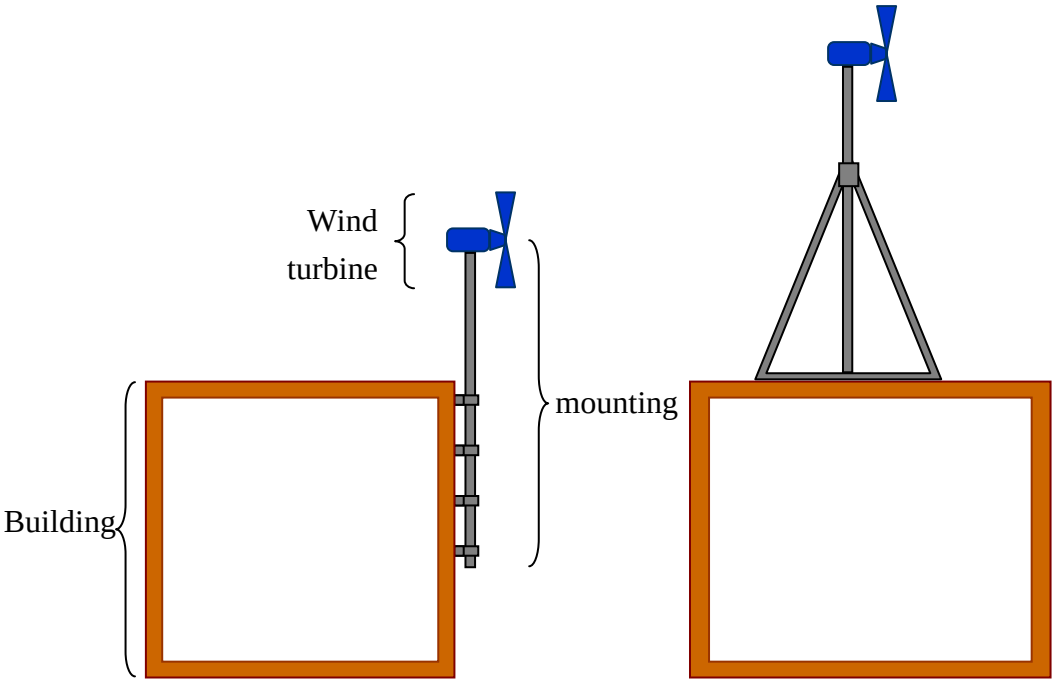

Figure 2: Schematic of installation showing WT (blue), mast (grey) and building (orange): left - wall mounted system; right - roof-mounted system.

The MWT itself is the source of any potential structure-borne sound and vibration. It is characterised by data obtained from measurements on an operational MWT (described in Section 3 of this report). The source strength is dependent on the wind speed at the time of the measurement and hence measurements are made over an extended period so as to capture a range of conditions. This data is presented in a MWT structure-borne sound database giving data under different wind conditions.

The mounting is the subsystem that transmits structure-borne sound from the MWT

into the building structure. Different designs of mounting can transmit more or less structure-borne sound depending on the design. The attenuation offered by a particular mount is obtained by a combination of measurements and calculations, as reported in Section 5.

As with the mountings, different types of building construction will transmit structure-borne sound and vibration to different extents. The attenuation characteristics of the building are obtained by a combination of measurement and calculation as described in Section 6.

The transmission paths from the source (the MWT) to the receiver (the occupant) are shown schematically in Figure 3. Note that it is necessary to include two transmission paths through the building, one leading to sound and the other to vibration.

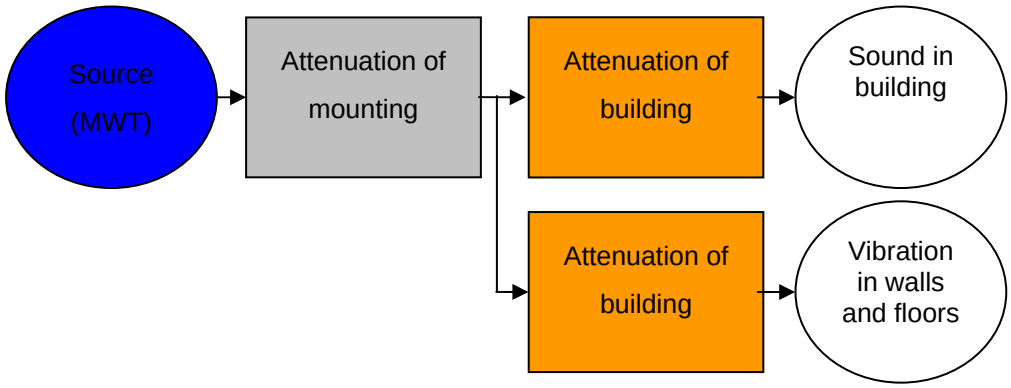

Figure 3: Schematic transmission paths of sound and vibration from the source (MWT) to receiver.

2.2 Criteria

Noise and vibration acceptance criteria were discussed in Part 1. It was determined that four separate criteria might be required to encompass different ways in which disturbance to residents could potentially occur:

- Structure-borne sound (audible sound caused by vibration of building surfaces)
- Tactile (feelable) vibration
- Rattling of fixtures and fittings
- Building damage due to vibration

It is not the role of this project to advise on the *levels* of noise and vibration that are

deemed acceptable, but we need to be aware of the form that such criteria might take in order to ensure consistent outputs from the prediction scheme. Unfortunately, existing standards for evaluating potential disturbance in the above categories define different timescales and measurement positions, e.g. 5 minutes near the centre of the room for structure-borne sound, 8 or 16 hours for tactile vibration etc. The proposed measurement positions, time and frequency ranges are summarised in Table 1.

Table 1: Proposed outputs for the prediction methodology

Output	**Parameter**	**Position**	**Frequency range**	**Evaluation time**
Structure-borne sound	$L_{Aeq,5\ minutes}$	Near room centre	To be determined	5 minutes
Tactile vibration	VDV	Centre of floor span	1-80 Hz	8 hours night 16 hours day
Building damage	PPV	Point of attachment to building	1-150 Hz	Instantaneous
Rattling	Peak acceleration	Walls in receiver room	To be determined	Instantaneous

2.3 Definition of the reference building

Each MWT will be characterised by the level of sound and vibration it would cause if installed in a 'reference installation'. The reference installation is a fictitious installation with well-defined properties but which is representative of typical wall-mounted installations. This form of presentation has been chosen in order to try to make the results more accessible and easily understood in the final form of the prediction methodology. It will become clear throughout this report that the standard terms and definitions used to describe structure-borne sources and transmission (in so far as they are standardised) are unfamiliar and can be confusing even to specialists. However, the reference installation approach will allow us to present the final results in terms of sound pressure level and vibration level which are more readily understood.

The reference installation consists of a wall-mounted mast and a building, defined as follows. The reference mast is defined as having a transmissibility as defined in Section 5. This performance is representative of a wall-mounting system comprising a 5m cylindrical pole with 3 connection points.

The reference building is defined as having:

a. a point mobility of 10^{-5} m/s/N at the point of attachment
b. a vibro-acoustic transfer function of 40 dB per N (see definition later)
c. a vibration transmissibility as defined in chapter 5

These properties are typical for buildings with solid brick walls onto rooms with wooden floors of volume 50 m^3 and reverberation time 0.5 seconds. The properties are explained and justified later.

In order to calculate sound and vibration levels for installations with different masts, different building constructions, room properties and layouts it is necessary to apply correction factors for different mountings, different wall constructions and room sizes. The appropriate correction factors will be presented throughout the report.

In the following section the characterisation of MWTs as sources of structure-borne sound is presented.

3 Characterisation of MWTs as source of structure-borne sound and vibration

3.1 Introduction

Source characterisation is a means of describing the operational behaviour of sound and vibration sources and their ability to transmit sound and vibration to the air around them or to connected structures. For the case of MWTs a source characterisation approach is required to allow predictions of structure borne noise and vibration to be made. A number of factors should be taken into account because wind conditions, building and turbine types may mean significant variations are observable from one site and system to another.

There are relatively few standard procedures available for characterising structure borne sound sources and unfortunately the standard test procedures which do exist are either impossible to implement (ISO 9611, 1996) or not sufficiently accurate (BS EN ISO 3822-1, 1999) for the current project. A particular difficulty which rules out many approaches is that a vibration source should be operated in a realistic way during measurements to obtain a representative source characterisation. A full review of characterisation methods can be found in Part 1 where the 'in situ blocked force method' was identified as the most appropriate method for MWTs.

3.2 The in situ blocked force method

The measurement of blocked forces in-situ is similar in many respects to the measurement of operational contact forces by inverse force synthesis. There are however two distinct advantages,

1. All measurements can be conducted on an existing installation without dismantling or modification.
2. Unlike contact forces the blocked force is an independent property of the source theoretically unaffected by the components which it is connected to.

The figure below shows a representation of a wind turbine installation. The wind turbine, marked W, is the component to be characterised. Attached to the wind turbine are the mount system (M) and the building (B). The vibration, forces and velocities, at any point on the installation are dependent upon the turbine, the mounting and the building, as is the structure borne sound observable in the rooms of the building.

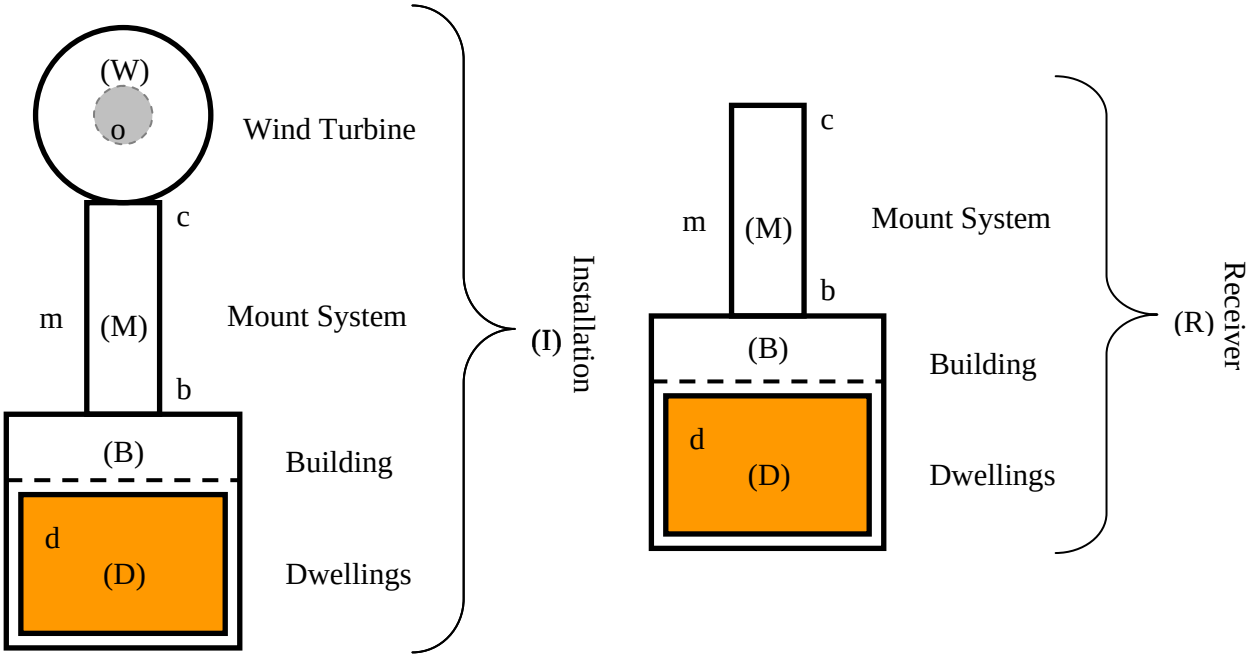

Figure 4: Left: representation of an MWT installation. Right: a building with attached mounting system, i.e. the receiver without the source.

The blocked force $\mathbf{f}_{bl}$ is found by solving,

$$\mathbf{v}_{Im} = \mathbf{Y}_{Imc}\mathbf{f}_{bl} \qquad 3.1$$

where $\mathbf{Y}_{Imc}$ is measured whilst the turbine is installed (Moorhouse et al. 2009). This approach therefore has all the advantages of inverse force synthesis including representative source operation with two significant further advantages. The source (wind turbine) can remain in-situ for all tests and the blocked force obtained is an independent property of the source not influenced by the mount system or building to which it is attached.

3.3 Measurement setup

For the purpose of source characterisation testing a flat roof mounting system was used because it can be most easily set up and accessed. Figure 5 shows an example of a flat roof mount. Flat roof mounting systems are available from at least two of the micro wind turbine manufacturers offering products to the domestic market in the UK and potentially bespoke flat roof mounts could be manufactured for any of the available turbines. The mount used had a height of 5m; above this was the central axis of the turbine the exact height depending on the geometry of the specific turbine

tested.

Whilst monitoring the installation it was found that stone slabs (used for ballast) in the base of the mounting were rattling. The vibrations caused would corrupt the results so a thin rubber sheet was applied between the slabs and the metal frame in order to prevent rattling. Some further adjustment was also required to prevent metal elements of the frame rattling.

Figure 5 Photograph of a "flat roof" mounting system on test site, also showing some of the accelerometers.

The site chosen for source characterisation tests was a rural/industrial area with high security to allow monitoring of the test turbines over a sufficient time period to capture a range of wind conditions (see Figure 27 for an aerial view of the site). The site allowed turbine installations at a height of 5m above ground level using the flat roof mounting system described above.

For each tested turbine a properly installed grid tie inverter system recommended by the manufacturer was used. This is of relevance because a turbine under electrical

load behaves differently to one which is free from load. It was not possible to take turbine electrical load into account during the source characterisation measurements. Thus, in the strictest sense the following results should be regarded as being individual cases of wind turbines which are connected to specific grid tie inverters and corresponding electronics. It is expected that in the future these systems may change which could potentially alter vibration output to some extent. However, over a reasonable period of time it should still be possible to capture a good range of loadings for a range of wind conditions.

An artificial wind source (such as a wind tunnel) could potentially have been used to provide a more controlled environment. This was not considered to be a viable option however as the variation of wind turbine vibration output with electrical load should be included in the characterisation and furthermore artificially produced uni-directional airflow may not be representative of real outdoor wind conditions.

During the source characterisation measurements the wind speed and direction at the site were continuously monitored and logged every second using a METEK sonic anemometer. A description of the wind conditions at the test site can be found in section 4. To ensure synchronisation with the logged vibration data the anemometer was programmed to time stamp every second according to the PC clock which was simultaneously monitoring vibration according to the same time reference.

Given that the link between wind speed and the vibration output of a turbine may not be easily identifiable a simple mechanism was used to monitor the rotational speed of the turbine during source characterisation measurements. A wireless system was required to allow free rotation of the turbine with respect to wind direction. This was achieved using a reed switch connected to a simple transmitter circuit and subsequently a receiver circuit connected directly to the recorder used to monitor vibration. Using this approach the rotational speed could be monitored in sync with the logged vibration data, it was also possible to trigger vibration measurements using this tachometer output so as to measure only when the turbine was rotating. This approach was employed to reduce the amount of stored data and to simplify post processing of the recorded time histories. Most importantly however, the purpose of measuring rotational speed in addition to wind speed was to introduce an intermediary step for linking wind speed to turbine blocked forces. This type of approach is often used when performing measurements on rotating machinery such as engines or motors. Such techniques, globally referred to as ‘order analysis’ (Randall 1987), allow like for like rotational speeds to be considered independently and this in turn

should allow for behavioural trends to be identified more easily.

In summary, the quantities required for source characterisation are a set of mobilities for the installation $\mathbf{Y}_{\mathbf{Imc}}$ and a corresponding set of operational velocities $\mathbf{v}_{\mathbf{Im}}$ measured at selected points on the installation, see equation 1. Section 3.4 describes the measurement of mobilities $\mathbf{Y}_{\mathbf{Imc}}$ and section 3.5 describes the measurement of operational velocities $\mathbf{v}_{\mathbf{Im}}$.

3.4 Mobility measurements on the installation

Part of the in-situ source characterisation procedure requires measurements of an installation's mobilities. These mobilities can then be used in conjunction with the operational velocities, described in the next section, to determine the blocked forces of a wind turbine.

Mobility measurements are usually performed by applying a known force whilst simultaneously measuring the structure's resulting velocity; the ratio velocity/force being the mechanical mobility. Measurement standards exist for the measurement of mechanical mobility (ISO 7626-2: 1990; ISO 7626-5: 1994) and even though measurements are performed in-situ,
the same general rules apply. Unfortunately however the standards do not give sufficient advice on how to deal with specific problems with specific geometries.

3.4.1 Dimensions of the problem

The blocked forces of the turbines that are to be measured are at the interface **c** (between the turbine and mounting system). To describe this interaction it may be necessary to include forces applied by the turbine to the mount in different directions and it may also be necessary to account for moments. Given that this information is not known in advance it was necessary to first account for all forces and moments which could couple. This was initially done using a series of laboratory tests which introduced complication in steps (Moorhouse and Elliott 2010). The main purpose of these preliminary tests was to ensure that important coupling directions were not neglected without good cause.

To begin with it was assumed that up to 5 degrees of freedom may have to be included to describe the interface between turbine and mount, these were the orthogonal x, y and z directions as well as rotations about the x and y axes. Rotations around the vertical z direction were not considered as the pivot shaft at the bottom of a turbine is coupled to the turbine through a bearing which should prevent coupling in

this degree of freedom.

Figure 6 gives an illustration of the type of connection between wind turbine and mounting system. Also included are the axes used to describe orientation. The z direction is always parallel with the pole so that the x and y axes are perpendicular.

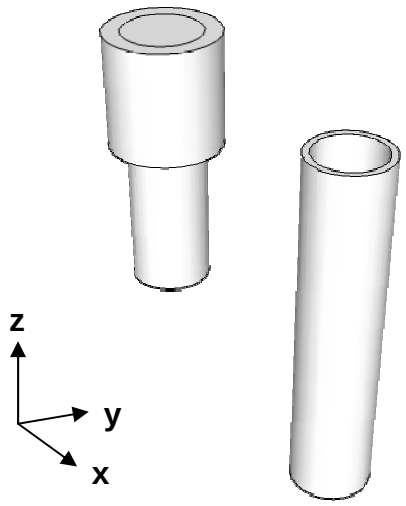

Figure 6: Pivot shaft at the bottom of a turbine left and a short length of mounting pole. The pivot shaft slots into the mounting pole and is held in place by grub screws. Also shown are the axes for orientation purposes.

As mentioned above, the importance of different degrees of freedom at the interface was investigated using a mock-up MWT in the laboratory (Moorhouse and Elliott 2010). During the course of laboratory testing it was found to be necessary to include all 5 possible degrees of freedom at the interface. This conclusion was drawn based on the quality of a predicted vibration velocity made using the measured blocked forcem. Using fewer than 5 degrees of freedom at the interface did not result in a serious error in the prediction, but using a controlled excitation there was a noticeable degradation in the predicted velocity as degrees of freedom were eliminated from the computation. Another important finding was that the blocked forces characterised in one installation could be used to predict vibration responses in a very different installation thus confirming the independence of the measured blocked forces.

Shown in Figure 7 is a schematic showing how accelerometers were mounted at the interface during mobility measurements. It can be seen that three accelerometers are oriented in the vertical z-direction to account for forces in the z-direction and moments about the x and y axes. As mentioned previously, moments about the vertical z axis were not included because of the bearing at the bottom of the pivot

shaft which will prevent such a coupling.

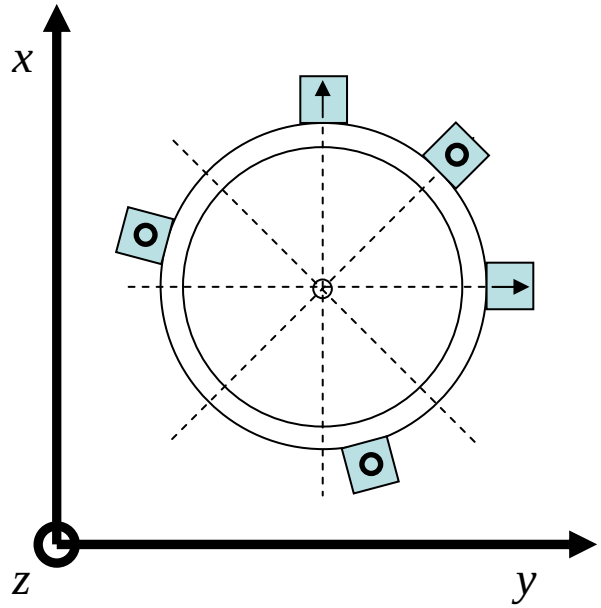

O = out of the page.

Figure 7 Above view of a mounting pole showing the orientation of accelerometers at the interface during mobility measurements of the installation. Directions x and y are each monitored by a single accelerometer. The vertical z direction however has 3 to allow for rotations about x and y to be included. In the field the x-dir was aligned to north.

3.4.2 On-site Measurements

According to standard mobility measurement procedures a measured force excitation can be achieved using either an instrumented hammer or shaker. In practice the instrumented hammer approach is often favoured for practical reasons and this is especially true for the current problem because injecting sufficient power to large structures below a few Hz would be particularly difficult by shaker. Furthermore, carrying out such measurements using shaker excitation would be excessively time consuming. Since the frequency range which is of importance to the current problem is not known in advance mobility measurements by hammer excitation are still not entirely straightforward however.

When there is sufficient prior knowledge to disregard specific frequency ranges in advance it is possible to prioritise mobility measurements accordingly. Unfortunately, in this instance there is no such evidence available. The most sensitive range for tactile or “feelable” vibration is between 1 and 10Hz and human hearing can be sensitive to a range covering at least 20Hz to 20kHz although for structure borne sound an upper limit of 2kHz should usually be sufficient. Based on this information

mobility measurements were performed so as to optimise the ranges 1-10Hz and 60-1600Hz in order to cover the most useful ranges with respect to tactile vibration and structure borne sound. Thus, in order to deal simultaneously with tactile vibration and structure-borne sound requires an extremely wide frequency range to be covered which presents particular measurement challenges.

Four different instrumented hammer type exciters were available for the measurement of mobility, each of which could be fitted with a number of tips to allow sufficient power to be delivered in a specific frequency range whilst also ensuring a good spatial accuracy. To measure acceleration responses (from which velocity can be determined) a range of small accelerometers with varying sensitivity (1-50mV/ms^{-2}) were also available, using these accelerometers structural loading should be of no great concern. The analyser used for these measurements has a dynamic range of 160dB. Some preliminary experimentation in the field was required to determine the most appropriate combination of transducers.

To cover the important frequency ranges described above two different hammer types were used one resembling a large lump hammer with rubber tip and the other resembling a pin hammer with a plastic tip. When performing mobility measurements the coherence was used as the main guide to quality of measurement. For some points the coherence was poor regardless of the excitation used due to non linear behaviour of the mount system. As the upper frequency limit was not known the mobilities were measured in two separate frequency ranges: 0 to 1600Hz in one quarter Hz resolution and 0 to 6400Hz in one Hz resolution. These measurements used window lengths of 4 and 1 seconds respectively. For the measurements made over the shorter (1 second) duration an exponential window was used to ensure that all signals had decayed before the end of the window. A uniform window could be used for the longer window measurements and for this reason the 1 to 1600Hz frequency range data should be more reliable. A 0.7Hz high pass filter was used during the measurements.

Eleven points on the mount system were excited during mobility measurements whilst accelerations were measured at the interface c where the turbine and mounting system meet. Ten of these excited points are to be used for the determination of blocked forces at the interface, the remaining point (treated separately) can then be used to serve as an on board validation as it allows a velocity prediction to be made which can be compared to velocity which is directly measured. This approach has been found to work well and helps to ensure that the blocked forces obtained are reliable. This eleventh point was situated at the base of the mounting system so as to represent as

best as possible an interface to a building, i.e. at the bottom of the mount pole.

Four of the excitation points were situated on the mounting system near to the edge of the base oriented in the z-direction. Two further points were situated on upright points of the base oriented perpendicularly to each other, these points lie in the xy-plane. The remaining four points were all on the mounting pole also oriented in the xy-plane staggered along a 2m length.

Shown in Figure 8 is an example of the mobilities measured in the x, y and z directions at the interface whilst exciting at the base of the mount.

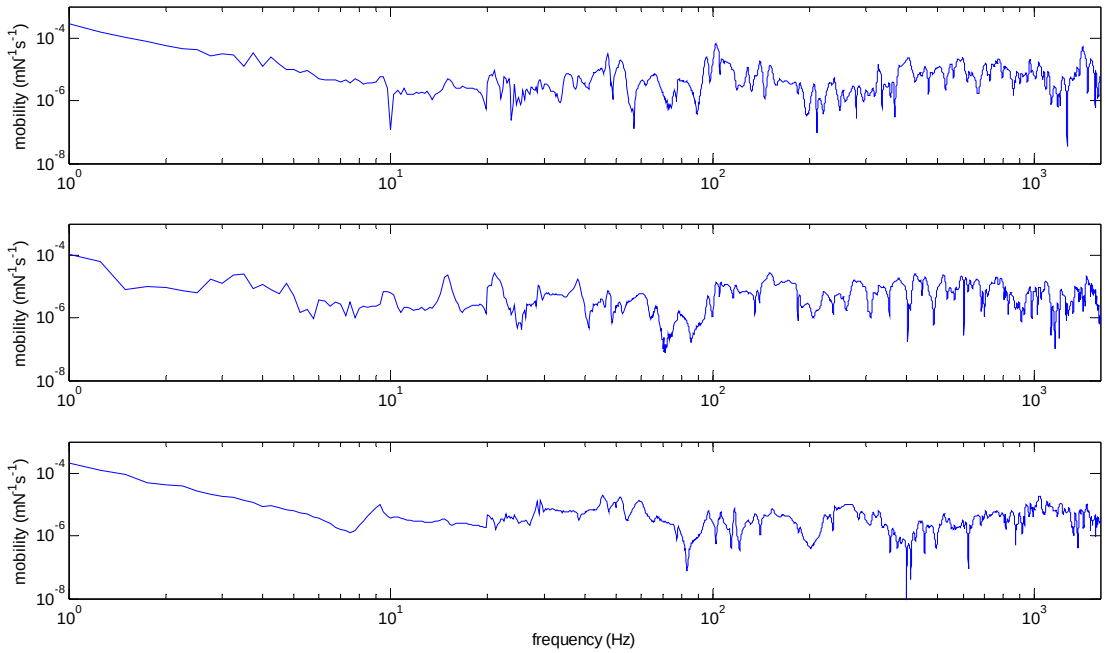

Figure 8 Transfer mobilities measured by exciting at a point on the mount's base with responses measured at c: Top plot - x-direction, middle - y-direction and bottom - z-direction.

3.5 Measurements on the operational MWT

The eleven points excited during mobility measurements were monitored using accelerometers whilst simultaneously measuring wind conditions and the rotational speed of the turbine. As described above, one of these points was included to serve as an on board validation. The remaining ten points were used to allow the computation of blocked forces. The orientation and positions of these chosen points was consistent with the points excited during mobility measurements.

Each of the points monitored on the structure were fitted with accelerometers having a sensitivity of 10mV/ms^{-2}. Measurements were triggered when the tachometer system delivered a voltage to the analyser, i.e. whenever the turbine was rotating. In some

instances a measurement was triggered erroneously,but this can easily be identified during post processing. Whenever the trigger level was reached a 10 minute uninterrupted recording was launched. This data was time-stamped according to the date and time at the beginning of the recording using the computer clock. Over each 10 minute period a small drift in time can be expected between the analyser and the computer clock but using such short recording time periods this should be negligible. Sampling was performed at a rate of 12800 samples per second on all channels (11 accelerometers and 1 tachometer) which should cover a far greater range than the current problem requires.

3.5.1 Measured velocity

Shown in Figure 9 are velocities measured at the corresponding point for which mobility plots were shown in Figure 8. The blue lines in the figure each show 30 four second velocities calculated from the recorded time history. Each line corresponds to a 4 second period weighted with a Hanning window. The black line is the linear average computed from 30 windows. A 50% overlap was used and as such the figure corresponds to a one minute time period. It can be seen that the vibration velocity varies significantly over a one minute period because the wind speed and the rotational speed of the turbine vary rapidly. It can be expected that sound and vibration in a dwelling may vary in the same way over a similar time period.

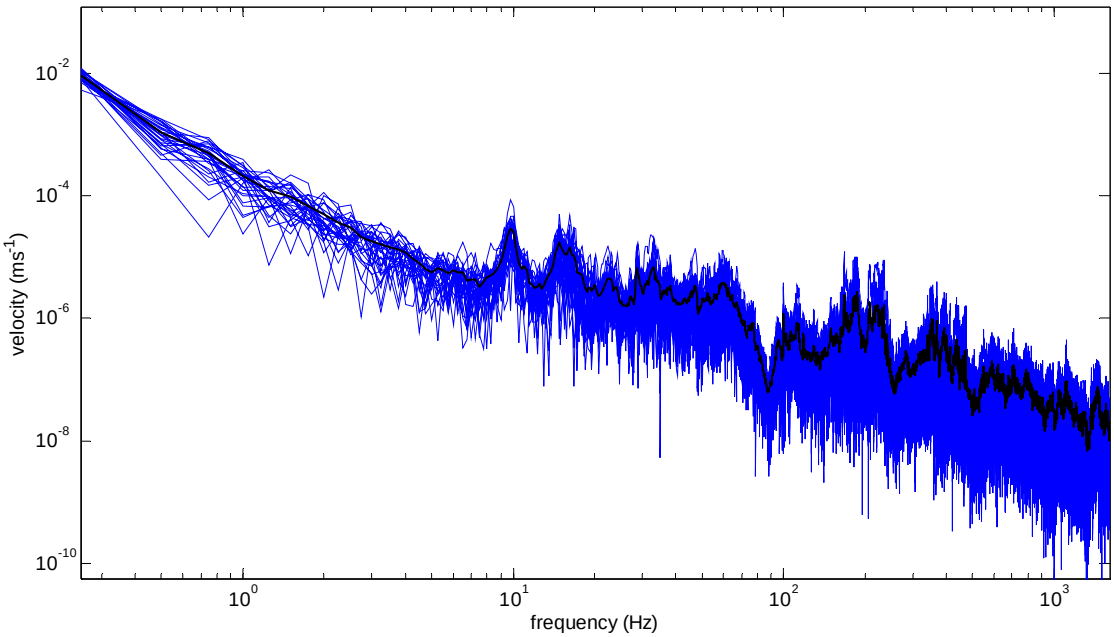

Figure 9 Measured velocities at a point on the base of the mounting. Multiple blue lines show 30 measured 4 second velocity FFTs. Black line shows the FFT average.

Section 7 of the report describes a number of field tests where the sound and vibration

in dwellings with attached turbines was measured. For these case studies it will be seen that the A-weighted sound pressure levels show a dominant peak approximately within the 100-300Hz range. This peak is also observable in Figure 9.

3.5.2 Tachometer measurements

As described previously the turbines were monitored using a tachometer connected to the same analyser used to record vibration data. To determine the rotational speed of the turbine from the tachometer pulses, FFTs of the tachometer signal were taken in the same way as for vibration measurements. The accuracy of the analyser used therefore ensured that the vibration and rotational speed measurements were well synchronised.

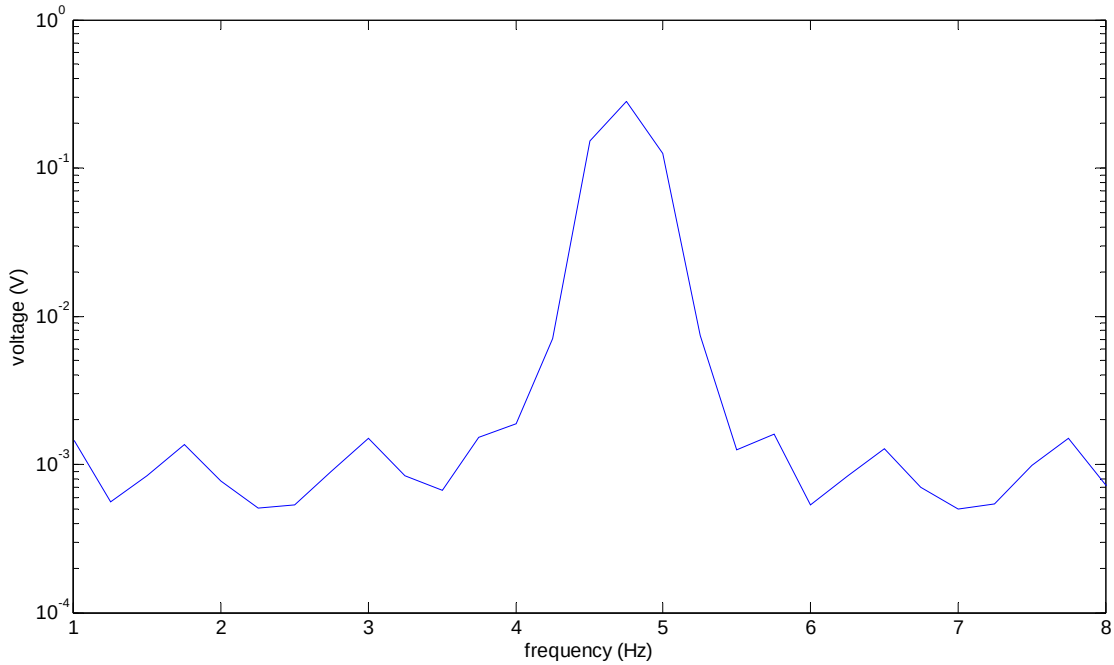

Figure 10 FFT of tachometer output voltage. During this four second time window the predominant rotational speed was 4.75 Hz or 285rpm.

Shown in Figure 10 is an example of the rotational speed monitoring system's performance. In this particular instance it can be seen from the FFT of the tachometer output that the rotational speed of the turbine was predominantly 4.75Hz during this 4 second window.

Using this approach it was possible to stamp every measured 4 second window of vibration velocity with a corresponding rotational speed of the MWT.

3.6 Blocked forces

The combination of measurements described above can be used to calculate the blocked forces of a wind turbine and these blocked forces which can subsequently be used to predict sound pressures or vibration in a dwelling. However, in order to have confidence in predicted sound pressures or vibration, a validation of the blocked forces is essential. The on board validation approach used allows this to be cross checked. Due to the variable and uncontrolled operation of the MWT this is the only cross check on the blocked force data.

Figure 11 shows the measured validation velocity on the mounting system compared to a prediction made from the measured blocked forces. The upper of the two figures shows the whole frequency range used for the study and the lower figure shows the audible part of that range. The measurement and prediction were averaged over a one hour period.

It can be seen that the audible peak at around 200 Hz observed during the field trials (section 7) is predicted well since it is within 2dB of the actual vibration level measured and that the range 10 to 40Hz is subject to the greatest error. This was however to be expected because the mobility measurements used to calculate the blocked forces were best suited to the 1-10Hz and 60-1600Hz ranges.

Overall Figure 11 shows good agreement between the measured and predicted velocity level in the optimised regions. A likely reason for the general underestimation of the velocity level is background noise occurring locally to the accelerometer used for the on board validation. Auralising a selection of velocity measurements revealed that some vibration measured on the mount system was not attributable to the turbine itself. Such events, caused by rain or creaks/rattles on the mount system, may be regarded as background noise. By using a combination of ten well-spaced accelerometers the calculated blocked forces were less susceptible to this local noise.

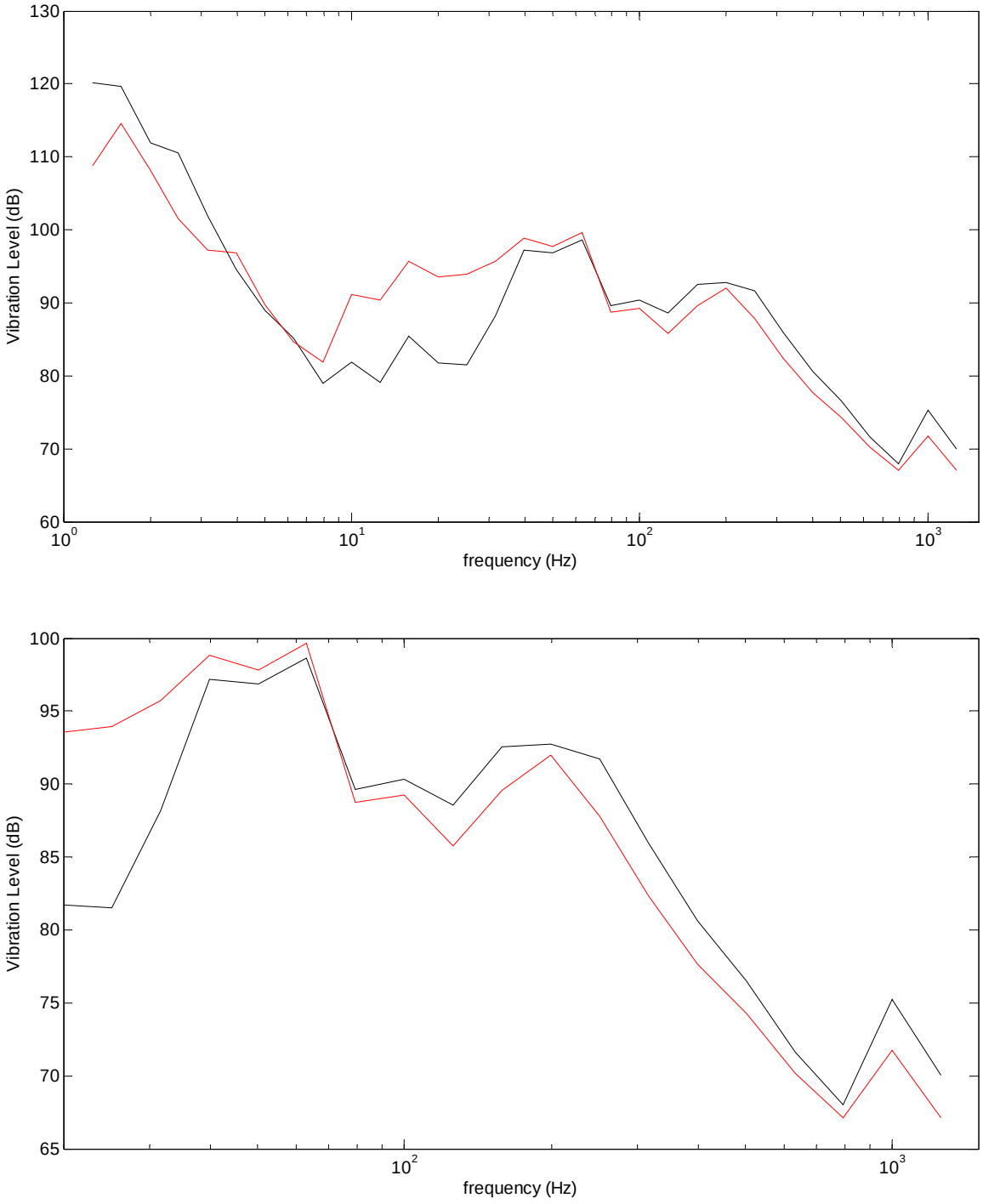

Figure 11 Velocity level (ref 10^{-9} $ms^{-1)}$ predicted as part of the on board validation compared with measured actual vibration level, red and black respectively, no frequency weighting applied. Upper plot shows 1 to 1600Hz and lower plot focuses on the audible range of 20 to 1600Hz.

3.6.1 Blocked forces versus rotational speed

As described earlier, every set of 11 measured velocities was stamped with a corresponding rotational speed for every 4 second window and since the blocked forces were calculated from these velocities the time stamp could be passed on. Using this approach blocked forces were calculated for a range of different rotational speeds. Using the measured rotational speed of the turbine it was then possible to single out events occurring at a specific rpm and by gathering together blocked forces at like for like rotational speeds a basic order analysis was possible.

Figure 12 shows blocked forces for two operational speeds of MWT1 averaged over approximately 200 seconds. The blocked force shown is the resultant of the blocked forces in the x and y directions only. The peak shown at 1 (or 10^0) for both operational speeds is the first order of rotation. With regard to structure borne sound this particular peak is of little interest however because it is outside the range of human perception. More interesting is the peak between 30 and 40 which is in the audible range at both operational speeds. Note that the range used on the x-axis is normalised by the rotational speed and that this axis cannot be interpreted directly as frequency.

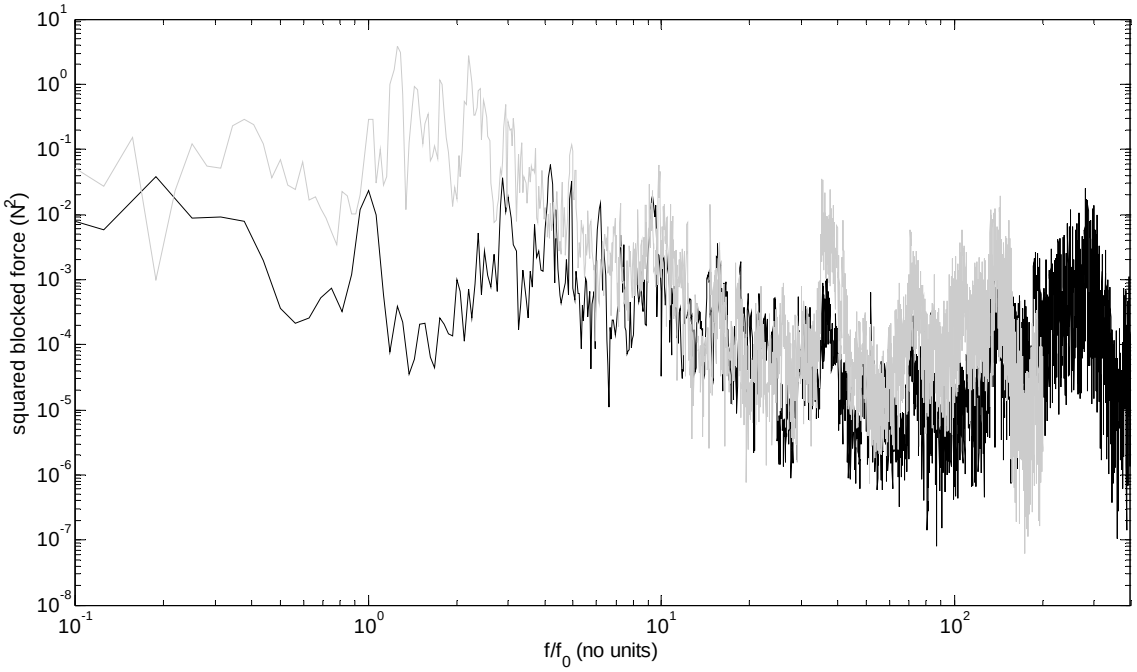

Figure 12 Blocked force calculated for two operational speeds, black line 240rpm and grey line 480rpm. The x axis is normalised by the rotational speed where f_0 is rotational speed in Hz and f is frequency also in Hz.

Shown in Figure 13 is the same data as shown in Figure 12 but converted to one third octave bands which have been A-weighted. The figure shows characteristic structure-borne sound power (as defined in EN12354-5 assuming a source mobility of 10^{-3} m/s/N) in dB plotted against a normal logarithmic frequency axis in Hz, i.e. not normalised by the rotational speed. Characteristic power is a measure of a vibration source's potential to deliver power to a connected structure; the actual power delivered is dependent upon the coupling between the source and receiver structures. Characteristic power can however in most cases be considered as an upper limit (EN12354-5:2009, Moorhouse 2001) .

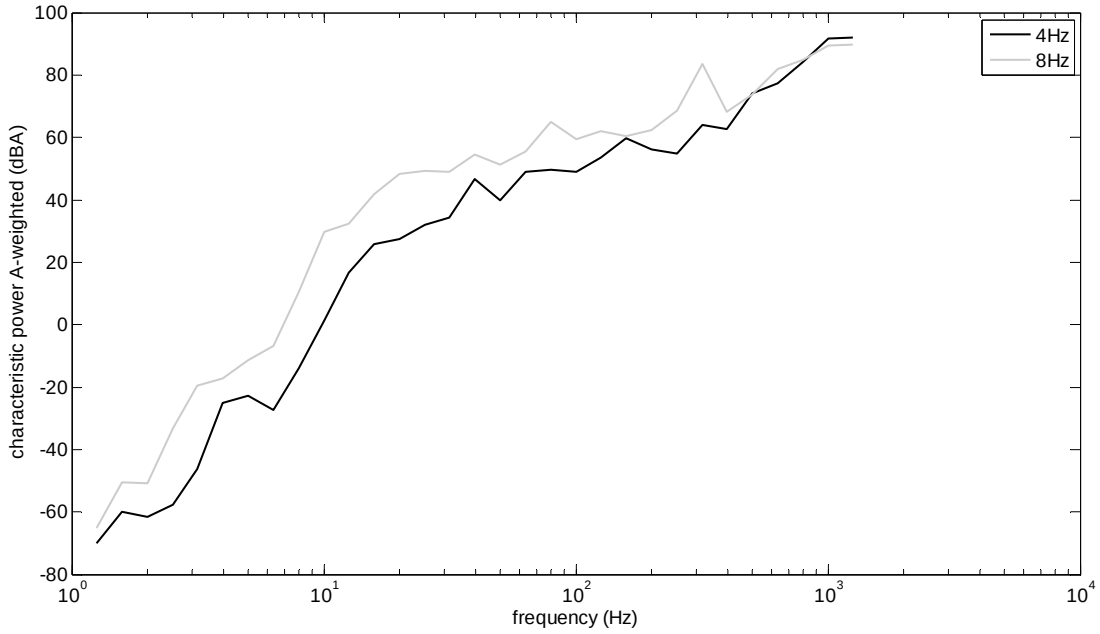

Figure 13 Characteristic power determined from blocked forces in the x and y directions for rotational speeds of 4 and 8Hz corresponding to 240 and 480rpm respectively, presented in third octave bands. The results are presented in dB and are A-weighted. (MWT1)

Figure 13 is included here mostly for comparison purposes between different rotational speeds. It can be seen that an increase in rotational speed from 4 to 8 Hz results in an increase of nearly 20dB when taking into account only the x and y directions. It is immediately clear from Figure 13 that a doubling of speed alters significantly the potential for noise and vibration output. A-weighting was used to illustrate more clearly the relationship to structure-borne sound but the attenuation of the mount and building have not been taken into account.

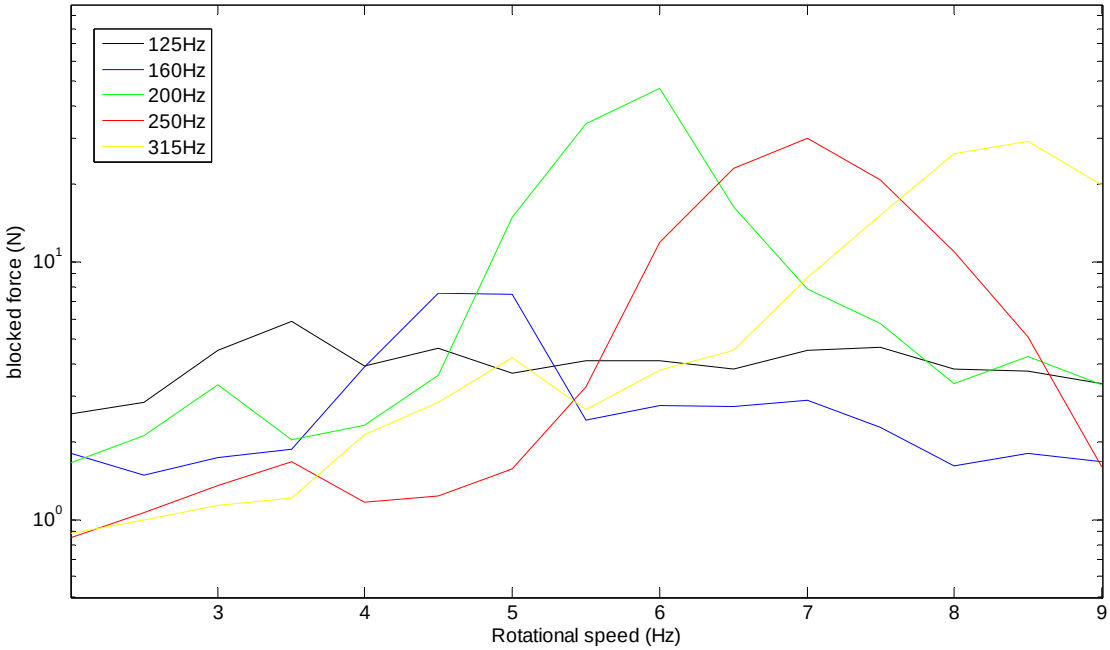

Figure 14 Blocked forces including the x, y and z directions for different rotational speeds. Black, blue, green, red and yellow lines correspond to the 125, 160, 200, 250 and 315 third octave band centre frequencies. (MWT1)

Figure 14 shows blocked forces in Newtons of a wind turbine as a function of rotational speed. Each line on the plot corresponds to a different third octave band in the identified problem region with respect to structure borne sound 125 to 315Hz (one third octave centre frequencies). The black line shows that the blocked force in the 125Hz band varies only slightly with the rotational speed of the turbine. The blue line (160Hz centre frequency band) shows a peak when a harmonic of the rotational speed passes through that particular one third octave band. The green, red and yellow lines then show the blocked forces in the 200, 250 and 315Hz bands which each in turn show a peak as the rotational speed of the turbine increases. Going beyond the 315Hz band the relationship between rotational speed and blocked force flattens again, similar to the 125Hz band. By combining the energy in the 160-315Hz bands a further figure can be generated to show blocked forces in the potentially problematic frequency range. This is shown in Figure 15.

It will be noted from Figure 15 that the blocked force does not increase linearly with rotor speed but levels off above about 350 rpm. This is most likely due to a resonance of the turbine itself being excited by this specific rotational speed.

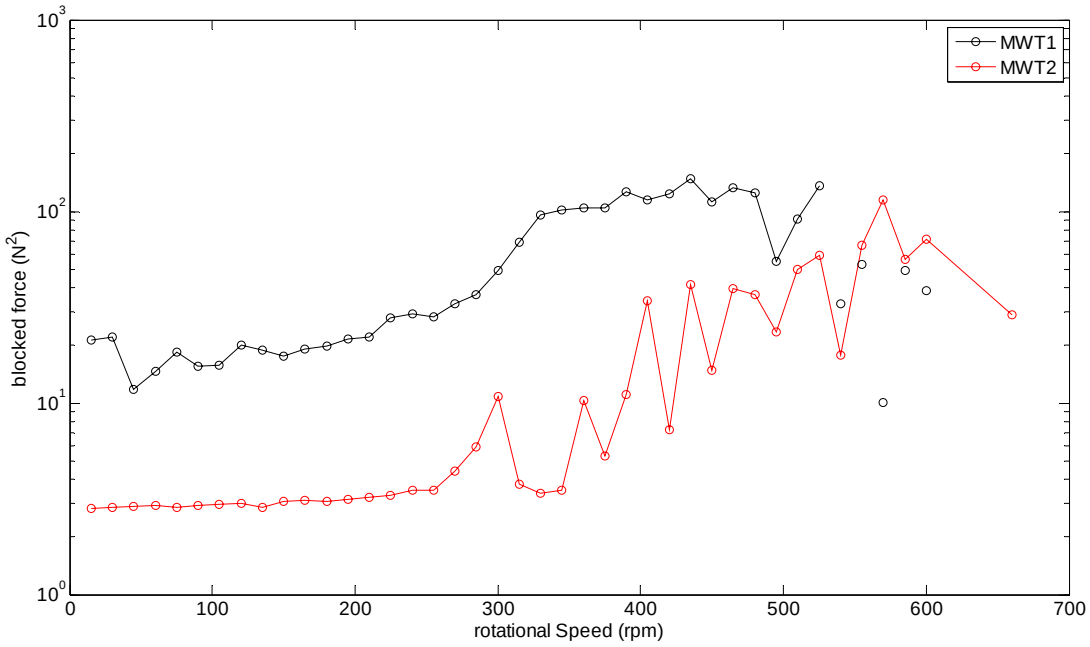

Figure 15 Blocked force (source strength) taking into account the x, y and z directions in the third octave bands 160-315Hz plotted against rotational speed. Black circles are indicative results for MWT1 based on the few samples that were available for those speeds.

Regardless of the mechanism it has been shown that for a specific turbine a higher rotational speed will not necessarily lead to a greater noise level. Micro wind turbines are required to be highly reactive to changes in wind speed and as a result they must be allowed to operate over a much greater range of rotational speeds than their larger counterparts. As such it should be possible to develop quieter devices by avoiding turbine resonances.

3.7 Structure-borne sound from pole flexure

This section briefly considers, as an aside, the structure-borne sound due to 'waggling' or flexing of the MWT mounting pole. Whilst the main source of structure-borne sound is thought to be due to MWT rotation, as discussed in the rest of this chapter, there was some anecdotal evidence to suggest that flexing of the mounting pole due to sudden changes of wind speed or direction could be a potential source of disturbance. This effect was not observed in the field trials but nevertheless a brief series of tests has been conducted in the laboratory in an attempt to quantify the effect.

A standard mounting system for MWT2 was installed on the outside wall of the reverberation chamber in the University of Salford laboratories. The pole was pulled back with a force of 200 N (20 kg), as measured by a spring balance, and then suddenly released. The resulting sound pressure level inside the reverberation

chamber was recorded. An instant unload of 200 N was selected on the basis that the maximum wind loading at the top of the pole, according to the manufacturer, is up to 500 N, however, we would not expect the full load to be removed instantaneously under real wind conditions.

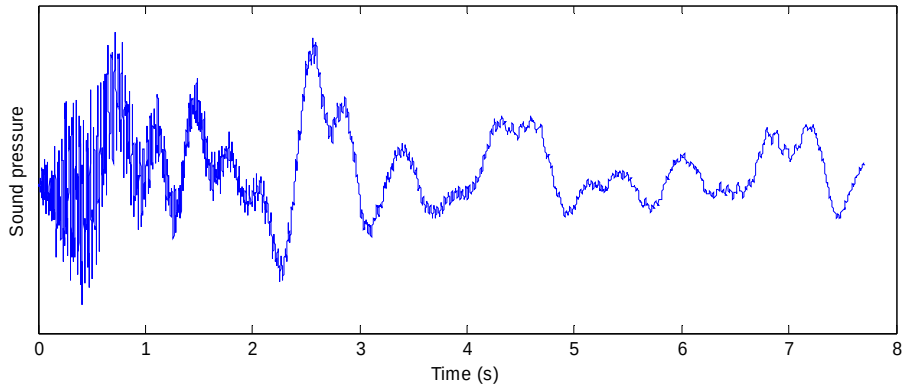

Figure 16: sound pressure inside reverberation chamber due to pole flexure.

Inside the chamber the 'waggling' of the mast was clearly audible accompanied by a soft 'rattle' due to the slight play in the pivot bearing of the turbine which was installed during the tests. Figure 16 shows the sound pressure recorded in the reverberation chamber. The maximum L_{Aeq} (Fast time constant) was 45 dB. It is difficult to draw decisive conclusions from this test without more definitive information on wind loadings. However, it seems feasible that rattling of the mast could be audible under highly variable wind conditions. This could be improved by reducing tolerances in the pivot shaft and/ or redesign of the mast.

3.8 Conclusions

The main purpose of this section was to describe how wind turbine source strength (blocked forces) was obtained from measurements during the project. Preliminary laboratory tests confirmed the feasibility of using the blocked force approach for a MWT and the method was then implemented on MWT1 and MWT2 in a field installation. Vibration on the MWT mounting, rotational speed, wind speed, direction and turbulence were all monitored simultaneously while the MWTs fed power to the grid under real wind conditions over a period of several months. Blocked forces were then calculated from the measured vibration data.

Rather than attempting to relate source strength directly to wind speed, an intermediary step was introduced in which the source strength was related to its rotational speed. Blocked forces corresponding to the same rotational speed were collected and averaged so as to quantify the source strength for a given speed over a range of loadings. The resulting curves, shown in Figure 15, are one of the main results of the study. They confirm the feasibility of obtaining an independent

characterisation of an MWT as a source of structure-borne sound and vibration from measurements taken in realistic operating conditions and expressing the result as a function of rotational speed.

Figure 15 shows that the structure-borne sound source strength of a MWT does not increase linearly with rotational speed and even shows a decreasing trend at some rotational speeds. This is likely to be due to structural resonances in the MWT. The implications are that as the rotational speed increases the sound level may increase and then decrease. Most airborne sound sources do not exhibit this behaviour, but it is not uncommon for structure-borne sound sources.

A brief test was conducted to assess the effect of 'waggling' of the MWT pole in rapidly changing wind conditions from which it appears feasible that this effect could produce audible sound in an attached property.

Having, in this chapter, expressed source strength as a function of rotational speed, the following chapter will consider the relationship with wind speed.

4 Relating MWT source strength to wind conditions

The aim of this section is to try to relate the blocked forces, obtained in the previous section, with wind conditions to which the MWT is exposed. In addition, a comparison is made of the wind conditions at the (rural) test site with those at an urban roof-top site in order to determine if there are particularly important differences.

It is well known that aerodynamic noise from wind turbines depends on wind and blade speed as well as on turbulence. The various well known mechanisms that produce aerodynamic noise, namely turbulent boundary layer trailing edge noise, separated flow noise, laminar boundary layer vortex shedding noise, tip vortex formation noise, trailing edge bluntness vortex shedding noise and turbulent inflow noise (Wagner et al. 1996) scale with the Mach number. This means that noise levels increase with increase in wind speed in the linear region of the power curve where the blade tip speed also increases linearly. Generated noise increases with 5^{th} power of blade tip speed. Similar increases in inflow turbulence noise are observed with increasing turbulence (Wagner et al. 1996). As with aerodynamic noise it is known that vibration also increases with both wind speed and turbulence (Hansen 2008). Hence an understanding of how wind conditions affect MWT operation and hence structure-borne sound source strength is needed.

4.1 Relationship between rotor speed and wind speed

In Section 3 the source strength of the MWTs was obtained under a range of wind conditions. Although source strength is known to depend on wind speed no attempt was made to express source strength directly in terms of parameters describing wind conditions since it was anticipated that the results would be subject to significant scatter. Instead, the source strength (blocked force) was expressed as a function of rotational speed of the MWT for which a more direct relationship is expected to exist. Using this approach clear trends in source strength behaviour were identified.

However, potential MWT sites are characterised in terms of wind speed rather than rotor speed and therefore in this section we aim to find a correlation between wind speed and rotational speed of the MWT. Should a satisfactory correlation be found then it may then be possible to relate source strength, via rotational speed, to wind conditions and thereby provide an estimate of source strength for a given site for which wind conditions are known (see Figure 17). The wind conditions examined are wind speed, in this section and turbulence in the following section.

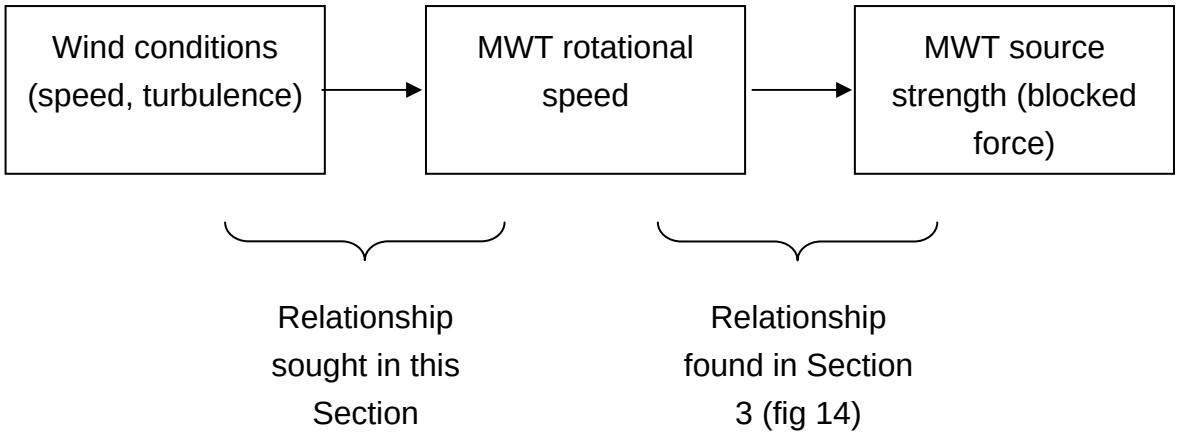

Figure 17: Relating source strength to wind speed via the intermediary quantity of rotational speed

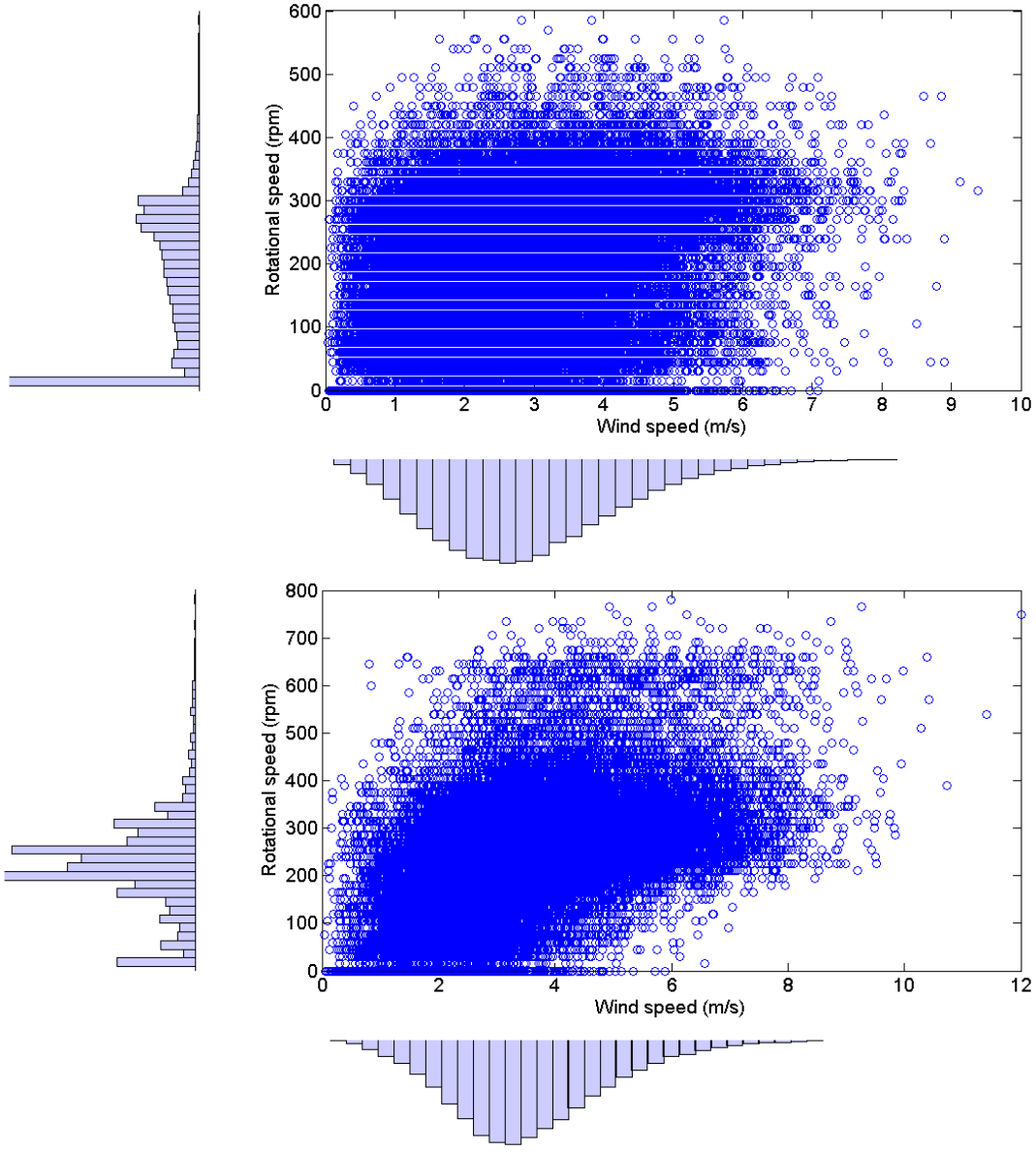

Figure 18: Rotational speed versus wind speed for four second samples also showing marginal probability distributions. Top: MWT1. Lower: MWT2.

Figure 18 shows a scatter plot of rotational speed plotted against wind speed both averaged over four second snapshot periods. (Wind measurements are described later in section 4.4). The marginal probably distributions are also shown which quantify the proportion of the time for which given wind speed and rotor speed occurred during the period of the measurements. The short four second window was selected since, as described in Section 3, the MWT rotational speed was observed to change over a period of a few seconds under normal wind conditions. However, significant scatter is evident in the plot to the extent that it does not seem worthwhile to quantify the relationship.

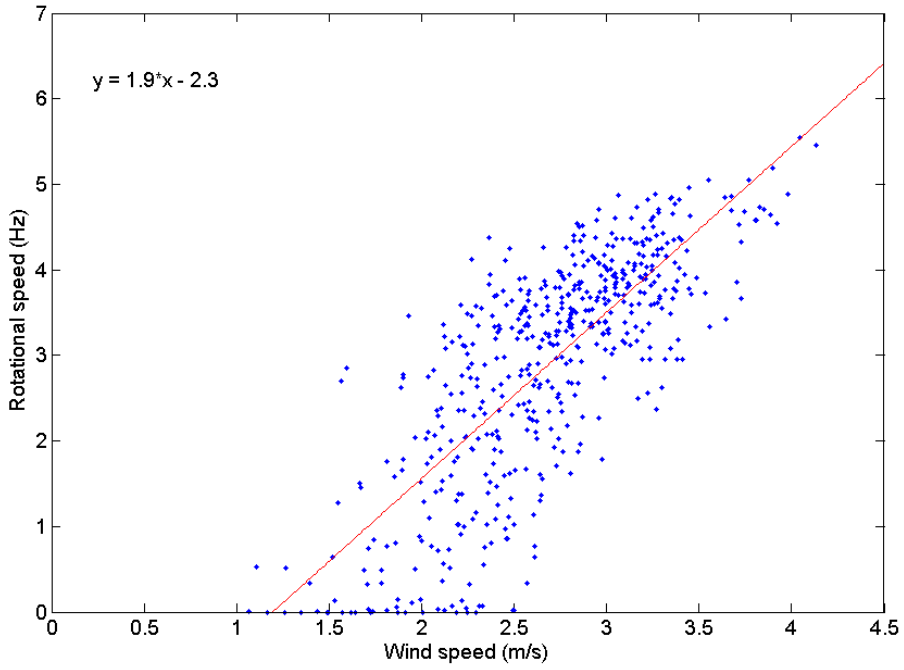

Figure 19: Rotational speed versus wind speed for five minute samples. MWT1

In an attempt to find a clearer cut relationship the averaging time was increased in steps up to ten minutes. Figure 19 shows the resulting plot for five minute averages taken from the same 37 hour period of continuously windy conditions. Some clearer trends are evident from this plot. First, the cut-out speed of the MWT can be seen with a number of zero rotational speed values (no rotation) occurring between 1 and 2.5m/s wind speed. Secondly, a positive correlation is seen between wind speed and rotational speed evidenced by the linear regression line. The fit could perhaps be improved as a predictor for high wind speeds by omitting points with zero rotational speed. Also, some of the points at lower wind speeds, which appear to depart from the linear relationship, could perhaps be omitted but the regression line as shown is sufficient for the current purposes.

Table 2 gives the regression coefficients obtained by producing plots similar to Figure 19 for various averaging times during the same 37 hour period. The correlation coefficients increase as the averaging time increases. It is also interesting to look at the slope of the regression line given as the coefficient of 'x' in the third column of Table 2. For the shortest averaging times different values are obtained for the slope, but for averaging times longer than two minutes the slopes are fairly stable. The MWT cannot be expected to respond instantaneously to variations in wind speed and as such there is a lag, sometimes greater than 4 seconds, between the rotational speed and the wind speed; this is especially true for periods where the rate of change of wind speed is high. These figures suggest that an averaging time greater than two minutes can be used to achieve an average without too much scatter caused by the 'response time' of the MWT . In view of this it seems sensible to use five minute periods since these correspond to the time period suggested for analysis of noise levels in Section 2. It is important to note that this does not invalidate the approach used in Section 3 of using short snap shot measurements to correlate source strength with rotational speed because source mechanisms are far more closely coupled to rotational speed than rotational speed is to wind speed. However, it does provide additional justification for the approach adopted in the previous chapter of using rotor speed as an intermediary.

Table 2: Correlation and regression coefficient between MWT rotational speed and wind speed for various averaging times

Time constant	**R^2**	**Regression line equation**	**Number of data samples used**
8.4 min	0.65	Y = 2.0 x + 2.6	265
4.2 min	0.60	Y = 1.9 x + 2.3	530
2.8 min	0.55	Y = 1.8 x + 2.0	795
2.1 min	0.53	Y = 1.8 x + 1.8	1060
1.05 min	0.46	Y = 1.6 x + 1.4	2120
31.5 sec	0.34	Y = 1.3 x + 0.6	4240
15.75 sec	0.22	Y = 0.9 x + 0.3	8480

Shown in Figure 20 is a similar result to that shown in Figure 19 but for a different wind turbine (MWT2). As before a five minute averaging period was used to generate the figure. An interesting point to note in Figure 20 is that above 4m/s the relationship between rotational speed and wind speed appears to separate which may be due to the load applied to the turbine. For example if the response time of the electronics was not sufficient to react to some rapid changes in wind speed which

occur in a 5 minute averaging period it is possible that no load would be applied for a portion of this time and a higher rotational speed would be produced.

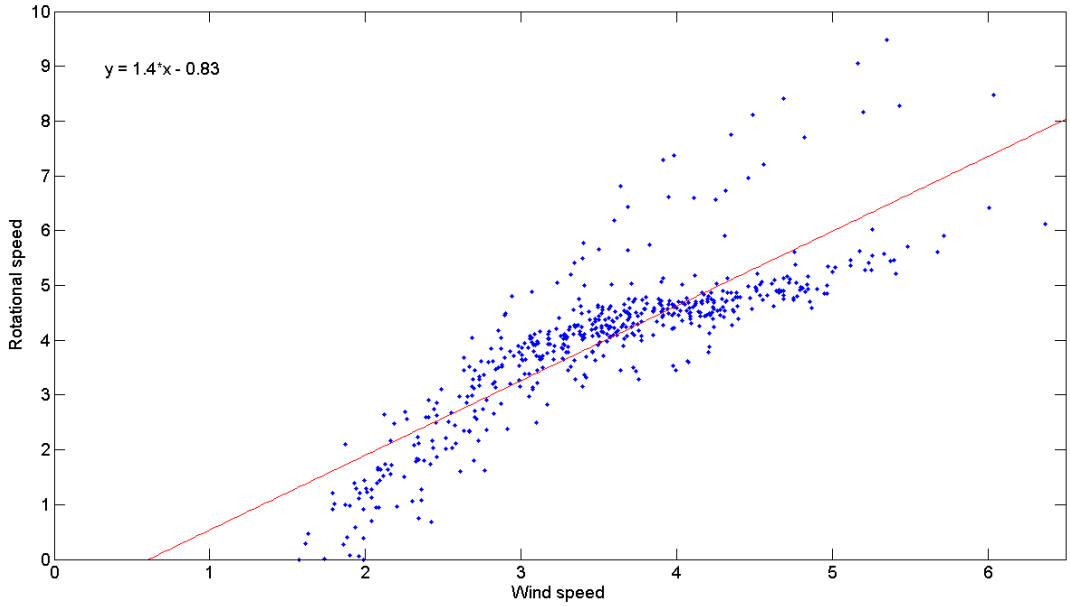

Figure 20 Rotational speed versus wind speed for 5 minute samples. MWT2

Having obtained a mathematical relationship between wind speed and rotor speed the obvious next step would be to reinterpret Figure 15 so as to provide blocked forces as a function of wind speed. However, this is not as straightforward as it may at first appear. Recall that in order to generate Figure 15 it was necessary to analyse data in sufficiently short periods such that the rotational speed effectively remained constant during the analysis window. Four second windows were used for this purpose. In contrast, it was shown above that significantly longer windows (five minutes) were required in order to find a stable relationship between wind speed and rotor speed. Since from experience the rotor speed is expected to vary significantly during any five minute period it is not necessarily valid to apply the five minute regression line shown in Figure 19 to the x axis of Figure 15.

4.2 Relating sound levels to wind speed distribution

In chapter 3 the MWT source strength was related to rotor speed and in the preceding section 4.2 a relationship between rotor speed and wind speed was found. Unfortunately, these two relationships could not be combined because of the different time scales used to derive each one. In this section we follow a statistical approach leading to a prediction of sound levels based on knowledge of wind speed.

Referring back to Figure 18 it is seen that the probability density for wind speed, shown under the horizontal axis, conforms reasonably well to a Weibull distribution which is the classical distribution expected for wind speeds (albeit using non-standard

2 second averages in this case). On the other hand, the distribution of rotor speeds, next to the vertical axis, does not conform to any standard probability distribution. In part, this is due to the high probability of a zero rotor speed, where the rotor is stationary, but in any case the rest of the distribution is not of any standard form for either MWT. This means that it will not be possible to find a general mathematical relationship between the wind speed and rotor speed distributions. For example, on a less windy site we would expect a narrower Weibull distribution with a greater density of low wind speeds, but we cannot predict how the rotor speed distribution would look under these conditions. Similarly, for a windier site a broader wind speed distribution would be expected but it cannot be inferred that the rotor speed distribution would broaden in the same way.

The implication of the above discussion is that the results of this section will be necessarily specific to the test site, or at least to sites with similar wind speed distributions. This was not the case for the source strength- rotor speed relationships established in Figure 15 which should be applicable for any site. Therefore, the relationship to wind speed will be less general but nevertheless useful, since wind speed information is more likely to be accessible than knowledge of rotor speed.

As a first step we extend Figure 15 to give, rather than source strength, the sound pressure level in the reference installation as a function of rotor speed. The procedure followed to obtain this plot will be described in chapter 7 and the resulting plot is shown in Figure 21. Figure 21 gives the sound levels predicted to occur in the reference installation if the MWT were to run (hypothetically) constantly at a given rotational speed. As was the case for Figure 15 this plot should apply to any site. The noise levels generally rise as rotor speed increases as might be expected. However, the curves level off above rotor speeds of about 350 rpm suggesting that there is an upper limit to noise levels, at least for these two models of MWT.

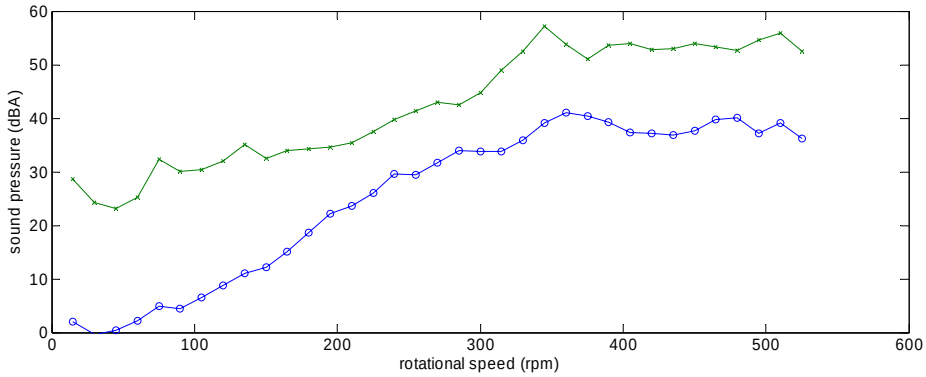

Figure 21: Sound pressure levels in the reference installation as a function of rotational speed. Upper curve: MWT1 (mast length 2.9m). Lower curve: MWT2 (mast length 2.4m).

The next step is to find a statistical relationship between sound levels and wind speed. We therefore consider the joint probability density function for rotor speed and wind speed shown in Figure 22. The plots are created from the same data as for Figure 18 and are based on 2 second averaged snapshots for MWT1 and MWT2. Each row of the grid corresponds to a given rotor speed and each column to a given wind speed, the lighter colours corresponding to more frequent occurrences. Note the white strips at the bottom of the plots which show that a static rotor is a frequent occurrence especially at low wind speeds, but also at higher wind speeds (presumably due to inertia in the system).

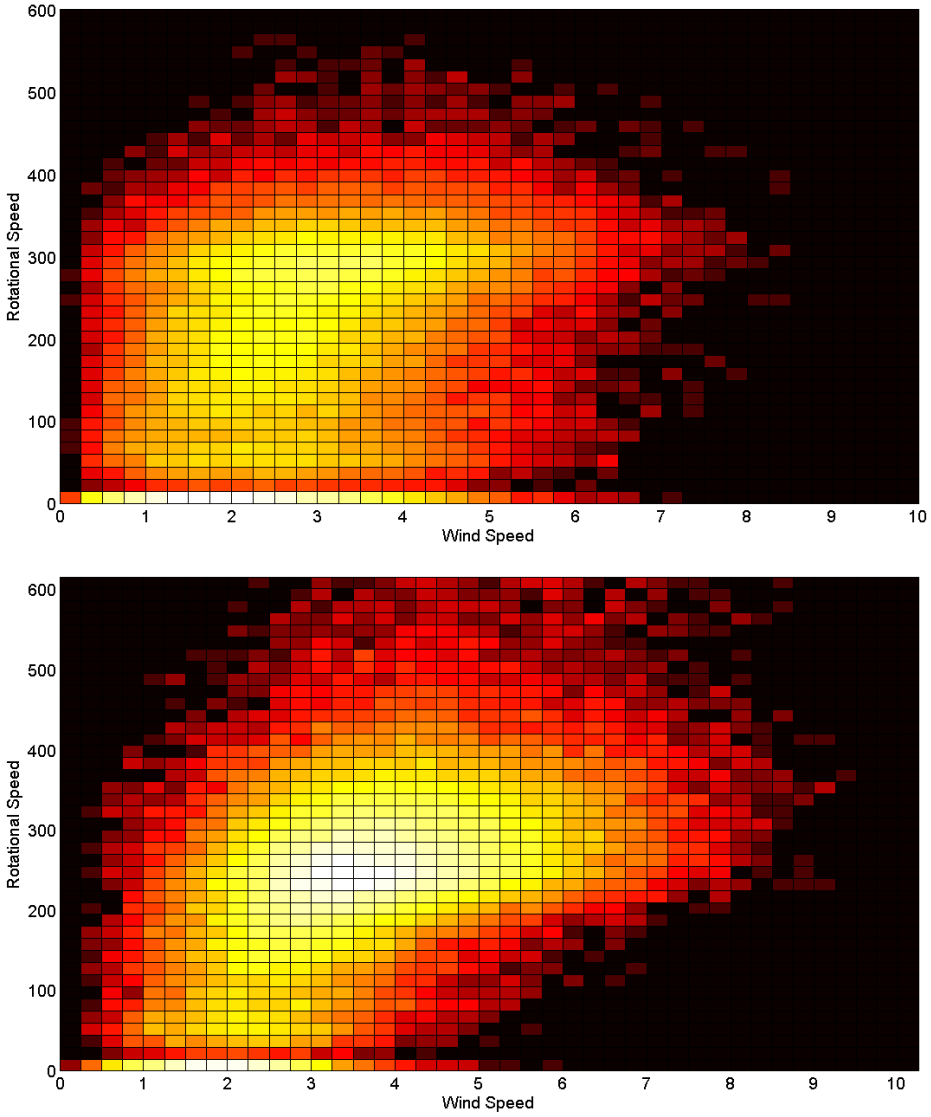

Figure 22: Joint probability density for rotor speed and wind speed. Upper: MWT1. Lower: MWT2.

Combining the data shown in Figure 22 with the relationship shown in Figure 21 we can group the data into 5-minute periods and average so as to create new scatter plots as shown in Figure 23. Figure 23 differs from the previous plots in that the vertical axis now gives $L_{Aeq,\ 5\ minutes}$ rather than rotor speed. The horizontal axis gives wind speed, but now averaged over 5 minutes rather than two seconds. For a site with wind speeds (5 minute average) distributed as shown at the bottom of each plot we can expect a distribution of $L_{Aeq,\ 5\ minutes}$ as shown to the left of each plot. It can be seen that under these particular wind conditions the $L_{Aeq,\ 5\ minutes}$ in the reference installation would be expected to vary between about 41 and 47 dB (31.5 and 34 dB for MWT2); levels around 45 dB (33 dB for MWT2) would occur most commonly and levels at the extremes would occur only rarely.

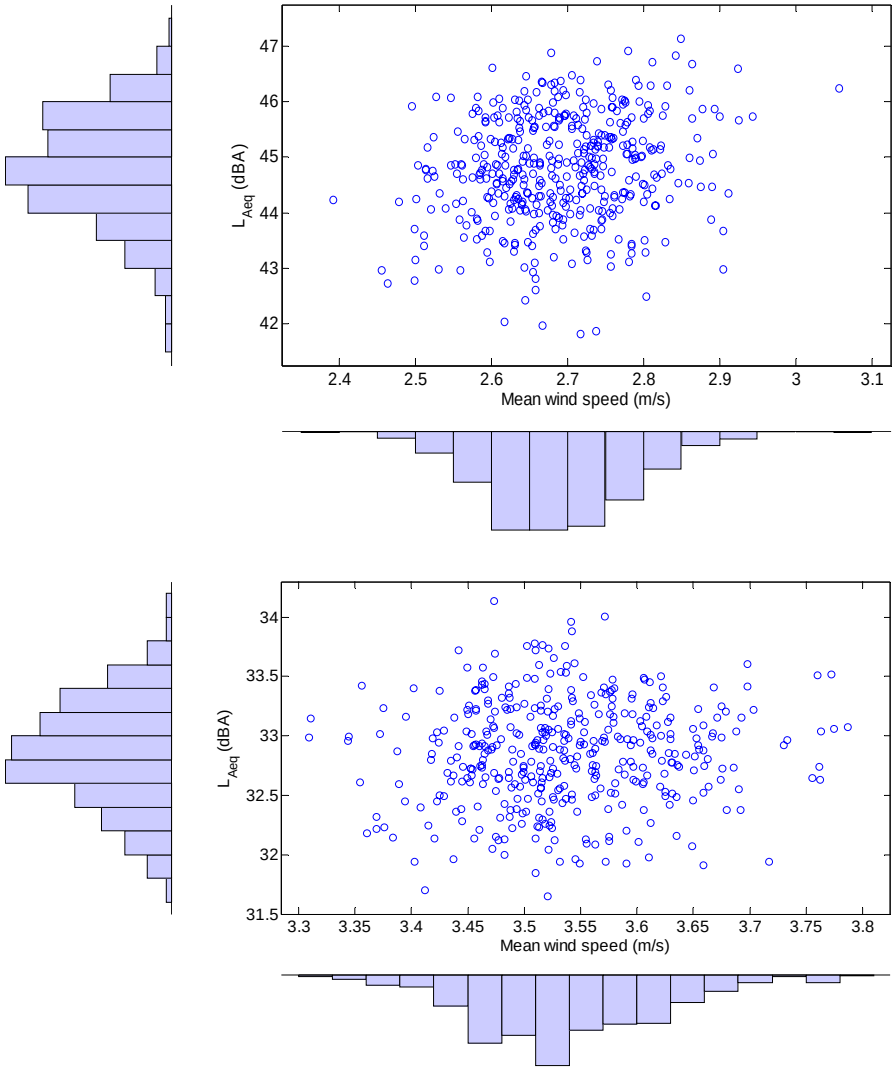

Figure 23: Distribution of $L_{Aeq,\ 5\ minutes}$ plotted against distribution of 5 minute averaged wind speed. Upper: MWT1. Lower: MWT2.

The above illustrates the essentially statistical nature of the noise levels from MWTs in fluctuating wind conditions. Since the criteria for structure-borne sound are likely

to be set in terms of a worst case $L_{Aeq,\ 5\ minutes}$ (see section 2.2) we need to look at the maximum values in the distribution. However, in a statistical analysis such as this the maximum value can be sensitive and it can be more reliable to select a percentile value, for example the $L_{Aeq,\ 5\ minutes}$ that is exceeded for 10% or 1% of the time. This point will be discussed further in section 7.2.

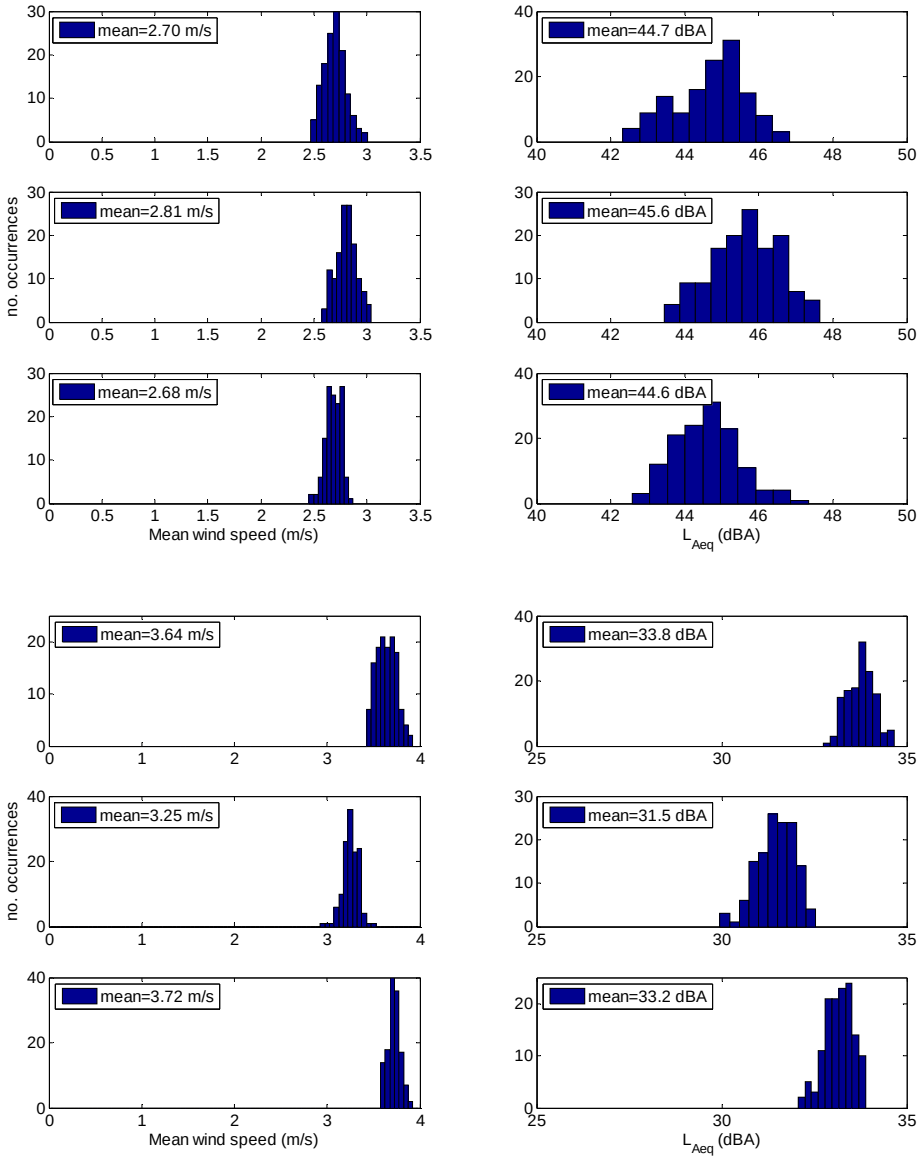

Figure 24: Distribution of $L_{Aeq,\ 5\ minutes}$ and corresponding distribution of 5 minute averaged wind speed. Upper three plots: MWT1 (mast length 2.9m). Lower three plots: MWT2 (mast length 2.4m).

The above analysis provides noise levels for one specific set of wind conditions with a mean wind speed of 2.7 m/s (MWT1) and 3.5 m/s (MWT2). In order to get an idea of how the distribution of $L_{Aeq,\ 5\ minutes}$ varies with wind speed we have extracted data for

3 separate days and obtained the corresponding distribution of noise level and wind speed (5 minute average). The resulting distributions are shown in Figure 24. It can be seen that the mean noise level generally increases in line with the mean wind speed but that the shape of the distribution may vary.

There is not a large difference between the mean wind speeds in each case and it is reasonable to ask what would happen at higher mean wind speeds. In order to answer this question fully would require more data obtained over a wider range of conditions. However, we can infer from Figure 21 that the noise levels will start to level off once wind speeds are sufficient to obtain a rotor speed of about 350 rpm.

4.3 Relationship between rotor speed and turbulence

Another aspect of the wind conditions which could potentially affect source strength of the MWT is turbulence. Inflow turbulence is known to have a pronounced effect on the noise generated by rotor blades (Wagner et al. 1996) and it is reasonable to expect that vibration of the MWT could be affected in a similar way.

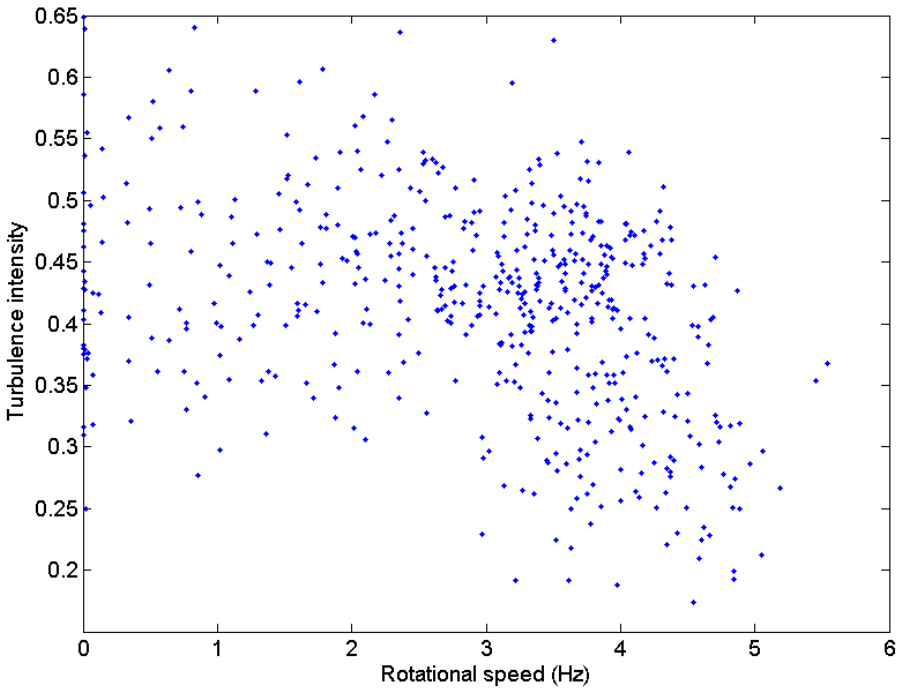

Figure 25: Turbulence intensity versus rotational speed: five minute samples

Turbulence is still an incompletely understood phenomenon and as such there do not exist universally accepted methods of characterising atmospheric turbulence in a comprehensive manner. The most widely used parameter is the 'turbulence intensity' which is defined as standard deviation divided by mean wind speed. The turbulence intensity is plotted against rotational speed in Figure 25. A negative correlation is seen which indicates that higher rotational speeds correspond to lower turbulence

intensities. However, it should be appreciated that the turbulence intensity is normalised by the mean wind speed so that low wind speeds are often associated with high turbulence intensity because wind direction may change more rapidly than in stronger winds. The negative slope may simply be a result of this effect.

One of the concerns about turbulence is that rapid changes in wind direction at high mean wind speeds may cause sudden yawing of the MWT which could lead to transient forces on the shaft which in turn could become potential sources of disturbance to occupants. The standard parameters used to characterise turbulence, such as turbulence intensity, do not appear appropriate parameters to address this concern for the reasons discussed above. In the absence of a widely accepted parameter we have investigated the use of a novel parameter, namely the rate of change of wind velocity. This is defined as the rate of change of the wind vector, so that a high value can be caused either by rapid direction changes or rapid speed changes. This appears to be more relevant to our concerns than turbulence intensity which, it can be argued, de-emphasises the higher wind speeds which are our main concern.

In Figure 26 rotational speed is plotted against this parameter. It is not easy to interpret the result but it does appear that there is not a strong effect of the rate of change of velocity on the speed, and by implication on source strength.

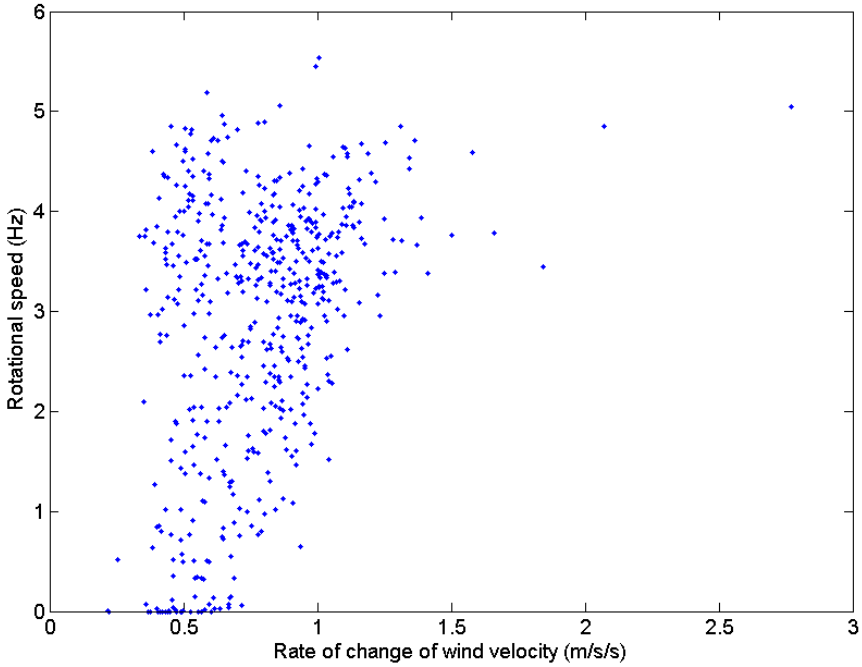

Figure 26: Rate of change of wind velocity: five second samples

4.4 Comparison of urban and rural locations

Having evaluated wind speed and turbulence at the test site in this section we conduct a comparison between this rural location and an urban site. The aim is to establish the extent to which the test conditions at the test site are representative of an urban roof-top location.

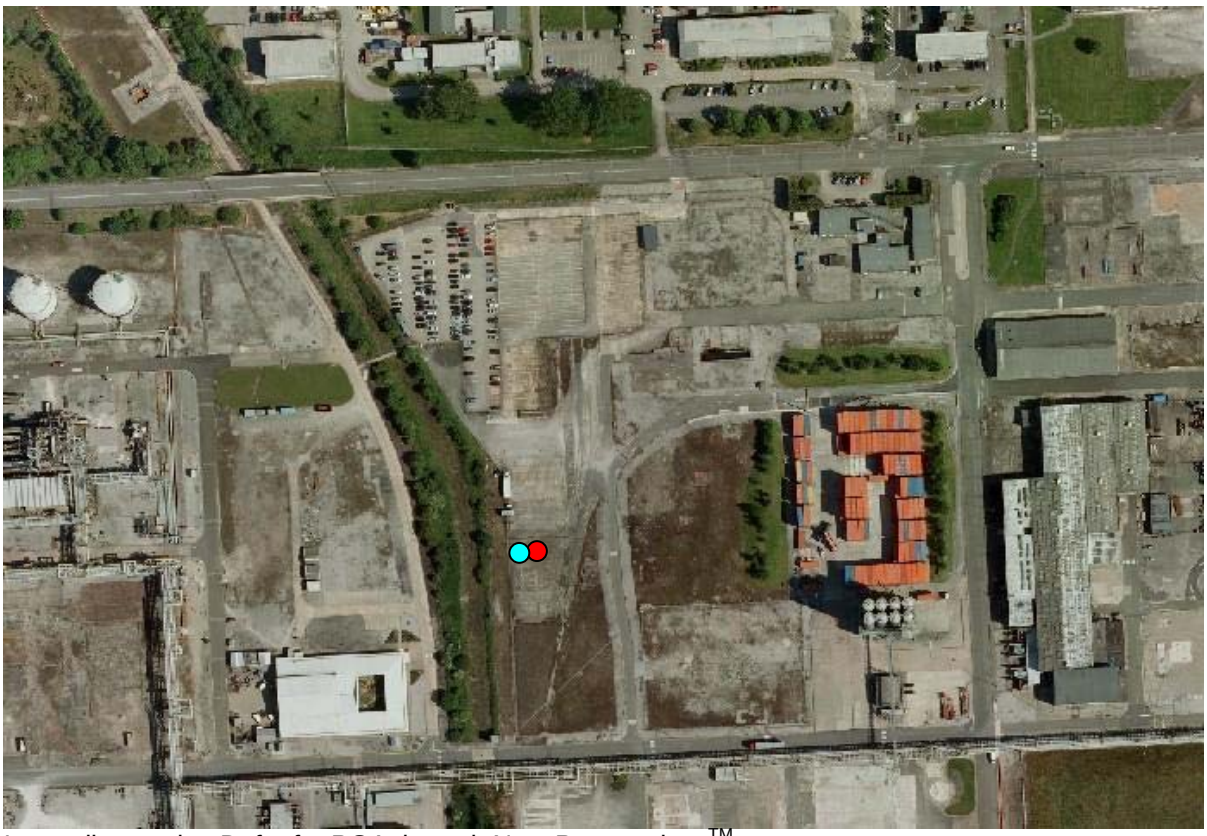

Image licensed to Defra for PGA through Next Perspectives™

Figure 27 Carrington measurement site with anemometer (blue dot) and MWT (red dot) position Indicated.

The wind resource measurements have been conducted at the Lyondell-Basell industrial plant at Carrington, UK. The flat site is characterised through industrial buildings, a disused, overgrown train track and a large tarmac area that was used for the measurements. Wind data were recorded using a sonic anemometer at 5 m above ground level (AGL), which corresponds to the hub height of the MWTs, and at a distance of approximately 10m from the MWT as shown in Figure 27 which was as close as possible whilst avoiding interference from the presence of the MWT. The measurement period analysed in this section covers the time from 9/4/2010 – 10/5/2010 during which simultaneous measurement of wind conditions was made on the roof of the Allerton Building on the campus of the University of Salford. The sonic anemometer was mounted 5 m above roof height on the Allerton building as seen in Figure 28. The building height is estimated to be about 30 m.

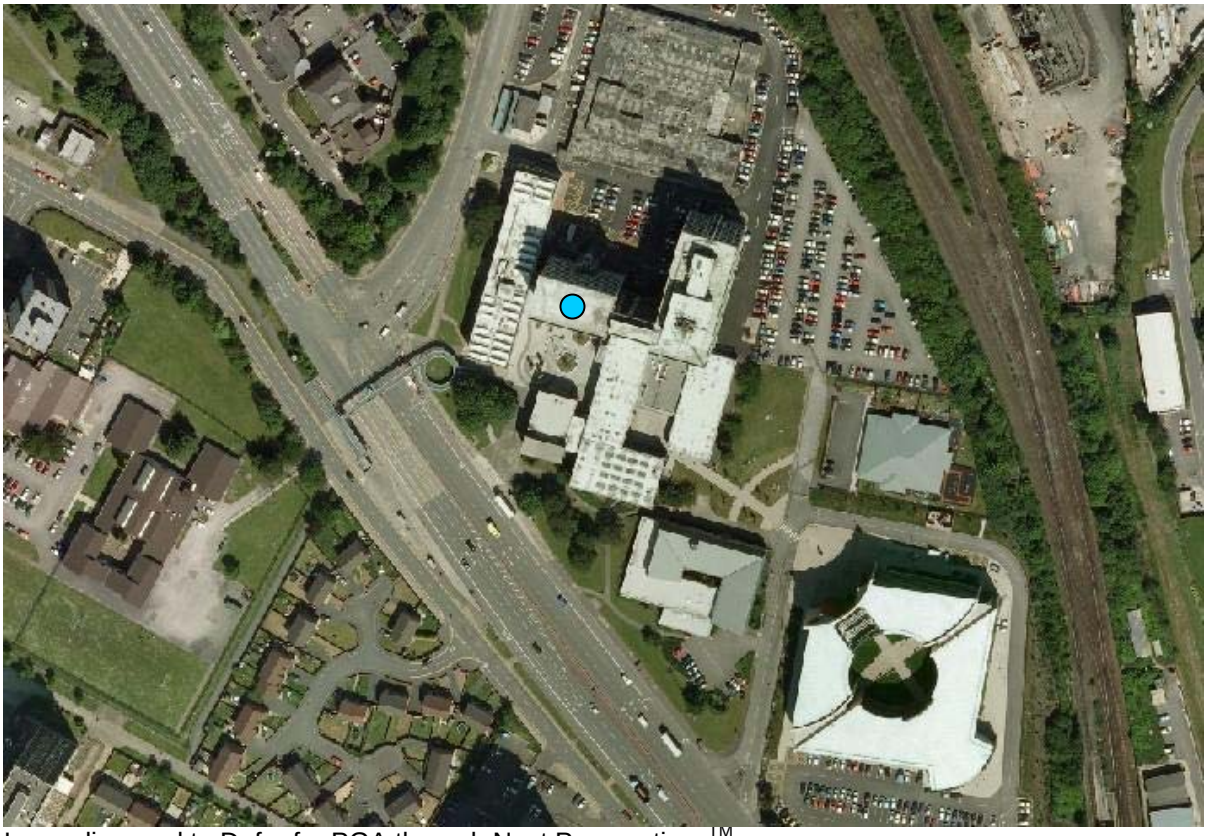

Figure 28 Allerton measurement site with anemometer position (blue dot) indicated.

Measured wind speed distributions at most sites fit best to a Weibull distribution which is therefore commonly used to predict power production for a suggested wind farm site. If noise levels from MWTs are proportional to the wind speed then these distributions will also be useful for the prediction of noise and vibration levels. Weibull distributions can be calculated from just two parameters: the scale factor 'c' which is a measure for the average wind speed and corresponds to the value that is published in the UK wind speed database (NOABL) which is the major source to determine the wind resource for MWT installations. The second parameter in the Weibull distribution, the shape factor 'k' describes how strongly the distribution is skewed towards lower wind speeds and is related with the terrain roughness where higher k values are expected in more exposed terrain with smaller roughness lengths. NOABL assumes a constant value of 2 for all sites.

Figure 29 shows that the wind speed distribution for Carrington displays a scale factor of about 2.9 ms^{-1} with a lower than average shape factor of 1.5. Compared to published BMWT case studies (Encraft, 2009) and (James et al. 2010) with an average scale factor of 3.5 ±0.28 and an average shape factor of 1.59 ± 0.04 these values are just slightly on the low side.

For the comparison between industrial and urban sites both Weibull distributions have been drawn on a semi-logarithmic plot to highlight the differences between the sites. The two distributions have very similar scale and shape factors with differences of about 8 % and 5 % respectively. The bars in Figure 29 show the measured percentage of wind speed occurrence. For high wind speeds this parameter was slightly above the distribution fit at Allerton whereas the same parameter was slightly below the distribution. And in fact the observed maximum wind speeds were higher at Allerton than at Carrington. This fact can simply be explained by the different measurement height above canopy where higher sites experience higher wind speeds. It is interesting in this context then that the average wind speed at Allerton is slightly lower than at the industrial site.

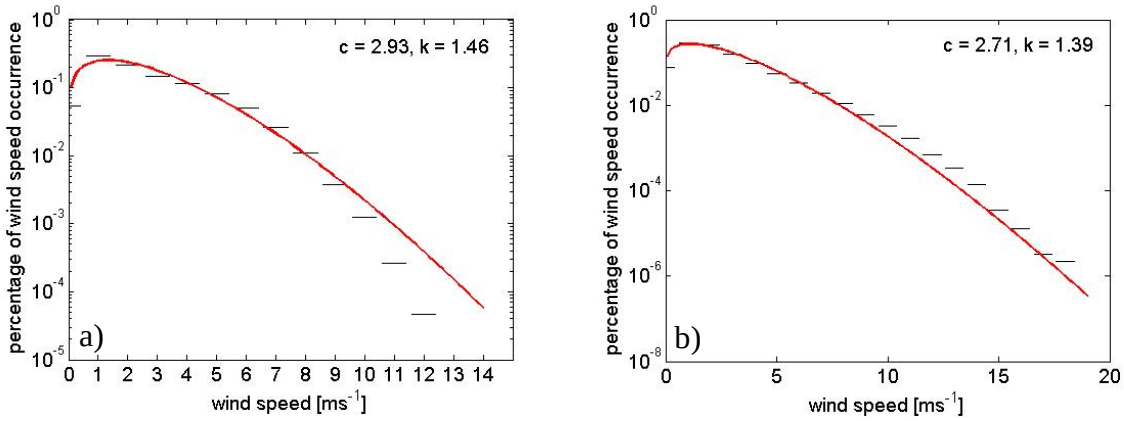

Figure 29 Measured wind speed distribution (bars) using 1 second data compared to respective Weibull distribution (red line) in the period from 9/4/2010 until 10/5/2010 at a) Carrington industrial site b) Allerton multi-storey urban rooftop.

Figure 30 shows the distribution of the occurrence of wind directions for 10 minute averaged values. It is evident that the main wind direction at Carrington during the measurement period was from the sector between 20^o and 80^o which corresponds to North Easterly winds. For Allerton there were two main wind directions with the predominant one being from Northerly directions whereas the second maximum was from the sector 160^o – 180^o that is Southerly winds. Figure 30 shows the wind directions more in terms of the main wind resource directions. High wind speeds in Carrington occur in a relatively wide section between 20^o and 70^o whereas the wind directions in Allerton are more narrowly aligned from three main wind directions at about 160^o, 290^o and 350^o with the highest wind speeds occurring in the 160^o sector. Such alignment can be produced by nearby objects that create channelling effects and will be different for every single site.

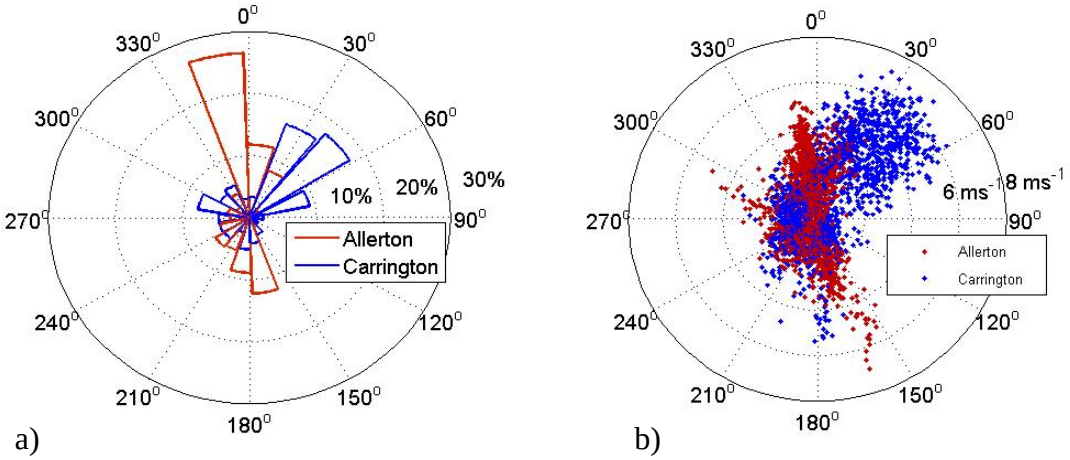

Figure 30 Measured wind direction distribution at Carrington industrial site (blue) and Allerton multi-storey urban rooftop in the period from 9/4/2010 until 10/5/2010. a) Wind direction histogram, b) Polar scatter plot of 10 min average wind speed values.

Turbulence has been assessed to predict aerodynamic turbulent inflow noise. This type of noise changes character depending on the ratio of blade chord dimension to turbulence scale. If the blade chord is small in comparison to atmospheric turbulence scales then the turbulence is expected to be a low frequency noise (dominant for BMWTs) and vice versa (Wagner et al. 1996). Therefore the scale spectra are the characteristic turbulence parameters. However there is a lot of discussion about how turbulence can reasonably be described and realistically measured and about what needs to be known to describe turbulence induced noise. The turbulence parameter that is commonly used to predict turbulent inflow noise is turbulence intensity which does not take account of the scale of the turbulence (Hansen 2008).

Turbulence intensity is defined as standard deviation divided by mean flow which can be measured by sonic anemometer instrumentation. This parameter is plotted in Figure 31 using 10 minute values to include all relevant scales of turbulence that impact on the BMWT. The Figure shows that the turbulence distribution is skewed towards lower values at Carrington and toward higher values at Allerton. Unlike the wind speeds the turbulence intensities do not follow a Weibull distribution.

Another measure to describe this behaviour is the so called roughness length. The rougher the terrain, the higher are the expected turbulence intensities. Roughness length is tabulated in the literature to be roughly 0.4 m for suburban or industrial areas and 2 m in urban areas with at least 15% of the buildings taller than 15m (Sockel 1994). These values can be verified by the sonic anemometer measurements however

there is one parameter that is very difficult to derive for a heterogeneous environment like the Allerton site and that is the average canopy height above which the logarithmic wind profile starts to develop (Kaimal and Finnigan 1994). The roughness length derived from the measurements at Allerton could therefore easily be between 3 and 9m. At Carrington it is much easier to define and is estimated to be about 0.5m. The values for both sites are roughly in agreement with the literature. In terms of turbulence Carrington can therefore claim to be characteristic for a suburban/industrial site whereas Allerton is more typical for an inner city site.

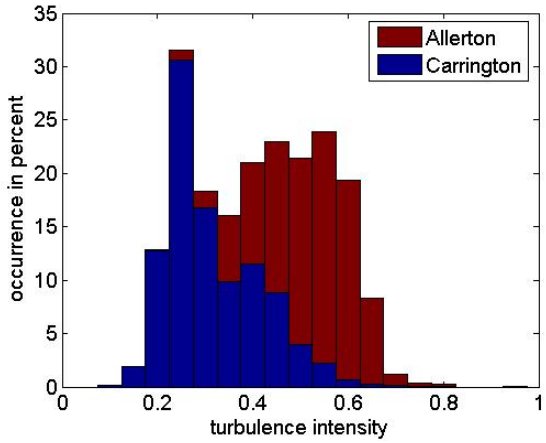

Figure 31 Distribution of measured 10 minute turbulence intensities at Carrington industrial site (blue) and on Allerton urban rooftop.

One interesting question is how the turbulence intensities scale with wind speed because it is plausible that high turbulence levels at high wind speeds might excite considerable vibration in a BMWT. In Figure 32 it can be seen that turbulence intensities show a weak negative correlation with wind speed. Also the spread of turbulence intensities increases towards lower wind speeds with some unrealistically high levels at very low wind speeds which might be due to measurement errors. It is apparent that the spread of turbulence intensities is higher at the Allerton site for all wind speeds. This could be another characteristic behaviour of urban sites.

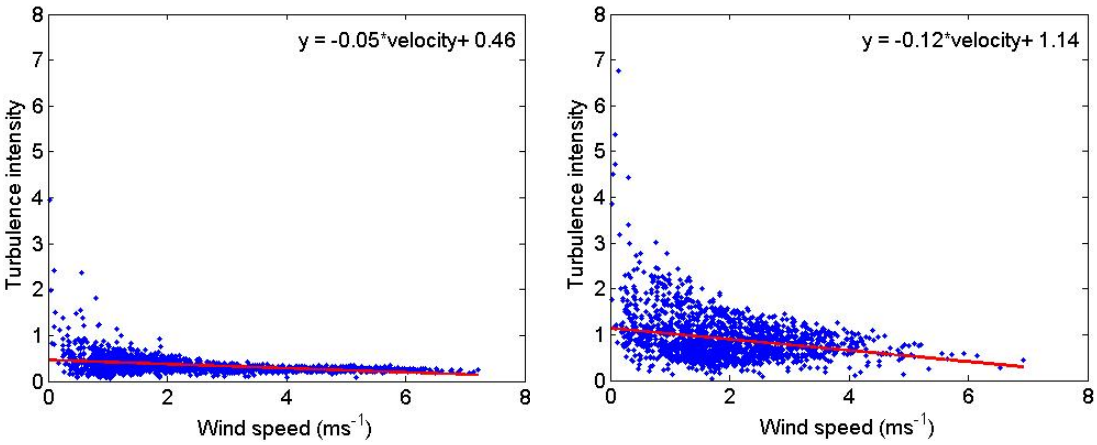

Figure 32 Correlation between wind speed and turbulence intensity for Allerton urban rooftop is obviously negative and can be approximated by a linear regression for wind speeds of 0.2 ms^{-1} and above. Left: Carrington industrial site. Right: Allerton multi-storey urban rooftop

Figure 33 is another way of showing that the highest turbulence levels occur at low wind speed. It adds the information about directivity: The directional spread of low wind speed values is large whereas at higher wind speeds the turbulence intensities are directionally much better aligned. This is true for both Carrington and Allerton. Additionally a "shadow sector" becomes apparent between 60° and 150°for the Allerton site.

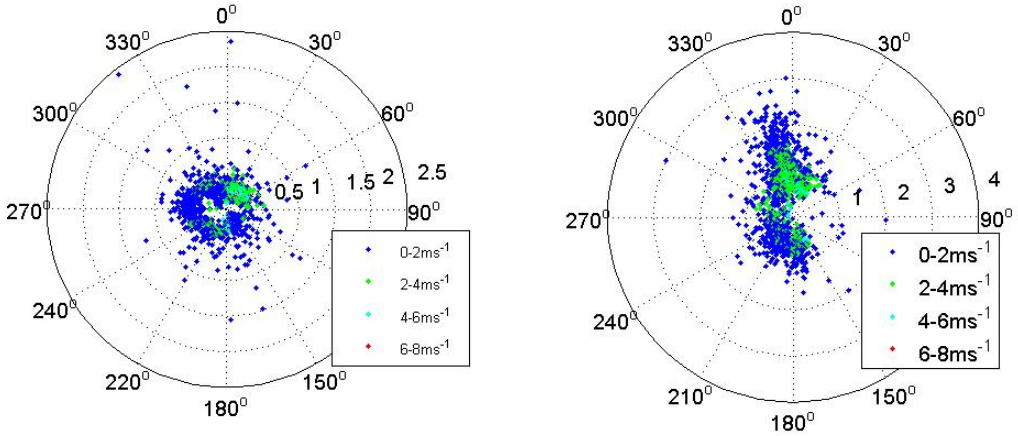

Figure 33 Measured polar scatter plots of turbulence intensity in 10 minute averaging intervals in the period from 9/4/2010 until 10/5/2010. Left: Carrington industrial site. Right: Allerton multi-storey urban rooftop.

For vibration excitation another important parameter might be the variability of the wind direction. It is a well known phenomenon that low wind speeds coincide with large direction changes as seen in Figure 34. For vibration excitation this is irrelevant

as rotational speeds at those wind speeds are going to be very small and potentially turbine inertia has stopped the blades from rotation altogether.

In contrast to the behaviour of the turbulence intensities the wind direction changes have been observed to be large at high wind speeds. Like in Figure 33 the direction changes at high wind speeds occur in well aligned narrow sectors of general wind direction. Wind direction changes could therefore be an influential factor in vibration excitation. Larger wind direction changes at high wind speeds have been observed at Carrington than at Allerton which should allow sufficient conclusions of the importance of wind direction changes on vibration.

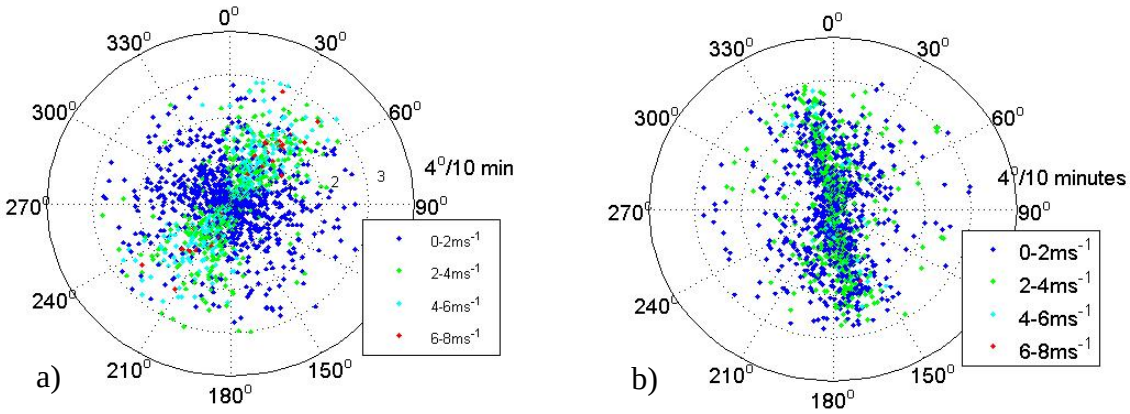

Figure 34 Measured polar scatter plots of wind direction changes from one 10 minute averaging interval to the next in the period from 9/4/2010 until 10/5/2010. Left: Carrington industrial site. Right: Allerton multi-storey urban rooftop.

4.5 Conclusions

In chapter 3 of this report we succeeded in relating MWT source strength to rotor speed in a fairly general way. In this chapter we have attempted to correlate source strength (and the resulting sound levels) directly with wind speed. However, this has proved more difficult, not because of the sound and vibration aspects of the MWTs, but because the relationship between rotational speed and wind speed is complicated and non-linear. It has therefore been necessary to use statistical relationships derived from data measured on site. Using this approach it has been possible to express the distribution of $L_{Aeq,\ 5\ minutes}$ for three specific distributions of wind speed. Since the rotor speed cannot at this stage be described as a mathematical function of wind speed it is not advisable to extrapolate these results to higher or lower wind speeds. Therefore at this stage, the predictions of $L_{Aeq,\ 5\ minutes}$ from wind speed are strictly only valid for the test site, or at least for sites with similar wind conditions and needs to be used with appropriate caution.

One of the concerns about turbulence is that rapid wind speed and direction changes could generate vibration. Therefore we have examined the correlation of turbulence and rotational speed which turns out to be negative i.e. the highest turbulence intensities occur at low rotational speeds. This suggests that the highest noise and vibration levels probably do not occur under the most turbulent conditions, as measured by the turbulence intensity. However, the standard turbulence parameters are not well adapted to the purpose and we have therefore carried out an analysis using a novel parameter, the rate of change of wind velocity which gives more emphasis to wind speed and direction changes at high wind speeds. This analysis shows that this unconventional turbulence measure does not have a strong influence on rotational speed.

Additionally in this Section a comparison has been made of wind conditions at the (rural/ industrial) test site with those at an urban roof-top site in order to confirm that the types of conditions found on the test site were reasonably representative of other sites. Simultaneous recordings of wind conditions were made at both sites over a period of one month. It was shown that Weibull distributions of wind speed obtained from both sites were similar. At the urban roof-top site higher turbulence intensities were obtained. However, since higher turbulence is associated with lower wind speeds and lower rotation speeds it does not seem likely that turbulence will be the dominant factor in structure-borne noise.

5 Transmission of structure-borne sound through mounting systems

In the two previous chapters we have considered the MWT itself as the source of structure-borne sound and vibration. In this chapter we look at mounting systems and, in particular, how they transmit structure-borne sound and vibration generated by the source into the building structure. Different designs of mounting can transmit more or less structure-borne sound and the main aim of this chapter is to quantify this effect, in other words to characterise mounting systems in terms of the transmission of structure-borne sound and vibration. This will be done by measurement of the 'transmissibility' of the mounts in laboratory tests, supplemented by analysis using a simple mathematical model.

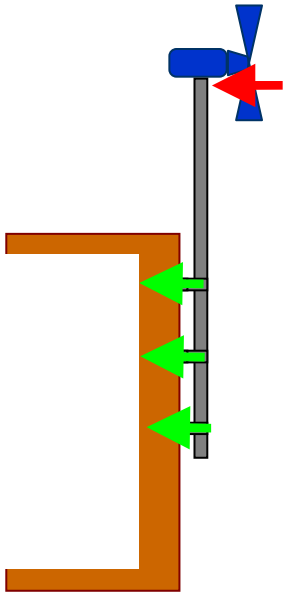

Figure 35: Schematic of wall-mounting system showing force applied at the top of the mast and the resulting forces acting on the wall of the building.

There are two main classes of mounting systems, roof-mount and the wall-mount as illustrated in Figure 35. Wall-mounting systems typically comprise a cylindrical pole connected to a wall via 2-4 mounting brackets, the MWT is connected to the top of the pole as illustrated in Figure 35. Wall-mounting systems come in a wide range of configurations with variations in the pole length, numbers of bracket and bracket spacing all potentially having an effect on the transmission of structure borne sound. Roof-mounting systems are less common and also show less variation, being typically provided in kit form.

A large number of measurements would be required to investigate the whole range of possible configurations for wall-mounts. Therefore, a more efficient approach has been adopted in which a simple mathematical model has been developed, the parameters of which can be changed easily so as to allow a wide range of configurations to be investigated. Development of the model is described in section 5.4. The results of an analysis are reported in section 5.5 in which sensitivity of the mast transmission properties to variations in mast length, bracket spacing etc. is investigated.

5.1 Measurement method

The quantity to be measured is the transmissibility. Transmissibility is a familiar concept in noise and vibration control being commonly used to describe the performance of resilient anti-vibration mounts. It is defined as the ratio of velocity (or acceleration) at the top of the mount to that at the bottom when the mount is excited from below.

In the case of a MWT mounting, the 'top' of the mast is defined as the point at which the MWT is connected to the mast. However, as discussed in chapter 3, it is necessary to account for velocity in the x, y and z velocities at this position, together with the rotational velocities. The 'bottom' of the mounting is defined as the points on the brackets which attach to the building.; there were two or three such points on the masts tested and it will be shown later in the report that data was required for all such points. Therefore, the usual concept of transmissibility needs to be extended to allow for the fact that more than one degree of freedom[1] is required at the top and bottom of the mounting. This extension has been achieved by using a matrix representation as described below.

The test is conducted by suspending the mast, complete with the attached MWT, on resilient hangers. The attachment points on the brackets are then struck with a force hammer as shown in Figure 36 while the velocity per unit excitation force (also called the mobility) at the top and bottom locations is measured. The mobilities at the bottom of the mount are organised into a matrix ($\mathbf{Y_c}$) one column for each excitation position and each row representing a response location. A second matrix ($\mathbf{Y_b}$) is constructed from the mobilities at the top of the mount. The transmissibility is then calculated as the 'ratio' of the two matrices or $\mathbf{T} = \mathbf{Y_c^{-1}Y_b}$. The result of this calculation is a

[1] All positions and directions requiring measurement are known as 'degrees of freedom'

transmissibility matrix relating all degrees of freedom at the top of the mounting to all those at the bottom. For the purposes of prediction it proved necessary to retain all degrees of freedom.

Figure 36: Set up for testing of the mount transmissibilities. Left: force hammer and accelerometer. Right: mast in suspended position for testing.

5.2 Measurement results

In Figure 37 and Figure 38 are shown the transmissibility of the wall mounts for MWT1 and MWT2 (three different lengths of mast for each). Results for the MWT1 roof mounting are shown in Figure 39. Since multiple degrees of freedom are required for a full description of the mount behaviour it has been necessary to calculate an average for plotting. Thus, these figures do not show the full picture for any of the mounts but the plots serve to illustrate general trends in behaviour.

The most significant observation is that strong fluctuations are present in the wall-mount results. These are due to resonances in the mast which essentially behaves as a long beam. These resonances could produce strong variations in the transmitted structure-borne sound as the excitation from the MWT moves up and down in frequency with rotational speed. Fluctuations are less evident for the roof mounting.

For the MWT1 mast there is a general trend for the frequency-averaged transmissibility to increase as the free pole length increases. Also it can be noticed that the average transmissibility for the roof mount is lower than that for the wall mounts; broadly this means that we would expect greater attenuation from the roof mount.

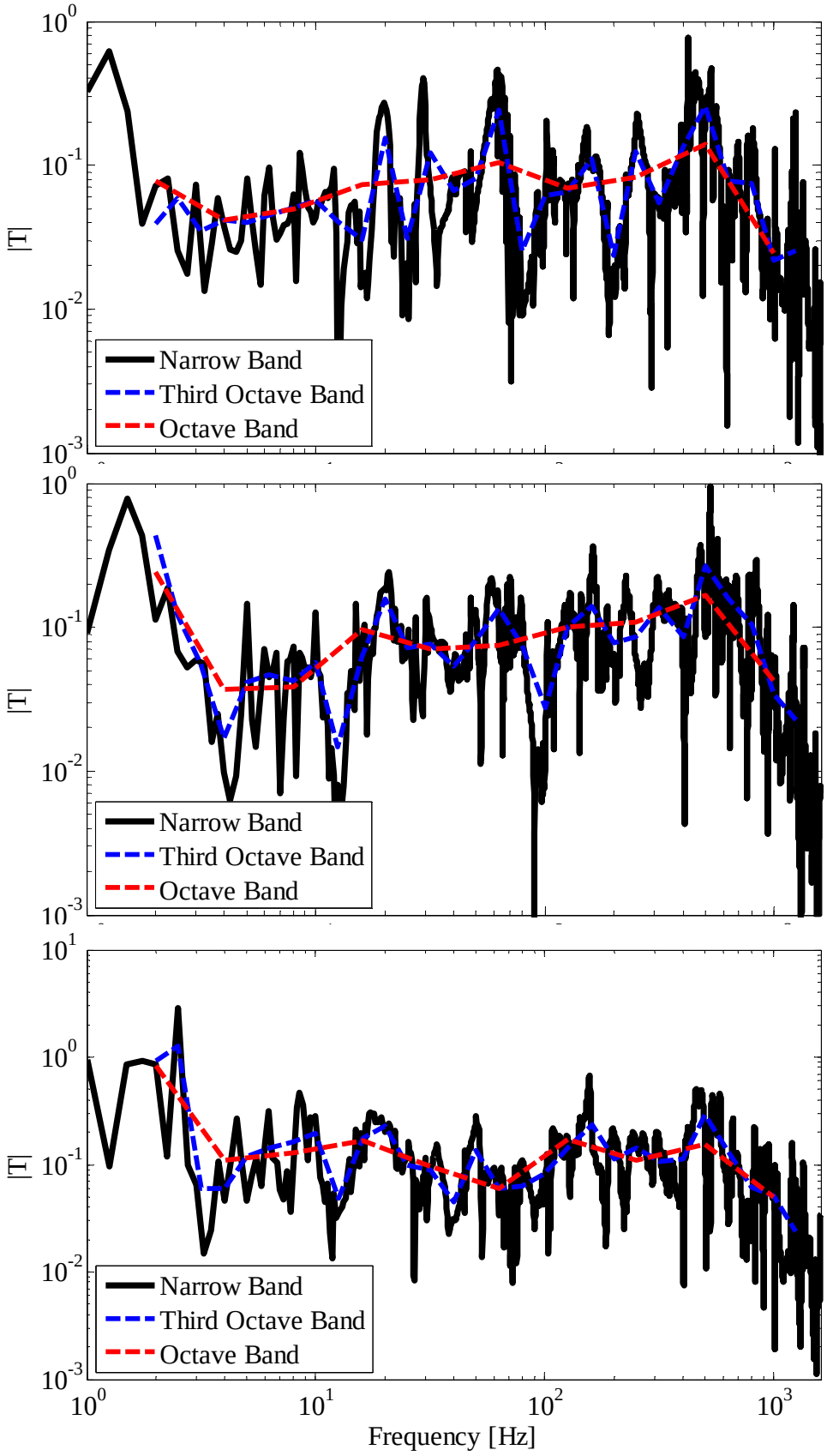

Figure 37: Mean transmissibility of wall mounts for MWT1 with free pole length from top to bottom: 2.2 m, 2.5 m, 2.9 m.

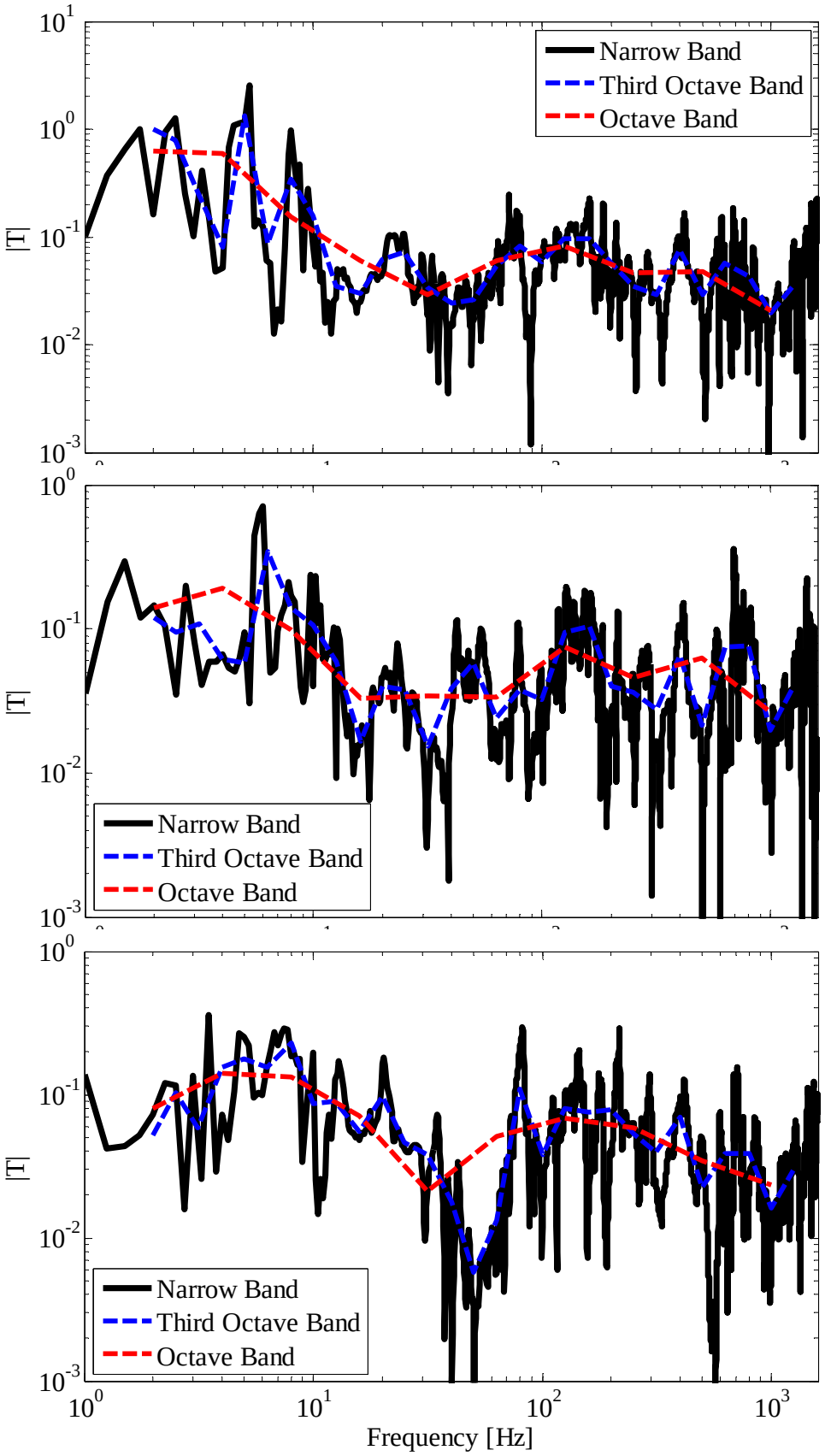

Figure 38: Mean transmissibility of wall mounts for MWT2 with free pole length from top to bottom: 1.5 m, 2.0 m, 2.44 m.

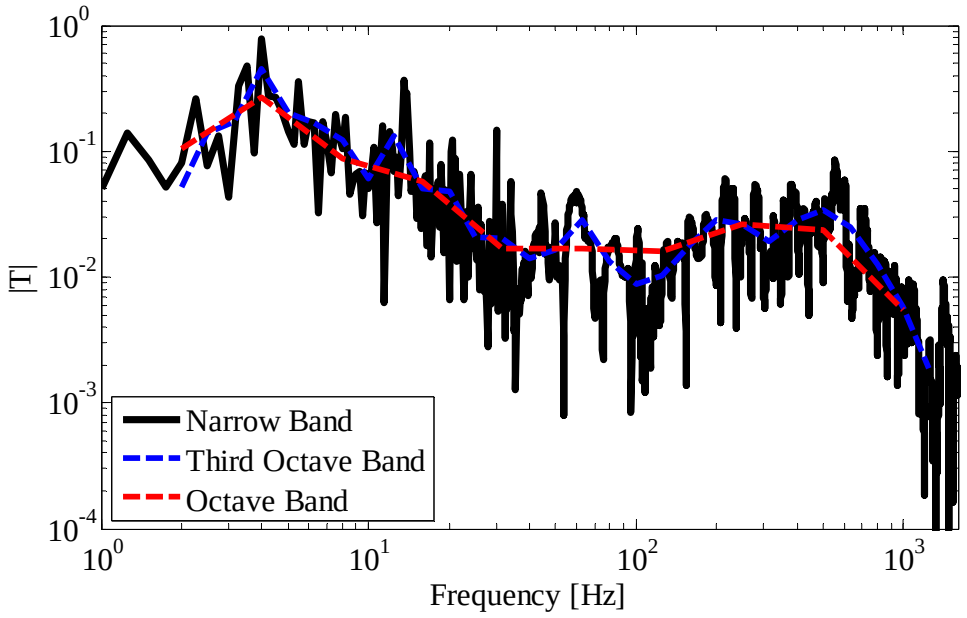

Figure 39: Mean transmissibility of roof mount for MWT1.

The differences due to mount length can be more clearly seen in Figure 40 which summarises results for MWT1. There are significant differences around 200 Hz where the predominant excitation occurs and these differences would be greater when plotted in narrow frequency bands. This indicates that we can expect some variation in the transmission of structure-borne sound depending on the length of the pole.

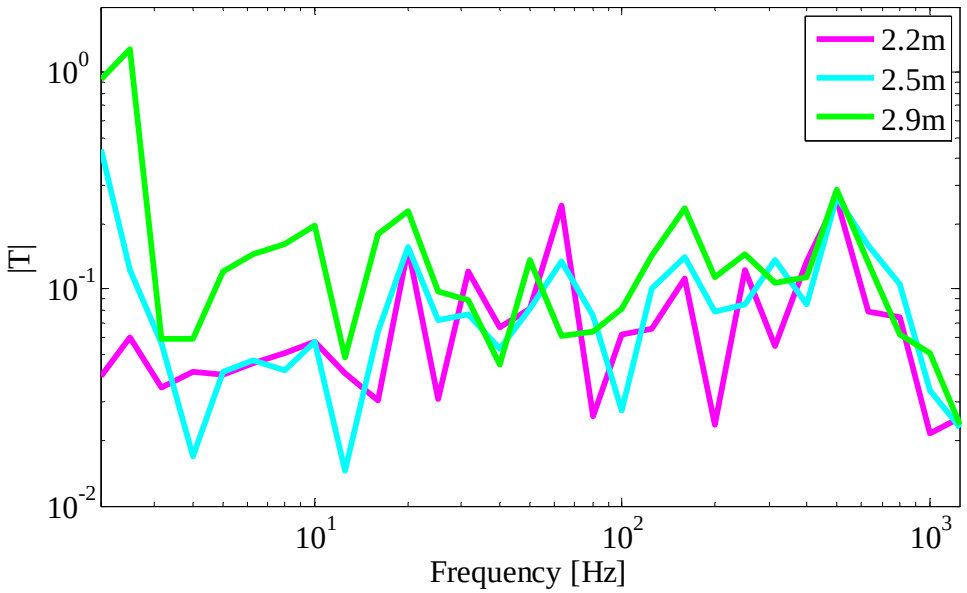

Figure 40: Mean transmissibility of roof mount for MWT1 for different mast lengths, shown in third octave bands.

Figure 41 emphasises the multiple degree of freedom nature of the problem. It shows averaged transmissibilities corresponding to x, y and z directions at the top of the mast. The plots are in third octave bands which omit some detail but allows trends to

be more easily seen. Transmissibilities for the z direction (vertical) tend to be somewhat lower than those for the horizontal directions indicating that transmission is less efficient. However, the importance of the three directions also depends on the amount of excitation in that direction. Again it may be mentioned that it has proved necessary to retain all degrees of freedom for the purposes of prediction.

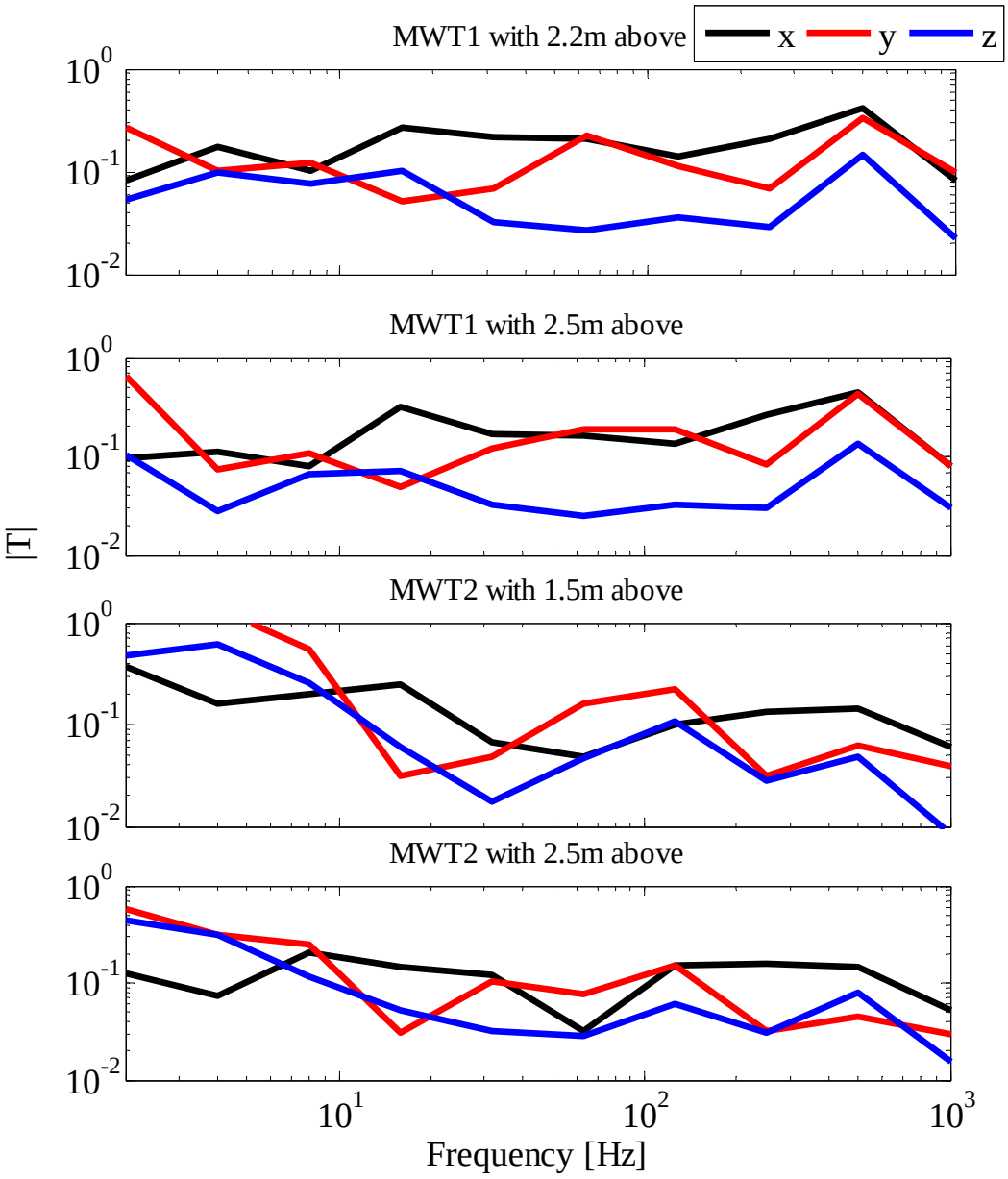

Figure 41: Mean transmissibility of roof mount for MWT1 for different mast lengths, shown in third octave bands.

5.3 Effect of mast on noise levels

As mentioned above the mount transmissibilities are strongly frequency-dependent, for example, stronger transmission will occur when an excitation frequency coincides with a resonance frequency.

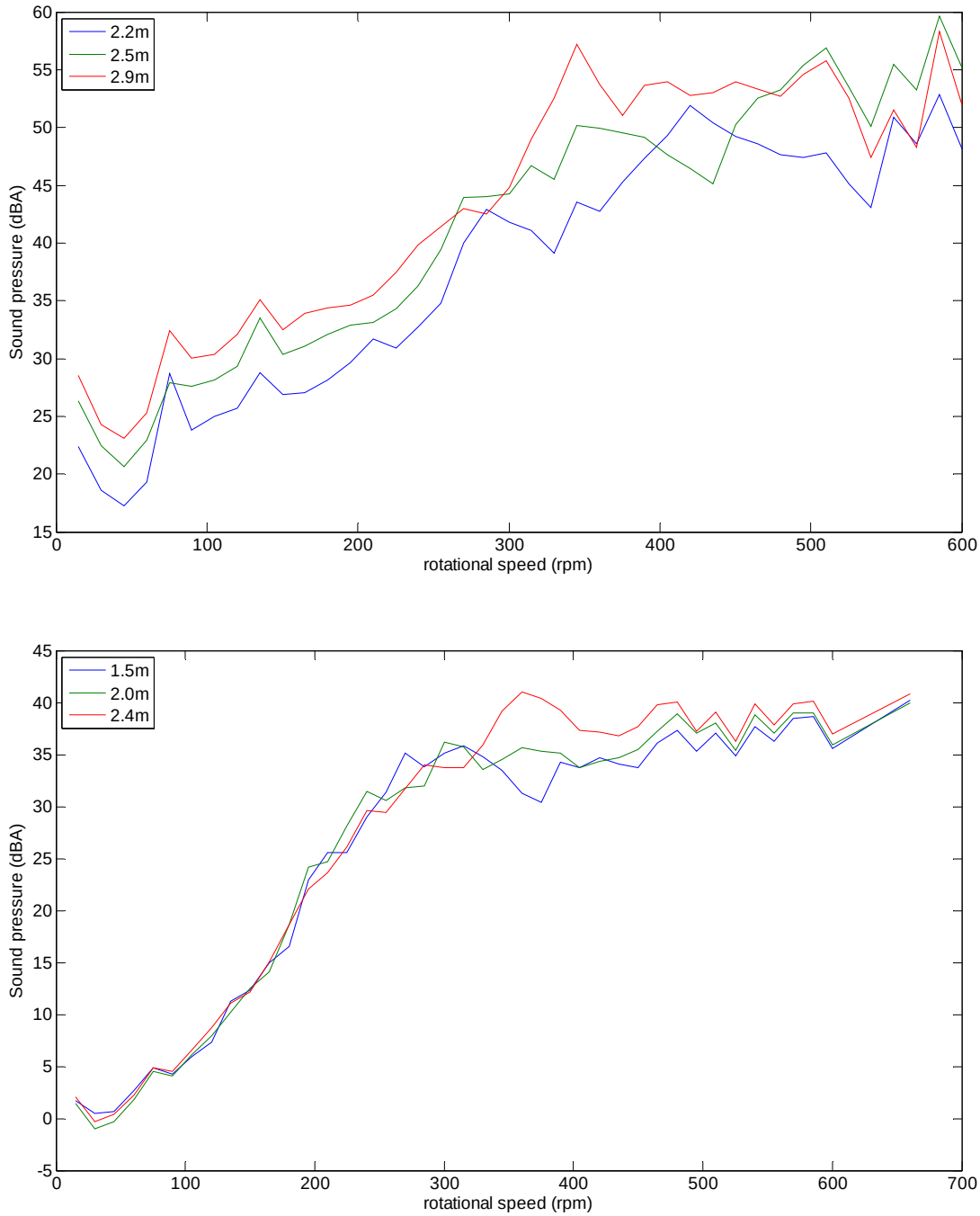

Figure 42: Sound pressure in the reference installation for three different mast lengths. Upper: MWT1. Lower: MWT2.

Therefore, in order to see the full effect we need to combine the transmissibility data with source strength data from chapter 3. We have therefore predicted the sound level in the reference installation (using a procedure described in chapter 7) for different mast lengths. Shown in Figure 42 are the A weighted sound pressure levels based on the dominant third octave bands (100 to 315 Hz) as a function of rotational speed. Significant differences are seen particularly around 300-350 rpm for MWT1. At these speeds the dominant excitation is in the region of 200 Hz which corresponds to the region identified in Figure 40 as subject to wide variations. Smaller, but still significant differences are seen for MWT2.

Shown in Figure 43 are the A weighted sound pressure levels as a function of rotational speed for MWT1 combined with the flat roof mounting system. Compared with Figure 42 this shows that the roof mount provides greater attenuation than the wall mount. If installed on a layer of resilient material, as is typical in order to protect the roof, a greater attenuation might be achieved.

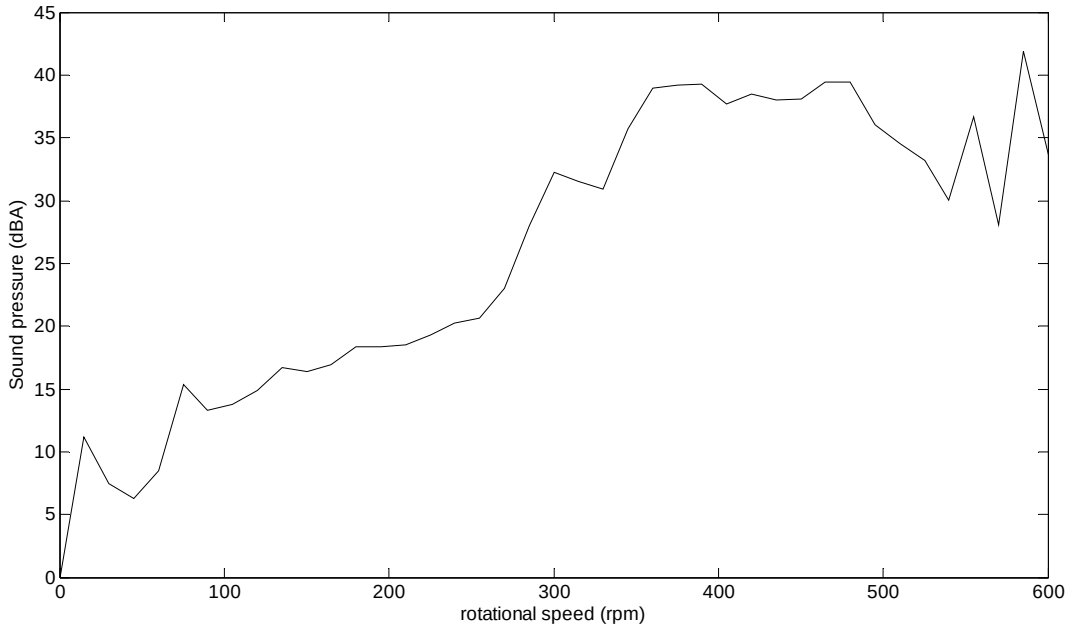

Figure 43: Sound pressure in the reference installation for the flat roof mount MWT1.

5.4 Simple model of wall mount

In this section an analytical model of the wall mounting system is introduced. The most reliable characterisation of a mounting system is through measurements along the lines of those reported above. However, a model can provide valuable insight into the behaviour as well as allowing more configurations to be considered.

Figure 44 shows a schematic of the modelled wall-mounting system. This system can

be modelled as a combination of three sub-components; a mass (to account for the mass of the turbine), a finite beam (pole) and springs (representing the stiffness of the brackets).

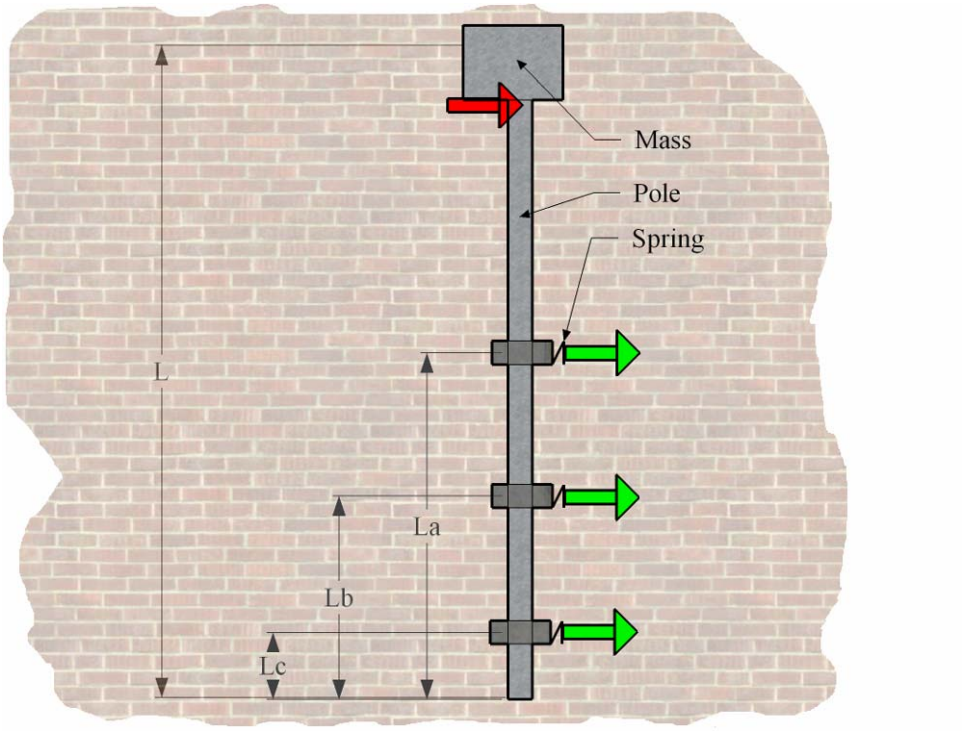

Figure 44: Schematic of wall-mounting system model.

Analytical models of the three sub-components are combined to form the complete model using the procedures for connecting lumped parameter one dimensional systems provided in (Gardonio and Brennan 2004) and the sub structuring methods described in (Elliott 2009).

The turbine is represented as a solid cuboid of a prescribed mass. The mobility of the mass is found at the point where it connects to the pole using the expression found in (Fulford and Gibbs 1999). The mass is attached at the bottom of the cuboid to the mounting pole via translational and rotational degrees of freedom. A finite Euler-Bernoulli beam (Gardonio and Brennan 2004) is used to model the mounting pole. The second area moment of a cylindrical tube is used and a mobility matrix is established describing the dynamics of the pole at the top and bottom of the mast.

To account for the stiffness introduced by the mount brackets, as well as the rubber collars used to grip the pole, springs are introduced whose stiffness is varied so as to

provide the best fit with measured data. Viscous damping is introduced into the stiffeners to account for the energy losses through the rubber collars. Expressions for the mobility of a spring and damper are found in (Gardonio and Brennan 2004).

In order to validate the model the mobilities and transmissibilities were calculated for one of the measured configurations and compared with the measured results. Figure 45 shows the mobility, i.e. the velocity at a point at the top due to a unit force excitation at a point on the bottom. It is not required or even intended that the agreement is exact since this would require a much more detailed model which would not provide the same insight. It is clear that the model captures the main trends in behaviour which is sufficient for the purposes of supplementing the measured results. Figure 46 shows the agreement in the transmissibility between the same two points. Again, a number of details are missing from the model but the general trends are comparable which is sufficient for our purposes.

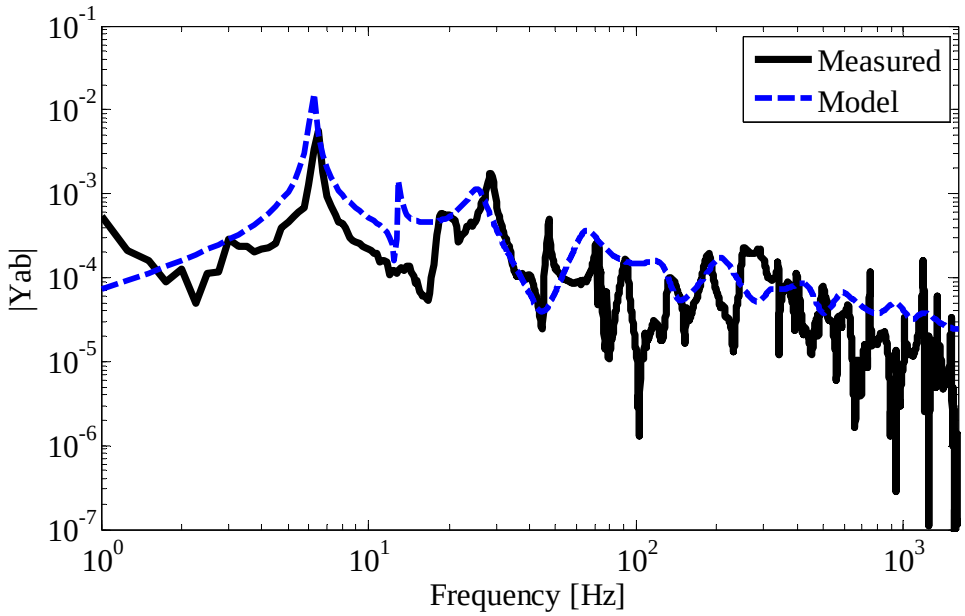

Figure 45: Comparison of measured and predicted mobility between top and bottom of the wall mount for MWT1 of length xx m.

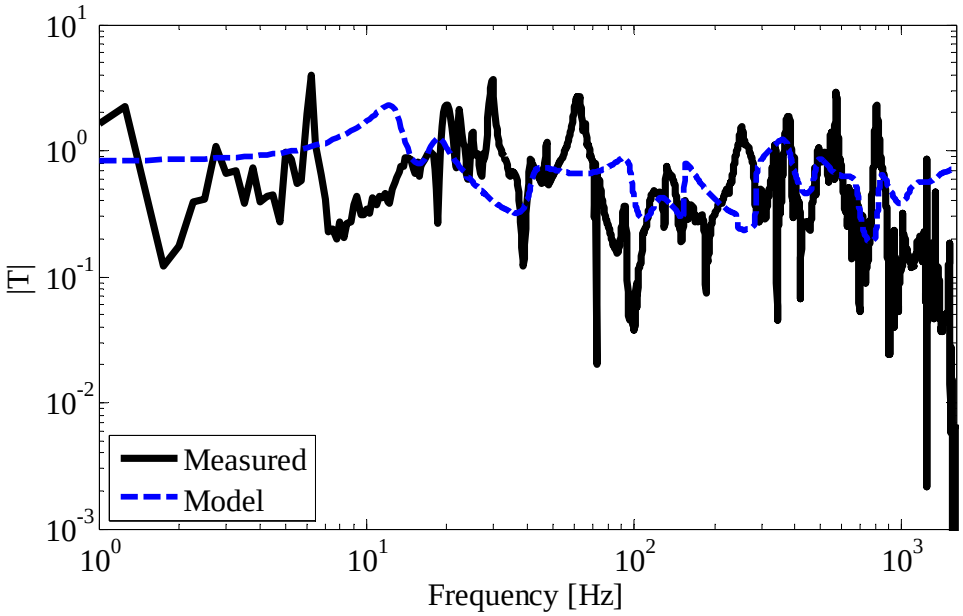

Figure 46: Comparison of measured and predicted transmissibility between top and bottom of the wall mount for MWT1 of length xx m.

5.5 Sensitivity analysis

Having developed the simple model it is relatively straightforward to vary the model parameters so as to determine the effect on the transmission of structure-borne sound. The effect of variations in bracket spacing and mast length are reported in this section.

To simulate variations in bracket spacing the position of the two lower brackets has been varied by ±0.35m. The position of top bracket is kept the same in order to maintain the same free pole length. In order to make the comparison we have calculated the sound pressure in a reference building due to a unit force at the top of the mount. This prediction is not a 'real' prediction of sound levels from the turbine but provides a basis for comparing different configurations. Results, shown in Figure 47 indicate that the standard deviation could be as high as 3-4 dB for variations in bracket spacing. These results are given in third octave bands, which obscure some detail but allows trends to be more clearly seen.

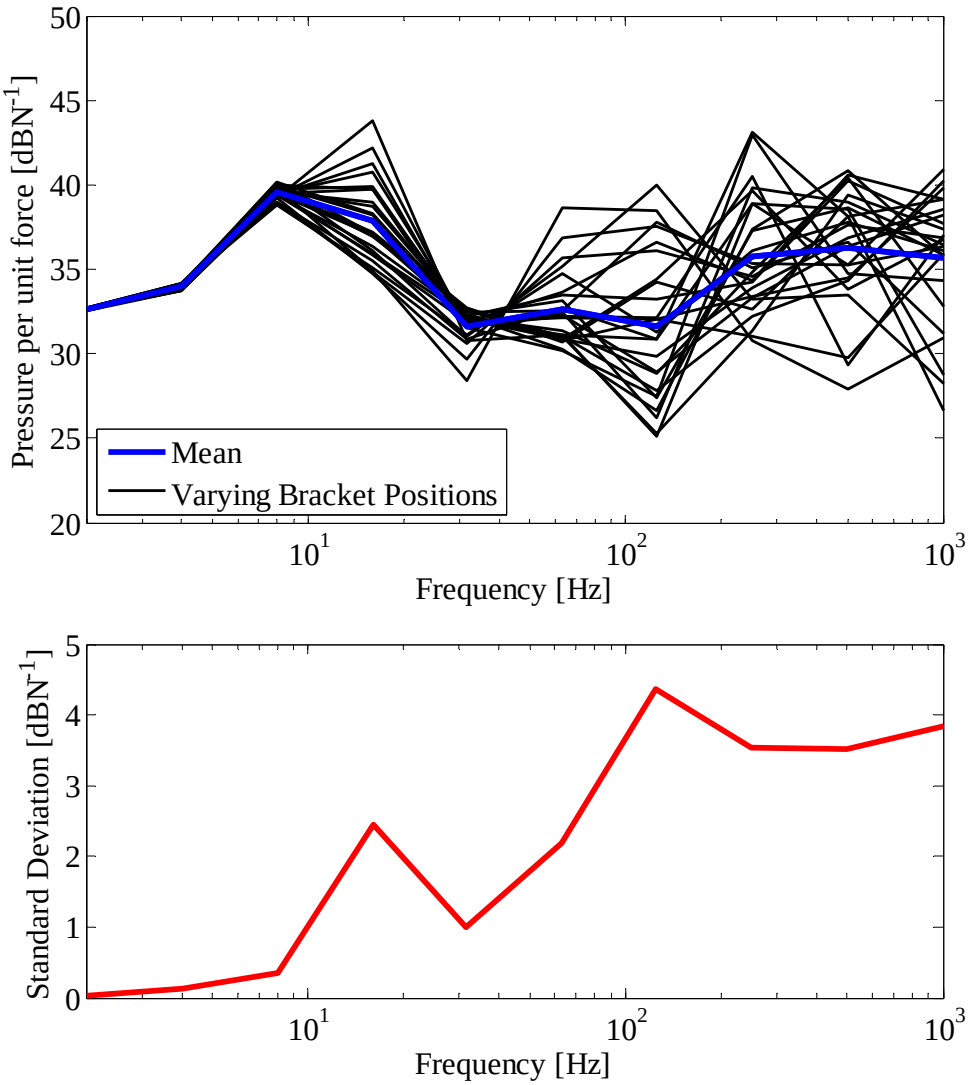

Figure 47: Effect of varying bracket position of MWT1 wall-mount given in octave bands. Upper: sound pressure level in a reference building with different bracket spacings. Lower: standard deviation.

A similar exercise was conducted to investigate the effect of variations in pole length. The results are shown in Figure 48. Again, differences are observed. Focussing on the region around 200 Hz, the standard deviation is around 2 dB which means that the 95% confidence limits would be expected to be ±4 dB. These differences are of a similar magnitude to those from Figure 37. Again, the implication is that differences could arise due to variations in pole length.

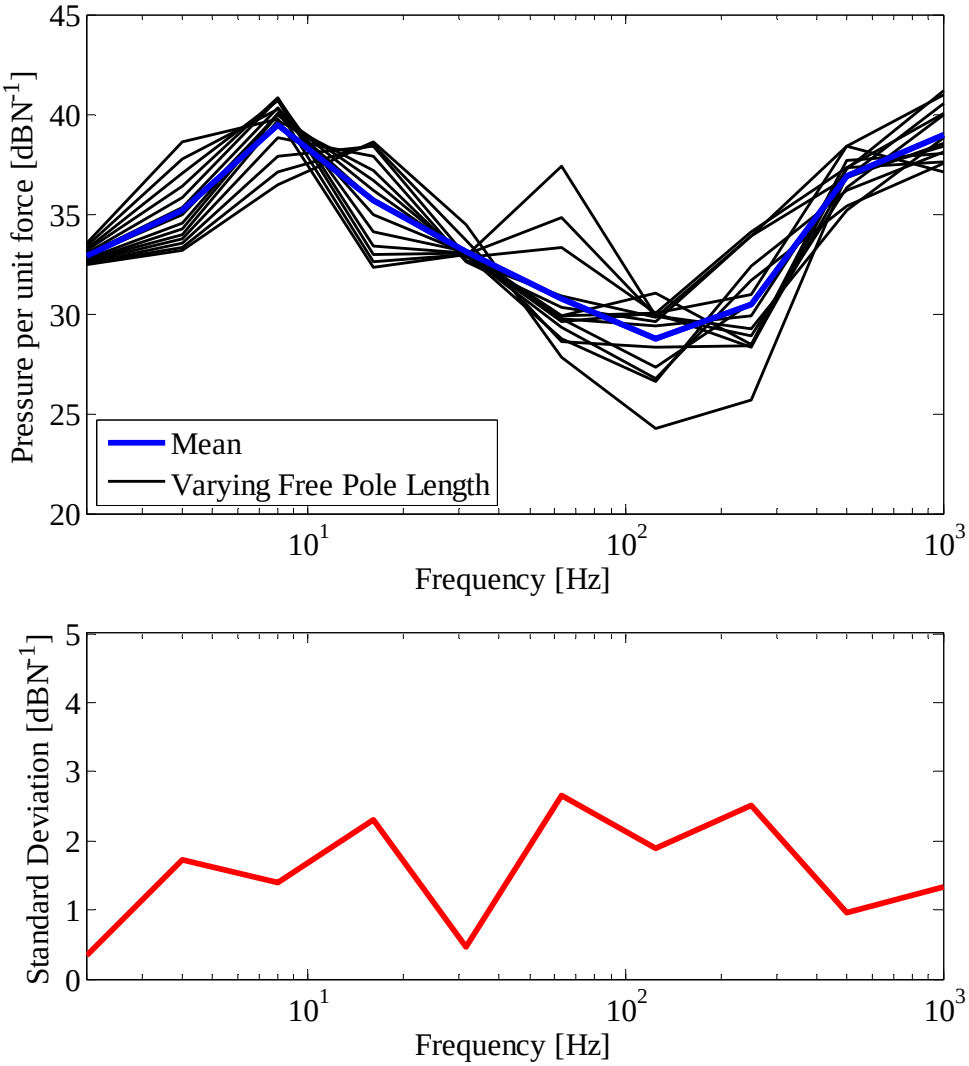

Figure 48: Effect of varying free pole length of MWT1 wall-mount given in octave bands. Upper: sound pressure level in a reference building with different pole lengths. Lower: standard deviation.

5.6 Conclusions

The transmission of structure-borne sound through mounting systems is a ‘multiple degree of freedom problem’, meaning that it is necessary to account for the vibration at various points at the top and bottom of the mount and to consider several directions of vibration simultaneously. The mount properties have therefore been characterised by a matrix of transmissibilities. In order to display the results, an average has been taken which does not include full detail but nevertheless allows some of the general trends in behaviour to be seen.

The transmissibilities of wall mounts show strong fluctuations with frequency due to mast resonances. These will tend to make the transmission frequency-dependent, i.e. the transmission could be more efficient at some rotational speeds than others. We also expect that differences of a few dB could result from variations in bracket spacing and pole length from site to site.

The roof mount investigated is expected to produce slightly larger attenuation than for wall mounts.

6 Transmission of structure-borne sound through buildings

Having evaluated source strength of the MWT in chapters 3and 4 and the properties of mountings in chapter 5, the aim of this chapter is to evaluate the properties of building structures that affect the input and transmission of structure-borne sound and vibration throughout buildings. The relevant properties are:

- The vibro-acoustic transfer function[2] from external wall to internal rooms.
- The vibration transfer function (measured as transfer mobilities).
- Mobility of the wall at the point of excitation.

Estimates of the vibro-acoustic transfer functions are required to feed into the prediction model so as to quantify the effect of the building construction and layout on the transmission of sound and vibration. Vibration transfer function measurements were made but are not analysed in detail here since, from the field trials reported in chapter 7, the main priority is structure-borne sound, rather than tactile vibration.

Although tables and databases of measured data for airborne and impact sound insulation properties of buildings are widely available, the same cannot be said for these structure-borne sound properties. Neither can these properties be easily predicted as discussed in Part 1; Although a standard is now available (EN12354-5) this has not to date been widely tested and is known to have limited accuracy at low frequencies. For these reasons it was considered advisable to obtain a set of measurements of the above properties for a range of building types. The resulting measurement survey and results are described in the following. The survey has focussed on obtaining a representative set of measurements for masonry constructions including solid brick, cavity brick and stone. Other structural types have not been included since, as described in Part 1, their properties are expected to vary widely which makes it difficult to generalise the results for use in a prediction model. However, it should be noted that the prediction method can still be applied to such constructions by using input data obtained from measurements, calculations or other estimates specific to the construction in question.

From the survey data a set of properties suitable for a reference installation will be derived. These will then be used to calculate the sound and vibration levels in the reference installation. A set of correction factors will then be derived so as to allow

[2] Strictly speaking the correct term is ‘frequency response function’ but ‘transfer function’ is much more commonly used and will be employed here.

the levels to be estimated in buildings of different construction and layout.

6.1 Measurement setup and procedure

The building transfer function measurements were carried out using the 'Bruel & Kjaer PULSE platform for noise and vibration analysis'. The pulse system has 5 channel inputs and data is logged directly to a laptop computer via ethernet cable. A force hammer was used to excite the external wall whilst simultaneous measurements of acceleration and sound pressure were made both on the internal surface of the wall and inside the building: Four accelerometers were used and four microphones in the room. The force hammer has changeable tips which have different frequency responses. There is a soft tip and a hard tip, the soft tip gives better low frequency response and the hard tip gives better high frequency response. Therefore for all the vibration transfer function measurements the soft tip was used and for all vibro-acoustic transfer function measurements the hard tip was used.

Two excitation points were chosen on the wall, at a point approximately 1m from the floor junction vertically and approximately 1m from the internal room junction, horizontally. The points chosen were dependent on the room size being tested. The two points were never in the same plane and never closer than 1m from any junction.

The mobility measurements were carried out using two accelerometers attached to the wall using beeswax and spaced approximately 200mm apart. The accelerometers were attached as securely as possible ensuring there was no 'play' in the wax, pushed hard on to the wall so the wax is holding fast and there is contact between the wall and accelerometer. Then the force hammer was used to impact between the two accelerometers five times at each location. The measurement setup has some similarities to that shown in Figure 36 but a much heavier hammer is used.

At the same time the internal velocity was also measured at two points of attachment to the same wall but internally. Therefore a vibration transfer function was formed using the recorded external force and the recorded internal velocity response.

The next step in the testing was to record the vibro-acoustic transfer functions which involved the four microphones being setup in the room of interest. The force hammer was again used to excite the wall externally at the chosen points on the wall. Five impacts and internal responses were recorded for each excitation point. These multiple impacts and responses were combined to give a spatially averaged vibro-acoustic transfer function.

6.2 Test sites

Test site details are summarised in Table 3 and further details, including sketches of each site are given in the appendix at the end of the report.

Table 3: Summary of test site details

Site	Construction Type	Building Type	Wall Thickness
Site 1	Brick Cavity	Detached	31cm with 7-8 cm cavity
Site 2a	Brick Cavity	3 storey flats	31cm with 7-8 cm cavity
Site 2b	Brick Cavity	3 storey flats	31cm with 7-8 cm cavity
Site 3	Brick Cavity with ties	3 storey flats	23cm with 3cm cavity
Site 4	Brick Cavity	Semi Detached	31cm with 10 cm cavity
Site 5	Solid brick and mortar with 4cm of render	Detached	23cm brick and ~ 4cm of render
Site 6	Large stone with lime render	Detached	~ 45cm

6.3 Wall mobility results

Mobility is important because it determines the vibrational power input resulting from an applied force. Measured wall mobilities are shown in Figure 49 in narrow band frequency resolution. In Figure 50 the same results are shown but in octave bands which allows the curves to be more easily distinguished. It can be seen that despite the differences between the constructions the wall mobilities lie within a relatively narrow range around 10^{-5} m/s/N. This was expected from the analysis in Part 1 where it was described that masonry walls tend to behave similarly to infinite plates of corresponding mass and thickness. In general the higher mobilities are for the cavity brick constructions and the lower values for solid brick and stone. Again this is expected because the outer wall of the cavity, which responds to the hammer blow in the tests, is effectively a half-brick thick plate whereas the solid brick constructions are twice as thick and the stone wall slightly thicker still. The inner leaf of the cavity would not be expected to have a strong influence on the mobility unless the excitation point was close to a wall tie.

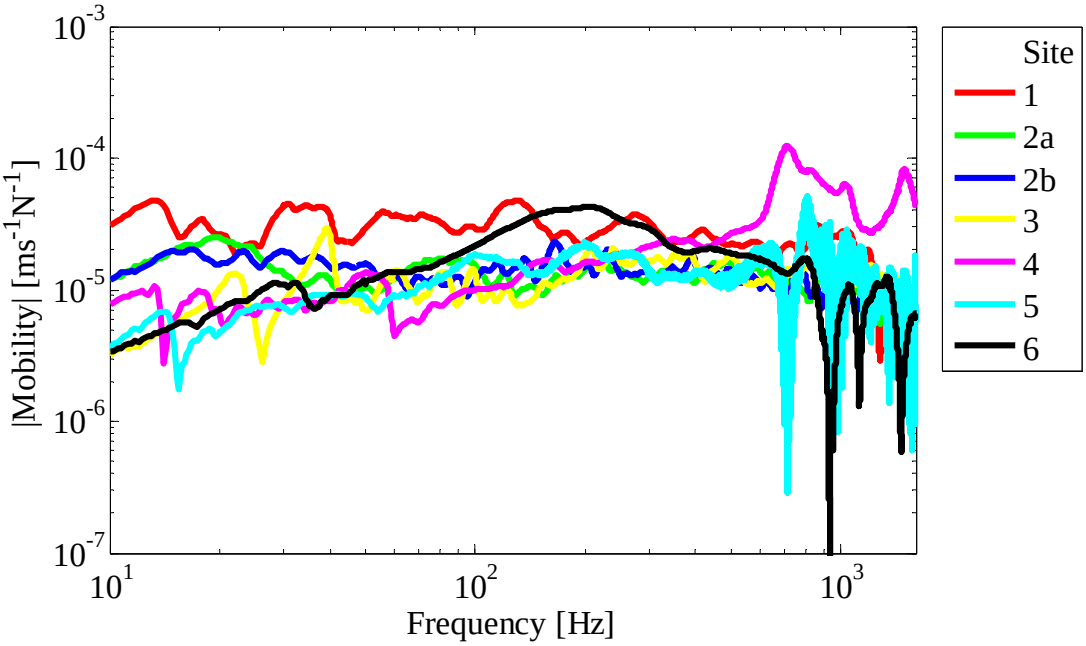

Figure 49: Point mobilities on external wall.

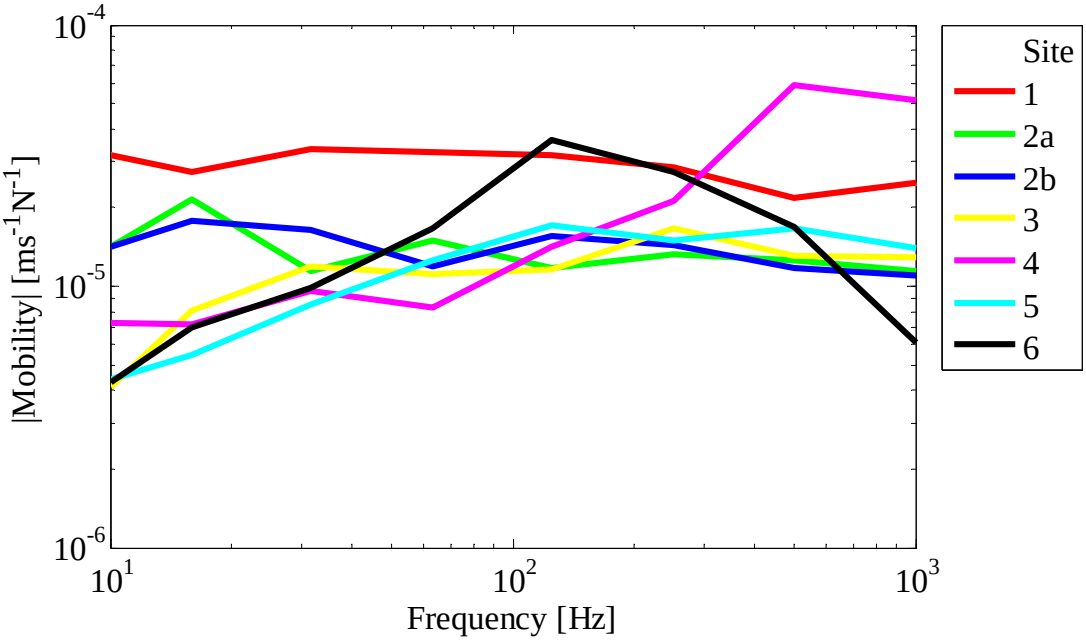

Figure 50: Point mobilities on external wall in octave bands.

6.4 Vibro-acoustic transfer functions to most exposed room

Vibro-acoustic transfer functions are measured by striking the wall with the impact hammer and measuring the sound pressure in a room. The transfer functions are displayed in units described as dB/N[3] which numerically equals the sound pressure

[3] This form of units is fairly widely used for vibro-acoustic transfer functions but mixes linear and dB dimensions so requires care for correct interpretation. It should not be thought of as 'dB per N', but

level which would be obtained with an exciting force of 1N at each frequency. The results shown in Figure 51 give an idea of the repeatability and variation from one excitation position to another. All these curves were obtained from the average of four microphone positions in the room.

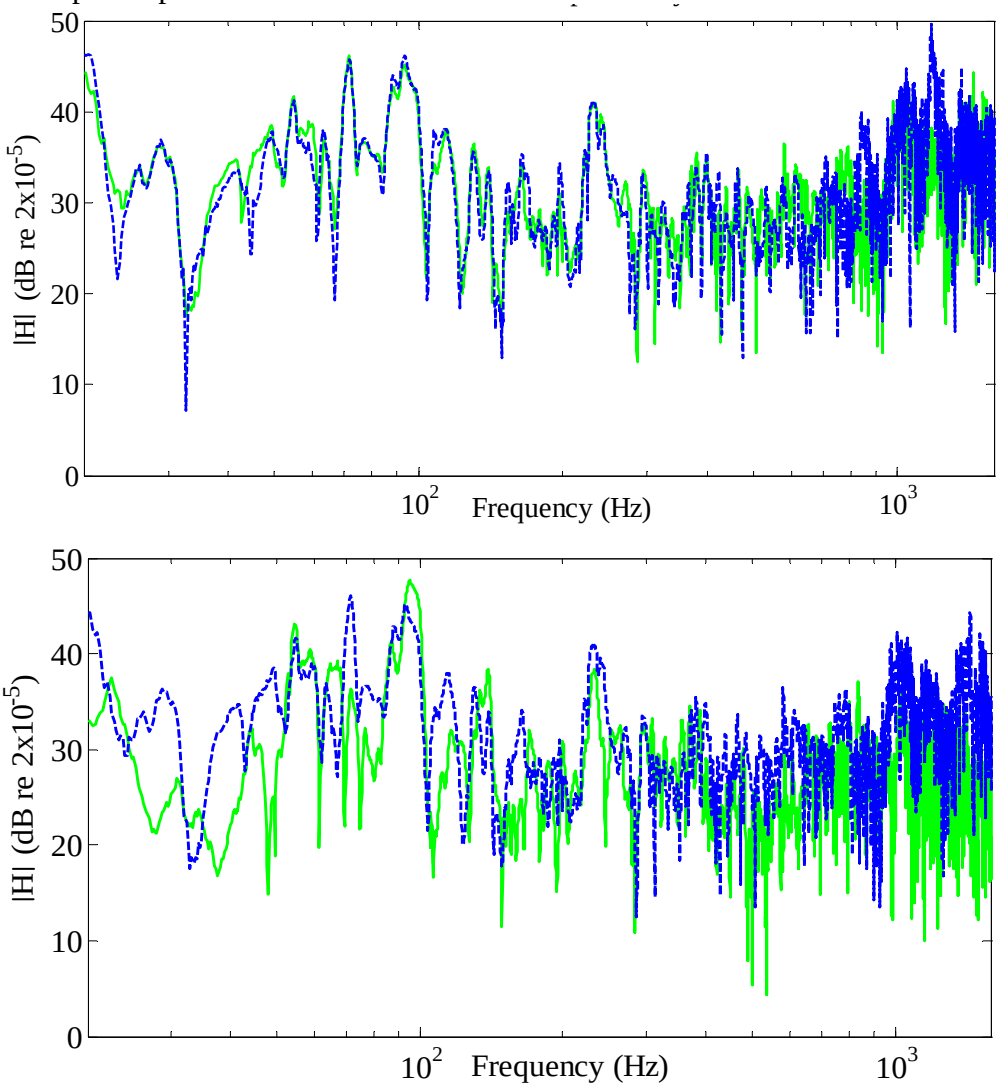

Figure 51: Magnitude of vibro acoustic transfer function averaged over several hits. Upper - repeatability. Lower- results for two different excitation positions.

Shown in Figure 52 are the transfer functions from a point on the façade to the room immediately behind the excitation point. Each curve is the average obtained from two excitation positions and for each position the signals from four microphone positions in the room were averaged. Curves for all test sites are shown on the same plot so as to provide an indication of the spread of the results. The same results are also shown in Figure 53 in octave bands from which it is easier to distinguish individual curves.

---

rather as the sound pressure level that would result from a 1 N input in a given frequency band.

The highest curve shown in Figure 53 (for site 3) illustrates different behaviour to the remainder of the curves. The other curves can arguably be formed into two groups: sites 4 and 5 show similar trends with transfer functions of the order of 40dB/ N across the range. These sites are both solid brick constructions. The remaining curves, for sites 1, 2a, 2b and 6, also show similar trends above 50 Hz with lower transfer functions of the order of 30 dB at 200 Hz. This group includes three cavity brick constructions (sites 1, 2a and 2b). Interestingly, it also includes the stone construction.

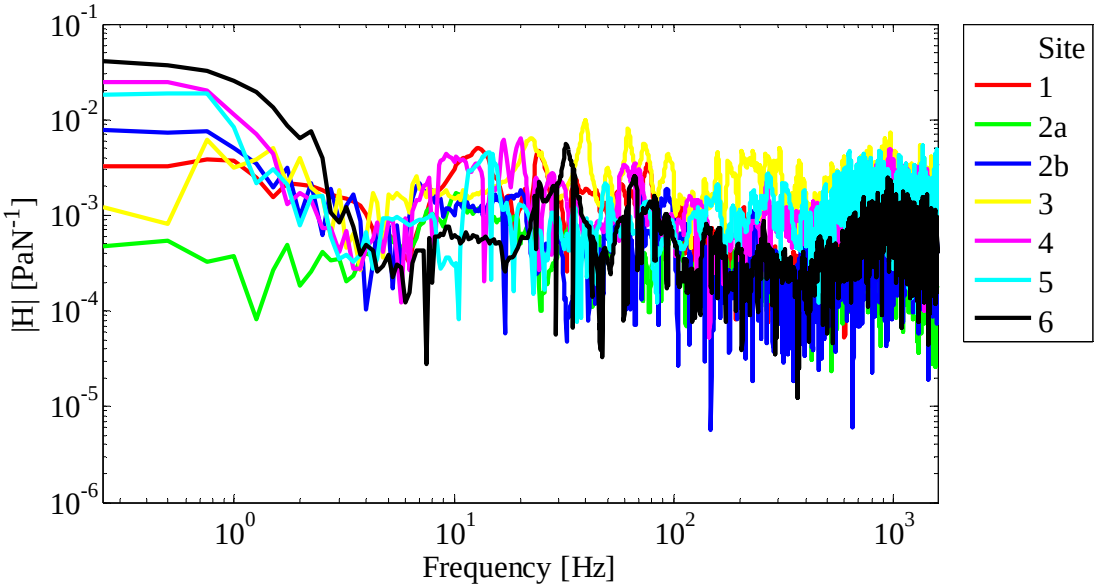

Figure 52: Narrow band spatially averaged vibro-acoustic transfer functions for various constructions.

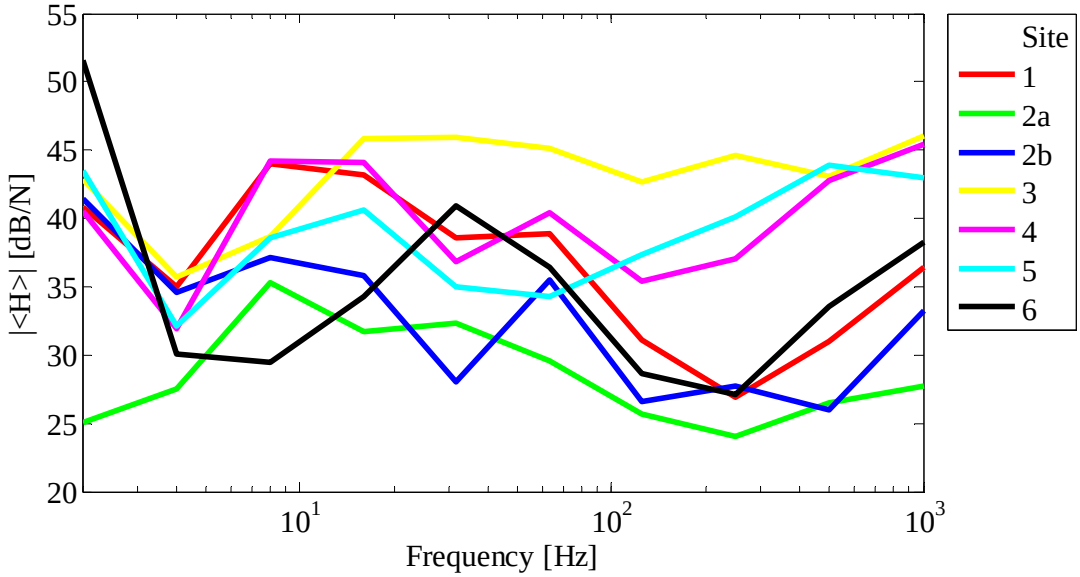

Figure 53: Octave band spatially averaged vibro-acoustic transfer functions for various constructions.

The results from these two groups have been averaged and the results are shown in

Figure 54. The 95% confidence limits, obtained from a student T test, are also plotted. The results from these curves are also tabulated in Table 4 and Table 5. In broad terms these groups can be interpreted as being representative of cavity and solid brick respectively as shown in Figure 54. Some caution is required with these labels however, first because of the small number of results and secondly because it should be remembered that the trends for site 3 (cavity brick) were anomalous and have been excluded. Nevertheless, some of the illustrated behaviour shows expected trends. In particular, the transfer functions are lower for cavity brick than for solid brick which would be expected because the inner leaf, from which sound is radiated into the room, is not directly excited in cavity constructions. Therefore, the radiation into the room would be expected to be higher for solid constructions.

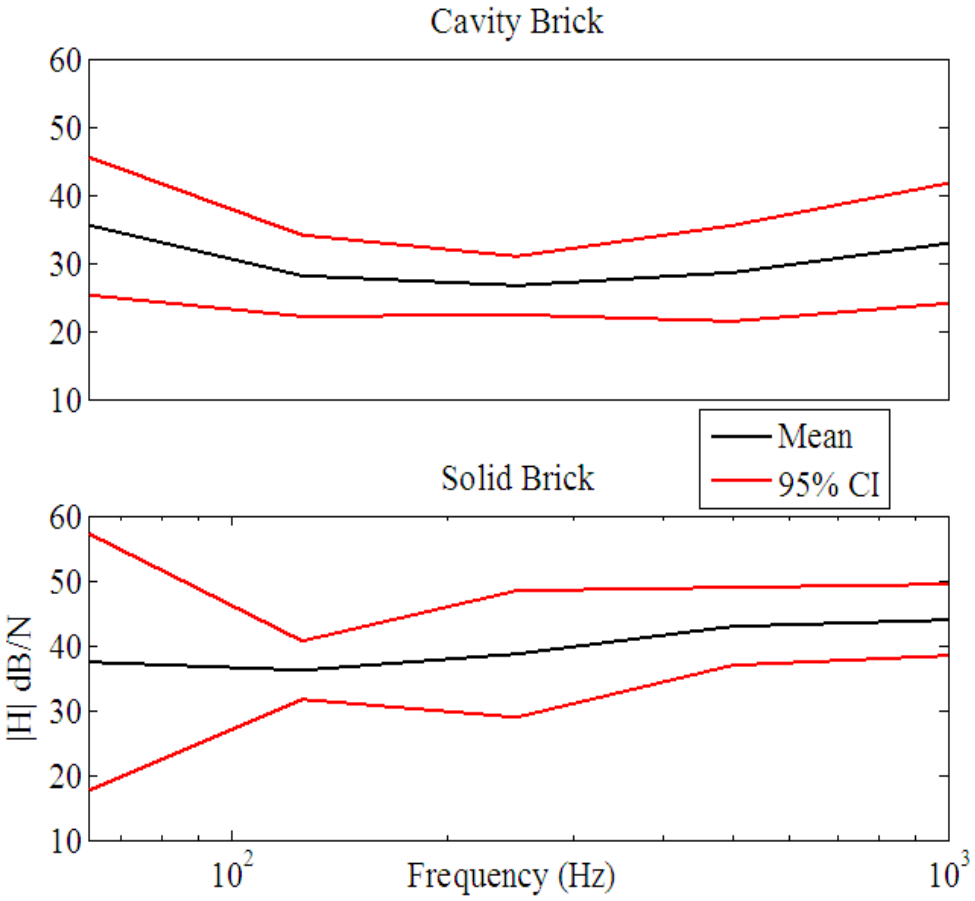

Figure 54: Octave band mean vibro-acoustic transfer functions together with ± 95% confidence limits. Upper: cavity. Lower: solid brick.

Table 4: Solid brick averaged vibro-acoustic transfer functions

Centre Frequency [Hz]	**31.5**	**63**	**125**	**250**	**500**	**1kHz**
Mean [dB]/N	36	37	36	39	43	44
95% confidence limit [dB]/N	±6	±20	±4	±10	±6	±5

Table 5: Cavity brick averaged vibro-acoustic transfer functions

Centre Frequency [Hz]	**32**	**64**	**125**	**250**	**500**	**1kHz**
Mean [dB]/N	34	36	28	27	29	33
95% confidence limit [dB]/N	±11	±10	±6	±4	±7	±9

The anomalous result for site 3 was investigated further. The coherence obtained during the measurement was similar to that for other measurements so it is not suspected that the result was corrupted by background noise. There are no obvious differences in the construction which would lead to the differences in behaviour but one possibility that cannot be ignored is that the excitation point may have been directly in line with a wall tie (for this site only one excitation point was used). In that case we would expect efficient transmission of sound energy into the inner leaf and a higher vibro-acoustic transfer function would result, potentially higher than for solid constructions at some frequencies, depending on the stiffness of the wall ties. In general the position of the wall ties cannot be known when carrying out the test so this possibility cannot be excluded. If this is the explanation for the anomalous site 3 result then it should be borne in mind that the same thing could happen in a MWT installation, i.e. that one of the brackets could be accidentally positioned to coincide with a wall tie. In that case a higher transfer function could result making the values in Figure 54, Table 4 and Table 5 un-conservative.

Generally, many variations can occur between cavity brick constructions in terms of wall ties, junctions and fixing conditions at the top, bottom and corners of walls. These details are known to manifest in variable sound insulation properties and it is reasonable to expect similar variations to occur in vibro-acoustic transfer functions. Therefore, it is advisable to treat the results for cavity construction with caution.

6.4.1 Comparison with impact sound insulation

The results given above are based on a relatively small sample of buildings; a larger sample would be required to derive statistically significant results. Furthermore, there are few results of vibro-acoustic transfer functions reported in the literature so it is

difficult to know how typical the above results are. One approach to increase the level of confidence in the results is to compare with impact sound pressure results which are fairly widely available.

The vibro-acoustic transfer function tests involve striking the wall with a hammer and measuring the resulting sound pressure impulse. Impact sound pressure levels are measured (according to ISO 140) using a 'tapping machine' in which a floor is subject to repeated impacts with small hammers and the resulting steady sound level is measured. The two methods therefore have significant similarities and it not surprising that a mathematical relationship exists between the results:

$$L_H = L_n - 10\log_{10}(0.8f) \qquad \textbf{6.2}$$

where:
L_H is the vibro-acoustic transfer function (sound pressure level for a 1 N force input), given in third octave bands
L_n is the normalised impact sound pressure level
f is the third octave band centre frequency.

This formula is derived from the formula for the force level of the tapping machine given in section F4.2 of EN12354-5:2009, together with the definition of the vibro-acoustic transfer function.

Unfortunately, we can only make limited use of this relationship for walls because impact tests only apply to floors and the constructions of walls and floors are generally significantly different, for example, no usual floor constructions resemble cavity brick. However, monolithic concrete floors are structurally similar to solid brick walls and it seems reasonable to compare impact results from solid concrete floors to the solid brick transfer functions. Table 6 and Figure 55 show results obtained from the results of impact sound tests of solid concrete slabs.

Table 6: Impact sound pressure and corresponding vibro-acoustic transfer function calculated from equation 6.1

		50	**63**	**80**	**100**	**125**	**160**	**200**	**250**	**315**	**400**	**500**	**630**	**800**
130 mm	$\mathbf{L_n}$	62	60	65	61	68	68	69	70	70	72	73	75	76
concrete	$\mathbf{L_H}$	46	43	47	42	48	47	47	47	46	47	47	48	48
140 mm	$\mathbf{L_n}$	56	63	63	68	70	66	71	72	72	72	72	73	73
concrete	$\mathbf{L_H}$	40	46	45	49	50	45	49	49	48	47	46	46	45

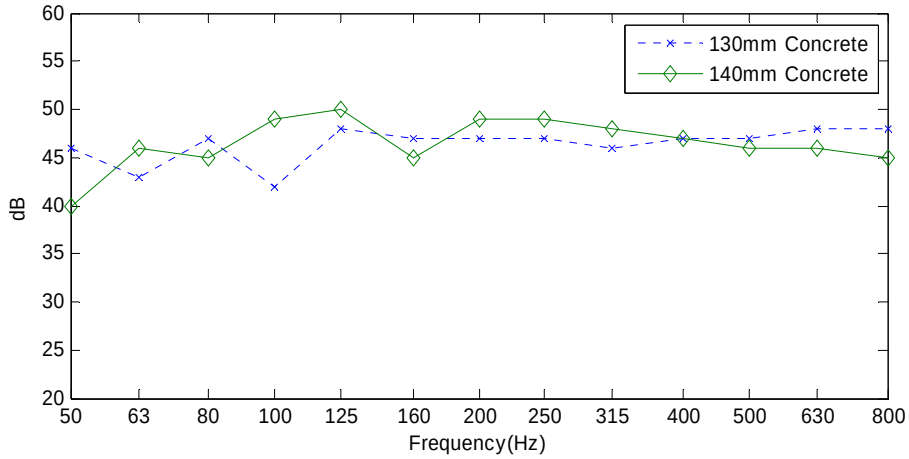

Figure 55: Vibro acoustic transfer functions obtained from impact sound insulation test results for 130 mm and 140 mm concrete floors.

The curves in Figure 55 are reasonably flat, especially above 125 Hz which was also observed in Figure 52 - Figure 54. The average level at 200Hz from Figure 55 is 48 dB but it should be remembered that the concrete slabs are about half the thickness (and mass) of a solid brick wall and would be expected to give results about 6 dB higher. Therefore, these results confirm that around 40 dB/ N seems a reasonable average figure for solid walls.

A further confirmation of these results came from a simple analytical model consisting of a rectangular acoustic volume driven by a single plate, itself driven by a point force (not described here). This model, which represents a room excited by one wall, produced results which were again consistent with a 40 dB/N transfer function.

6.5 Transmission to remote rooms

In the above we have looked at sound transmission to the room immediately behind the excited wall. However, in many MWT installations the receiving position will be in a more remote room. Hence, in this section we look at transmission to a room once removed from the excited wall. There are three possible configurations: to the room below, horizontally into the building and horizontally so as to share the same façade. These three directions are referred to as z, x and y respectively as shown in Figure 56.

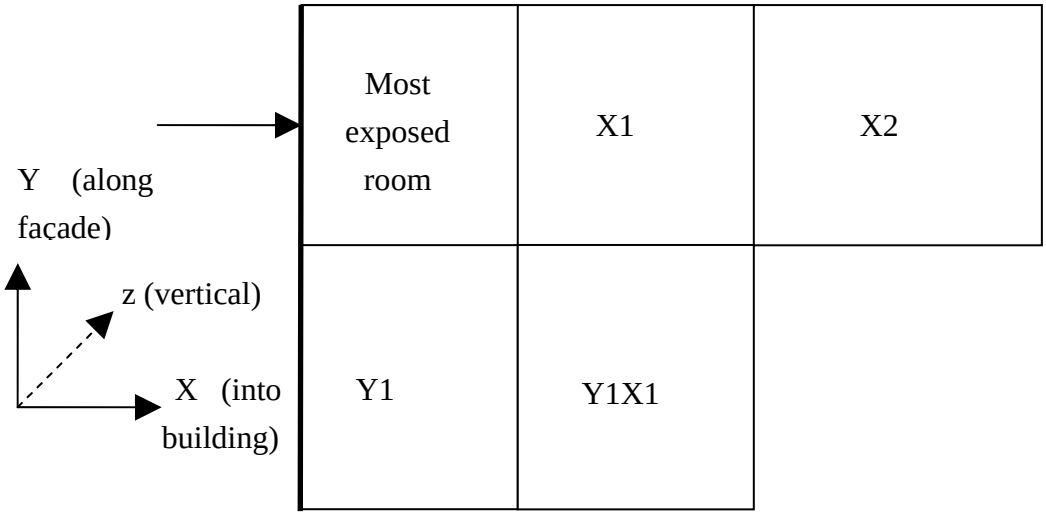

Figure 56: Labelling system for building layout

The results in the following figures and tables show the 'second room loss' (SRL) which is defined as the difference in dB between the average sound pressure level in the second room, i.e. adjacent to the most exposed room, compared with that in the most exposed room. This corresponds to the correction that would need to be applied to calculate sound pressure in remote rooms. Results from the different sites are displayed in the same groups as were described in the previous section.

Table 7: Second room loss, mean and 95% confidence limit cavity brick X direction

Centre Frequency [Hz]	**2**	**4**	**8**	**16**	**31.5**	**63**	**125**	**250**	**500**	**1kHz**
Mean [dB]	3	2	6	3	1	3	2	4	5	7
95% confidence limit [dB]	±6	±6	±3	±3	±1	±2	±7	0	±7	0

Table 8: Second room loss, mean and 95% confidence limit solid brick X direction

Centre Frequency [Hz]	**2**	**4**	**8**	**16**	**31.5**	**63**	**125**	**250**	**500**	**1kHz**
Mean [dB]	5	2	4	4	3	6	8	12	14	13
95% confidence limit [dB]	±12	±8	±6	±2	±8	±4	±1	±3	0	±3

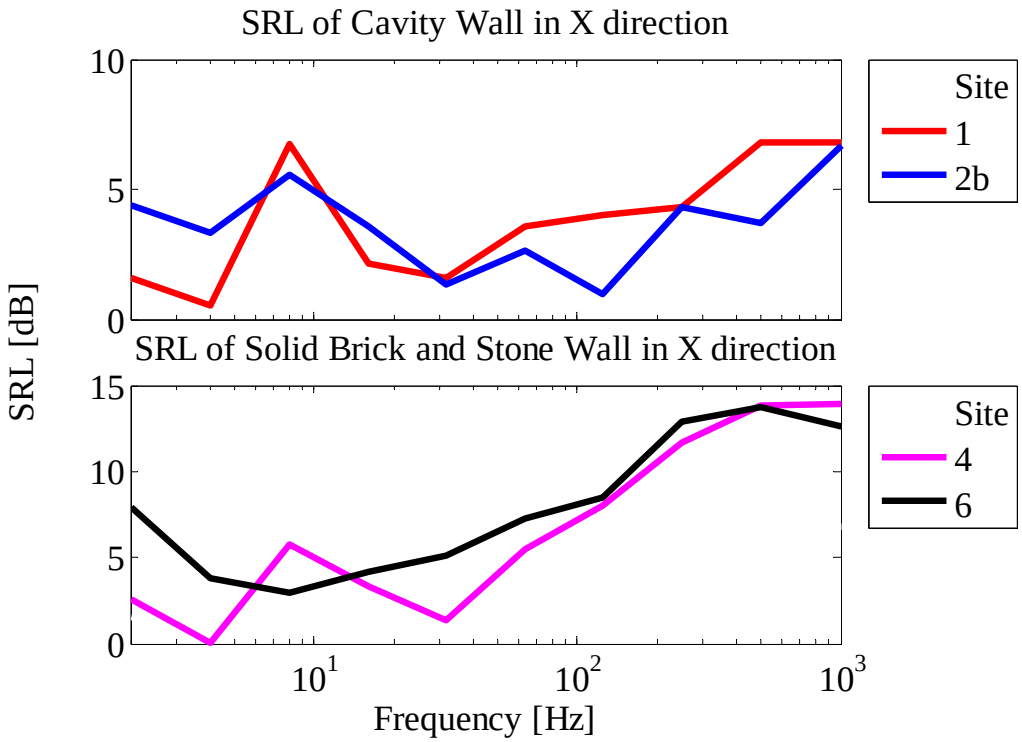

Figure 57: SRL in X direction (into building) for cavity, solid brick and solid stone wall construction types.

Results in Figure 57, Table 7 and Table 8 show the results for the X-direction, i.e. into the building away from the excited façade. Results for the grouped sites follow similar trends. Greater attenuations are seen for the solid constructions with more than 5dB reduction per room (compare Table 8 with Table 7). The cavity constructions show a lesser reduction although still significant, of the order of 5 dB above 250 Hz.

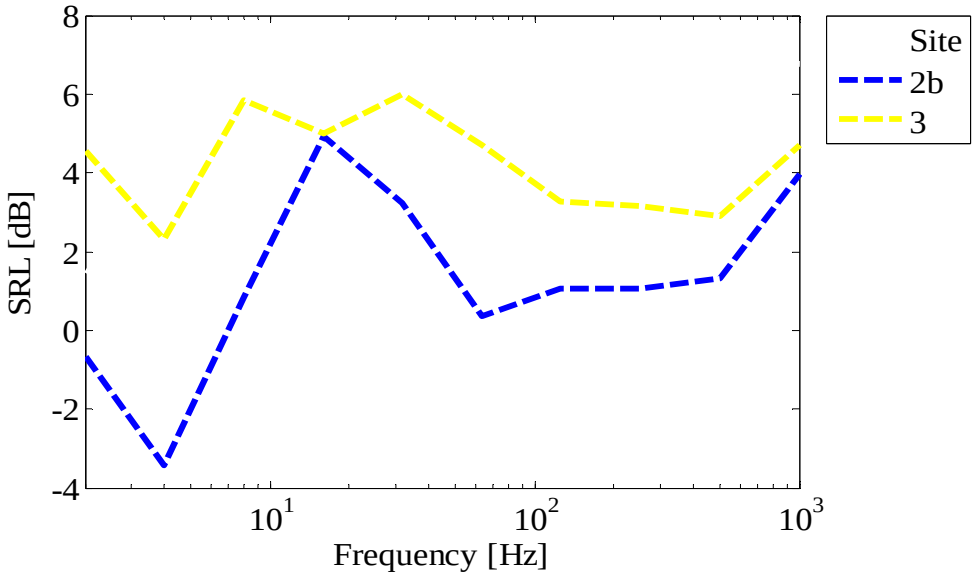

Figure 58: SRL in Y direction (along facade) for cavity wall construction.

Table 9: Second room loss, mean and 95% confidence limit cavity brick Y direction

Centre Frequency [Hz]	**2**	**4**	**8**	**16**	**31.5**	**63**	**125**	**250**	**500**	**1kHz**
Mean [dB]	2	-1	3	5	5	3	2	2	2	4
95% conf. limit [dB]	±12	±13	±11	±0	±6	±10	±5	±5	±4	±2

The corresponding results for the Y–direction, horizontally along the façade, are shown in Figure 58 and Table 9. Only cavity wall results are available for this direction. The reduction is seen to vary between 1 and 4 dB above 63 Hz.

Z-direction results are shown in Figure 59, Table 10 and Table 11. For the cavity brick constructions the attenuations average around 2 dB. These results are similar to those of the Y-direction which is to be expected since there are no significant structural differences encountered by vertical and horizontal travelling waves in the outer skin of the façade. Also shown in Figure 59 is the result for a solid wall construction which indicates attenuations of up to 5 dB in the 250 Hz band.

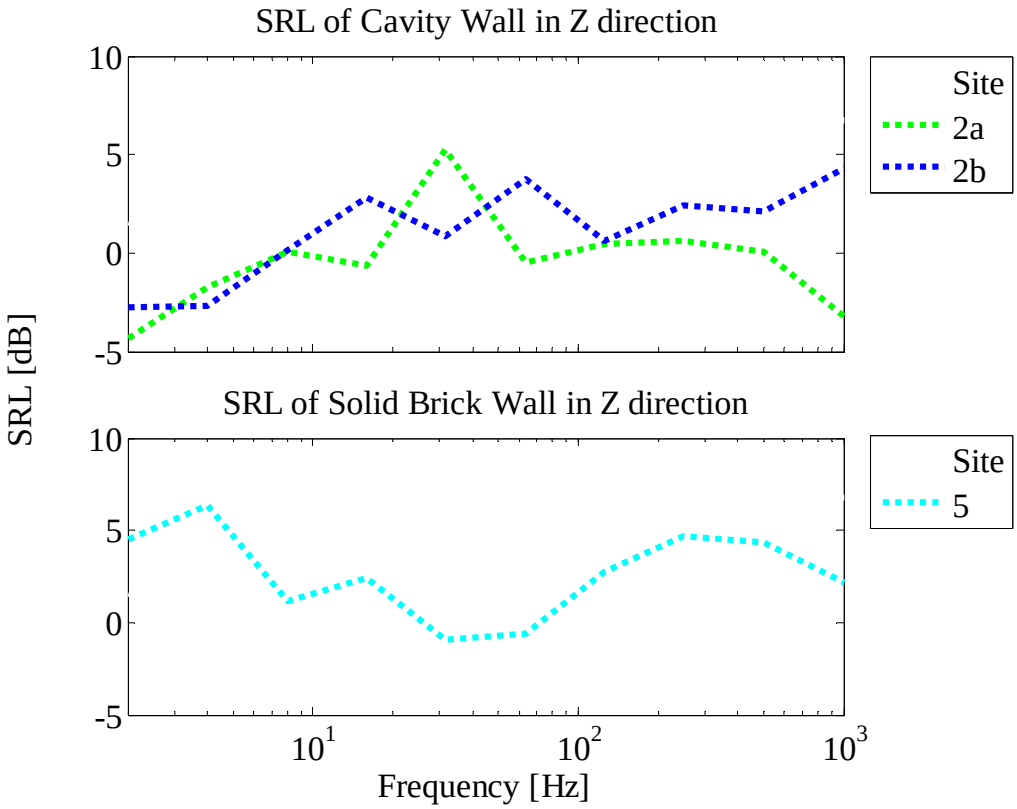

Figure 59: SRL in Z direction (up facade) for cavity and solid brick wall constructions.

Table 10: Second room loss, mean and 95% confidence limit cavity brick Z direction

Centre Frequency [Hz]	**2**	**4**	**8**	**16**	**31.5**	**63**	**125**	**250**	**500**	**1kHz**
Mean [dB]	-4	-2	0	1	3	2	1	2	1	1
95% confidence limit [dB]	±3	±2	0	±8	±10	±9	0	±4	±5	±17

Table 11: Second room loss, mean, solid brick Z direction

Centre Frequency [Hz]	**2**	**4**	**8**	**16**	**31.5**	**63**	**125**	**250**	**500**	**1kHz**
Mean [dB]	5	6	1	2	-1	-1	3	5	4	2

The results above can be grouped into two categories, one where the two rooms in question do not share a common façade, and one where there is a common façade irrespective of whether the transmission is vertical or horizontal. Smaller attenuations were obtained in general for the latter category i.e. when the façade, which is the element subject to the excitation, is shared by the two rooms. This is believed to be because the most direct transmission path is along the façade whereas for rooms 'behind' the most exposed room sound would need to be transmitted round at least one junction (round a corner of the building) in order to reach the second room.

A second trend is that the attenuation to the second room was lower for cavity than for brick constructions. This trend can be interpreted in the light of the schematic shown in Figure 60. In the upper figure it is shown how vibration travels through the façade of solid wall constructions and has to pass through a wall junction before it can reach the second room. Attenuation by junctions has been studied by a number of authors and a nominal attenuation of up to 5dB would be expected to occur at a 'T' junction such as this. The lower figure in Figure 60 shows how vibration transmission occurs through the outer skin of a cavity wall façade. In this case the main transmission to the inner leaf, and hence to the room, occurs through wall ties (as well as to some extent through the air in the cavity). The important point is that transmission through the outer skin to the second room does not benefit from the attenuation of a junction.

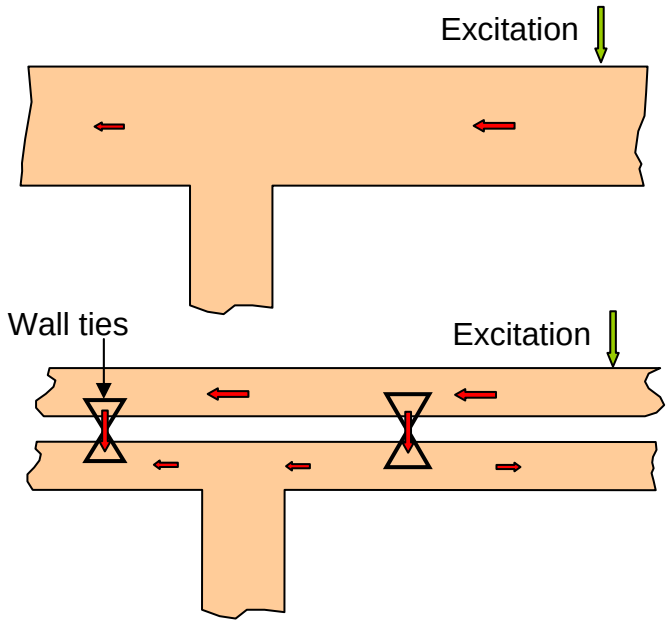

Figure 60: Schematic showing vibration transmission from the excitation point along the facade for a cavity and solid masonry construction

Even for cases without a shared façade (transmission 'into' the building, X-direction) lower attenuations were observed for cavity as opposed to solid brick constructions. The reason may be an extension of the arguments above: whereas the external walls of solid brick constructions are 'compartmentalised' by junctions with internal partition walls, this is not the case for the outer skin of cavity constructions. Vibration may then be transmitted round the whole of the outer shell of the building with relatively little attenuation from where it may be transmitted via wall ties into the inner skin and hence into the room.

One of the most striking findings from the results above is that the attenuations obtained to the second room are numerically rather small. For purely airborne sound transmission, the attenuation between rooms would typically be of the order of 45-50 dB, however, for structure-borne sound excitation, as studied here, we see that attenuations of less than 5 dB are typical going from room to room. In principle this phenomenon has long been recognised in the study of structure-borne sound but from the point of view of MWT installations it is disappointing that so little attenuation can be expected for rooms away from the point of attachment. It is likely that the attenuation is additive for further rooms but no measurements have been conducted to confirm this.

6.6 Correction factors

In this section the above results are presented in the form of correction factors which can be used to adjust the prediction results for different construction types and

building layouts. The reference installation is defined as the most exposed room of a hypothetical solid brick building, the room being 50 m^3 in volume and with a reverberation time of 0.5 seconds. From Table 4 the average transfer function for solid walls is of the order of 40 dB for a 1 N force input. We can therefore define the reference installation as having a transfer function of 40 dB across the frequency range.

6.6.1 Correction factors for construction types

Lower sound levels are expected to arise from the same excitation on a cavity wall as compared with the reference installation (solid wall) as indicated in Table 5. Therefore, we need to apply a correction factor to be able to predict the sound level in buildings of cavity wall type construction. The relevant correction factors are calculated as the difference in the vibro-acoustic transfer function for the two constructions and are shown in Table 12. The average value of the correction factor in the dominating octave bands (125 and 250 Hz) is -10 dB, i.e. on average the same MWT would be expected to cause 10 dB lower sound levels on a cavity wall as opposed to a solid wall for the same excitation.

Table 12: Correction factor for transmission into the most exposed room for cavity constructions

Centre Frequency [Hz]	**31.5**	**63**	**125**	**250**	**500**	**1kHz**
Solid [dB]	36	37	36	39	43	44
Cavity [dB]	34	36	28	27	29	33
Correction factor for cavity brick [dB]	-2	-1	-8	-12	-14	-11
Average of 125 and 250 Hz bands = correction factor for cavity brick = -10 dB						

6.6.2 Correction factors for building layout

The correction factors for rooms next to the most exposed room are derived in this section based on the results of Figure 57 through Figure 59 and Table 7 through Table 11. The results are summarised in Table 13. For the MWTs studied the most important octave bands are 125, 250 and 500Hz octave bands and taking an average across these bands the following results (summarised in Figure 61) are obtained:

Solid brick, X-direction (into building)	-11 dB
Cavity brick, X-direction (into building)	-3 dB
Cavity brick, rooms on shared façade	-2 dB.
Solid brick, rooms on shared façade	-4 dB.

Table 13: Correction factors for rooms once removed from the most exposed room

Centre Frequency [Hz]	**31.5**	**63**	**125**	**250**	**500**	**1kHz**
Solid brick X-direction(into building) [dB]	-3	-6	-8	-12	-14	-13
Cavity brick X-direction(into building) [dB]	-1	-3	-2	-4	-5	-7
Cavity brick Y-direction(along facade) [dB]	-5	-3	-2	-2	-2	-4
Cavity brick Z-direction(along facade) [dB]	-3	-2	-1	-2	-1	-1
Solid brick Z-direction(along façade) [dB]	1	1	-3	-5	-4	-2

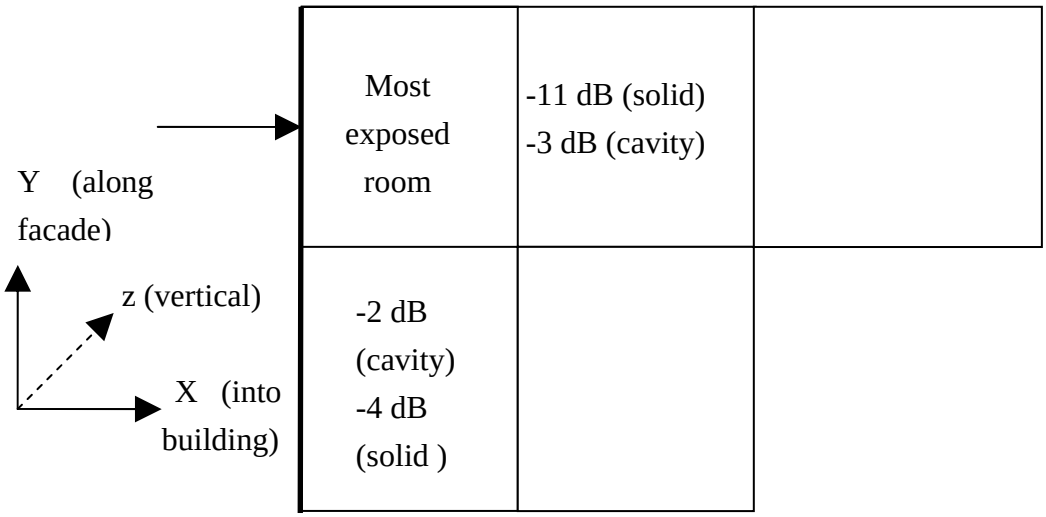

Figure 61: Summary of correction factors for remote rooms

These figures should be treated with caution because of the number of assumptions made in their derivation and because of the small number of results on which they are based. Nevertheless, the results should provide a useful overall picture.

6.6.3 Correction factors for room volume

Correction factors are calculated as the ratio of the volume to the reference room volume ($50m^3$) expressed in dB as shown in Table 14. This assumes that the reverberation time remains constant at 0.5 seconds.

Table 14: Correction for room size

Volume (m^3)	**30**	**40**	**50**	**60**	**80**	**100**	**120**	**150**
Correction (dB)	2	1	0	-1	-2	-3	-4	-5

6.7 Conclusions

Based on the tests reported here, the vibro-acoustic transfer functions for solid brick walls, for transmission into the most exposed room, tend to be around 40 dB/ N. Some scatter would be expected, for example due to varying structural reverberation time and the surface area of the excited wall. However, this figure has been shown to compare reasonably well with the adjusted results of standard impact sound insulation tests of solid concrete floors. Furthermore, results from an analytical model (not shown) were consistent, which again increases confidence.

In broad terms the transmission into the most exposed room should be about 10 dB lower for cavity walls than for solid walls. A correction factor of -10 dB can therefore be applied for cavity brick construction, although in reality the figure is likely to be variable depending on the specific details of the cavity wall construction, such as wall ties.

Correction factors have also been derived for transmission of structure-borne sound into adjacent rooms both along the same façade and into the building. Only about 2 dB attenuation is expected to adjacent rooms vertically or horizontally along the same façade as the excitation point for cavity walls, and about 4 dB for solid walls. For adjacent rooms behind the most exposed room we can expect the order of 11 dB attenuation for solid walls but only about 3 dB for cavity walls. In perceptual terms the only scenario providing a significant reduction is for rooms behind the most exposed room for solid masonry construction.

Finally, a note of caution is required since the transmission of sound from excitation on an external wall into rooms is a complicated phenomenon. We would expect results to depend on many factors such as the size and damping factor of the wall and, for cavity constructions, the type of wall ties and details of joints. Therefore, where possible the results should be backed up by additional measurements or calculations for a specific building. Furthermore, in order to simplify the results for the prediction model we have averaged the results over the frequency bands found to be dominant for MWT1 and MWT2. Therefore, caution is required if used for different MWTs or mountings which may result in other frequency bands becoming important.

7 Prediction methodology

The aim of this chapter is to pull together the results of the preceding chapters, relating to the MWT, mounting and buildings, into an overall prediction methodology. First, a prediction procedure is described in which the sound level is predicted as a function of rotor speed. This is a general procedure which should be applicable to any site for which rotational speed data is available. Example results from this procedure are reported in the following chapter for each of three Case Studies of real MWT installations. The second part of this chapter describes the procedure for estimating sound levels based on wind speed. For reasons discussed in chapter 4 these results are strictly applicable only to sites with comparable wind conditions to those occurring during the test programme, although with further data the approach could be extended.

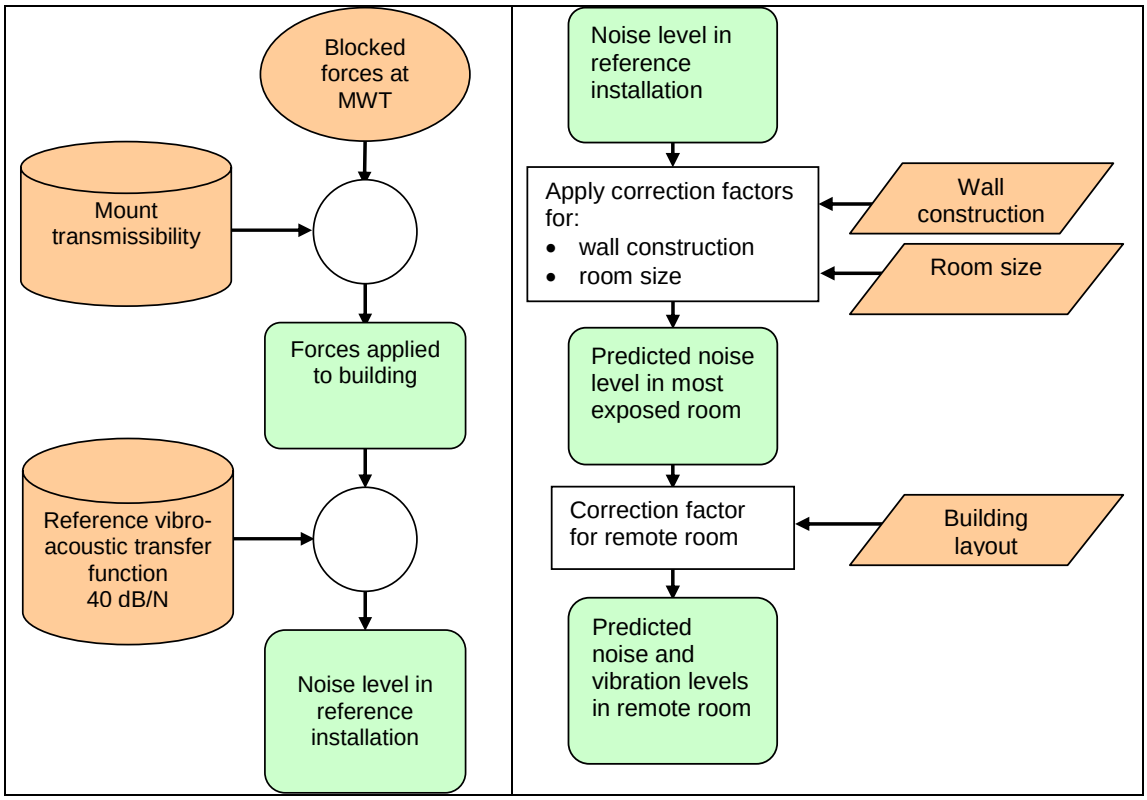

Figure 62: Flow chart for prediction of noise levels as a function of rotor speed. Left: prediction of sound levels in the reference installation. Right: correction for construction type, room size and building layout.

7.1 Prediction in terms of rotational speed

The full procedure followed for predicting noise levels as a function of rotational speed is shown in flow chart form in Figure 62. The left side of Figure 62 shows the

steps required to calculate sound levels in the reference installation. These procedures necessarily require significant complication and could not be reproduced by non-specialists. The right side of Figure 62 shows how adjustments may be made to the reference installation levels to predict sound levels in other buildings. These adjustments are relatively straightforward and could be made by non-specialists. If reference installation levels are available for a particular MWT then the right hand side of Figure 62 may be used as a simplified prediction procedure. Example predictions are given in the following chapter.

7.1.1 Prediction of sound level in the reference installation

The prediction (summarised in the left of Figure 62) is based on the blocked force data (source strength) for the MWT as obtained in chapter 3. For each rotational speed a matrix of blocked force spectra is stored. The following procedure applies for a given rotational speed and would be repeated for other rotational speeds of interest. Each blocked force matrix contains 5×5 spectra so as to provide information about the magnitude and relative phase of the blocked forces at the five degrees of freedom at the top of the mast. The next step is to calculate the forces applied to the wall of the building. This is achieved by a matrix multiplication of the blocked force spectra with the transmissibility matrix as described in chapter 5. The result is a set of force spectra, including magnitude and phase, one for each connection point at the base of the mount. These forces are then multiplied by the vibro-acoustic transfer function of the building, taken as a constant value of 40 dB per N (see chapter 6).

The results of these calculations give the sound levels in the reference installation for a given MWT with a given mast length and are plotted in Figure 42.

7.1.2 Prediction of sound level in other rooms

Having obtained sound levels in the reference installation as described in the previous section, adjustments may be made for construction type, room size and room layout by making use of the correction factors developed in chapter 6. The process is summarised in the right of Figure 62 and in Part 3 of this report. Specifically, Table 12 may be used to correct for cavity brick constructions and Table 13 for remote rooms. Thus for many cases the sound levels in the reference installation may be used as a starting point. Only for different models of MWT or mast designs will it be necessary to recalculate reference installation levels.

7.2 Prediction in terms of wind speed

As described in chapter 4, sound levels can only be related to wind speed on a statistical basis. This is because, as yet, no mathematical relationship between wind

speed and rotor speed exists. Shown in Figure 63 are the cumulative probability density functions showing how the $L_{Aeq,\ 5\ minutes}$ varies statistically for a given set of wind conditions. The rightmost curve of each plot was shown in a different form in Figure 24 and the two other curves have been added so as to provide predicted levels for different mast lengths. The curves show that noise levels are expected to vary over any given period and one can extract the mean or maximum $L_{Aeq,\ 5\ minutes}$ or alternatively one can use a percentile value, for example the level exceeded for 10% of the time. The percentile figure gives a near maximum value without the uncertainty associated with an actual maximum. Table 15 summarises the mean and 10% values of $L_{Aeq,\ 5\ minutes}$ for the two different MWTs, each for three different mast lengths and for wind conditions on three separate days (as was used to generate Figure 24).

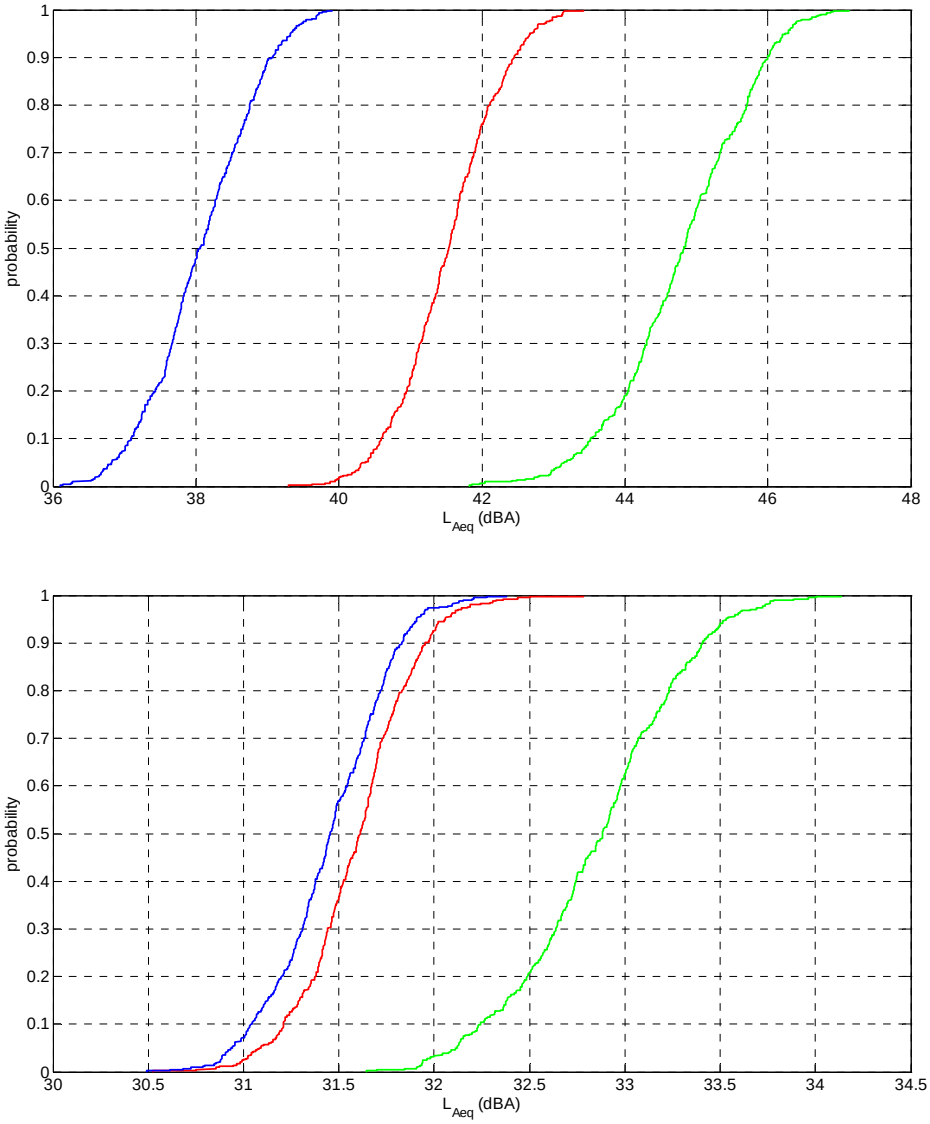

Figure 63: Cumulative probability density function for $L_{Aeq\ 5\ minutes}$. Upper: MWT1 for mean wind speed of 2.7 m/s, mast length 2.2, 2.5, 2.9 m from left to right. Lower: MWT2 for mean wind speed of 3.5 m/, mast length 1.5, 2, 2.4 m from left to right.

Without more definitive information on the relationship between rotor speed and wind speed it is not possible to generalise these results to different wind speeds. It is tempting to employ the curves derived in Figure 19 and Figure 20 but for reasons explained in section 4.2 this is not advisable. However, referring to Figure 42 it appears that for both MWT1 and MWT2 the noise levels do not continue to rise for rotor speeds above about 350 rpm. In continuously high wind speeds we would expect relatively high rotational speeds but provided the rotor speeds do not rise above about 600 rpm (the maximum for which vibration data is available) the $L_{Aeq,\ 5\ minutes}$ should not rise above the noise levels shown in Figure 42.

MWT1 with mast length 2.9m			
Mean wind speed	2.7	2.8	2.7
Mean $L_{Aeq\ 5\ minutes}$	45	46	45
10% highest $L_{Aeq\ 5\ mins}$	46	47	46
MWT1 with mast length 2.5m			
Mean wind speed	2.7	2.8	2.7
Mean $L_{Aeq\ 5\ minutes}$	41	42	42
10% highest $L_{Aeq\ 5\ mins}$	42	43	42
MWT1 with mast length 2.2m			
Mean wind speed	2.7	2.8	2.7
Mean $L_{Aeq,\ 5\ minutes}$	38	39	38
10% highest $L_{Aeq\ 5\ mins}$	39	39	39

MWT2 with mast length 2.4m			
Mean wind speed	3.6	3.3	3.7
Mean $L_{Aeq\ 5\ minutes}$	34	32	33
10% highest $L_{Aeq\ 5\ mins}$	34	32	34
MWT2 with mast length 2.0m			
Mean wind speed	3.6	3.3	3.7
Mean $L_{Aeq\ 5\ minutes}$	32	31	32
10% highest $L_{Aeq\ 5\ mins}$	32	31	32
MWT2 with mast length 1.5m			
Mean wind speed	3.6	3.3	3.7
Mean $L_{Aeq\ 5\ minutes}$	32	31	32
10% highest $L_{Aeq\ 5\ mins}$	32	31	32

Table 15: Summary of statistics of wind speed and $L_{Aeq,\ 5\ minutes}$ from Figure 24

8 Field trials of the proposed methodology structure-borne sound through buildings

In this section the results of four case studies carried out on existing MWT installations are described. The sites were selected so as to provide a range of wall and roof mounted installations, a mixture of cavity and solid brick constructions and to include examples of both MWT1 and MWT2 as studied in the site tests reported in chapter 3.

8.1 Measurement procedure and data analysis

Noise and vibration measurements were taken within the properties at the four case study sites detailed within this section. Measurements were carried out using the 'Bruel & Kjaer PULSE platform for noise and vibration analysis'. The pulse system has 5 channel inputs and data is logged directly to a laptop computer via ethernet cable. Equipment details are listed in Table 16. Four channels of the Pulse system were connected to microphones which were located diagonally across the room of interest with equal spacing. This method was used to allow for instantaneous spatial averages via microphone response averaging.

The fifth channel of the Pulse system was used to monitor vibration via an accelerometer. The accelerometer was attached internally in the room of interest using bees wax. The accelerometer was located on the internal wall as close to the external attachment of the turbine as possible, measuring in the horizontal direction perpendicular to the wall.

Table 16: Equipment used for the case studies

'Bruel & Kjaer PULSE platform for noise and vibration analysis'
1 Accelerometer – B&K, DeltaTron, Type 4507.
4 Microphones – G.R.A.S. ½" CCP Pre-amp and 01dB Microphone Type 26CA.
Anemometer wind logger – Metek Ultrasonic Anemometer USA-1

Continuous measurements were taken at a sample rate of 16384 samples per second. The on-site conditions, of background noise and varying wind conditions, meant that the turbine noise could either be heard, masked by background noise, or the turbine was not rotating therefore not producing any noise. This meant that all measurements had to be manned in order to note down 'clean' periods of turbine noise for later analysis. Also the method of measurement using the PULSE platform made it possible to listen back to the recorded data during analysis.

In order to try to match wind data to the turbine noise, an anemometer was also setup. However, on all sites there were problems in obtaining an accurate measure of the wind speed at the MWT hub either due to locally varying wind conditions caused by obstacles, difficulties in access or both. An alternative strategy was therefore devised which was to establish the rotational speed of the turbine through frequency analysis of the recorded data. The MWT rotational speed was considered to provide a more reliable indication of the actual wind conditions at the hub than the anemometer readings.

Notes were taken of the noise climate and the subjective perception of the turbine noise characteristics. Also, although no formal interview was conducted, any comments made by residents about their perception of the noise from the turbine and their attitude to it were noted.

Audio recordings were taken in the room closest to the turbine attachment point. Notes were taken of noise environment during measurements in order to mark the measurement data with either 'good clean' noise from the turbine or background noise occurring. Audio recordings were edited into recordings of clean turbine noise, by listening. The time periods used were either four seconds or five minutes. However, it was not possible at all sites to extract a full five minutes of clean data; therefore some results are shorter than five minutes. The resulting edited audio was plotted as a narrow band spectrum and A-weighted third octave bands.

Four seconds was used as a time period in order to have 'snapshots' of turbine noise with a long enough period to achieve spectral data of sufficient resolution but short enough that the rotor speed was more or less constant during the time window. The resulting 'snapshots' were used as data points to plot dB(A) level against rotational speed. Spectral plots of 5 minute periods were also plotted, this time period was used to allow for comparison to the proposed criteria of $L_{Aeq(5\ mins)}$. Narrow band spectral analysis (FFT) and A-weighted third octave band analysis was carried out on the four second snapshots of varying rotational speeds of the turbine. The noise level and rotational speed extracted from the analysed snapshots of data were used as data points in order to plot dB(A) level against rotational speed, which in turn can be related to wind speed.

8.2 Case study 1

Details of the site are given below.

- End Terrace property
- Solid brick construction
- Turbine on gable end approximately 2m above roof level
- Four fixing brackets
- Turbine type – MWT1
- The property and turbine are owned by the occupier.

Comments on measurement period

- Prevailing wind was from a North Easterly direction.
- The turbine was operational for majority of time.
- Tests were carried out between 13:30 – 16:30 on 25th May 2010.

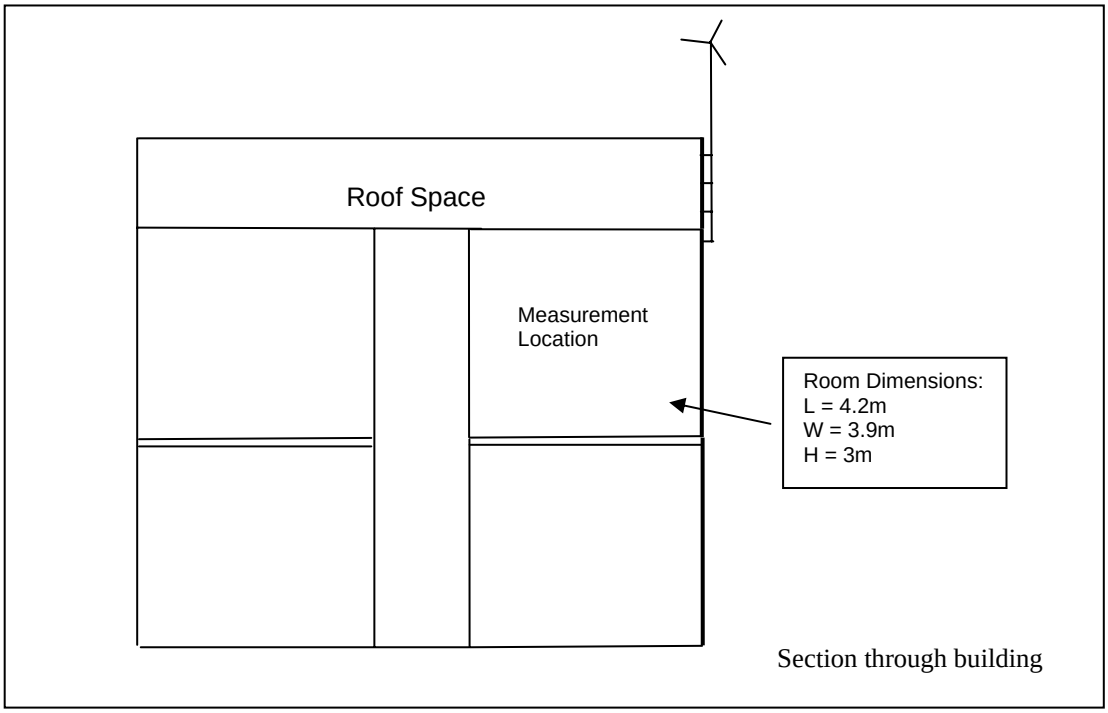

Figure 64 Site details for Case Study 1.

8.2.1 Subjective description of sound and vibration

The turbine noise was audible above the background noise in rooms along the side of the property to which the MWT was attached. The background noise consisted of passing road traffic. The turbine noise could be described as 'humming and whining' and sounded tonal. There was also a knocking noise as the turbine speeded up or slowed down. Even though the turbine could be heard during operation the resident reported not being annoyed by the noise experienced. However the residents' bedroom was on the other side of the house and although the turbine was just audible the level was low enough to not bother them.

There was no tactile vibration noticed during the measurement period and the resident informed us that they had never experienced any vibration from the turbine operation.

No perceptible rattling of fixtures or fittings occurred during the measurement period.

8.2.2 Results

It can be seen in Figure 65 that the turbine noise predominantly lies within the 200Hz and 250 Hz third octave bands. The FFT plot shows the noise from the turbine, over the five minutes, is concentrated around 200Hz. The peak due to the rotational speed is smeared out due to the speed changing over the five minutes.

Spectra for short snapshot measurements are shown in Figure 66 through Figure 68. These figures are intended to provide a useful picture of the instantaneous spectral content although the lower frequency bands should not be relied on for an absolute level in view of the short averaging time.

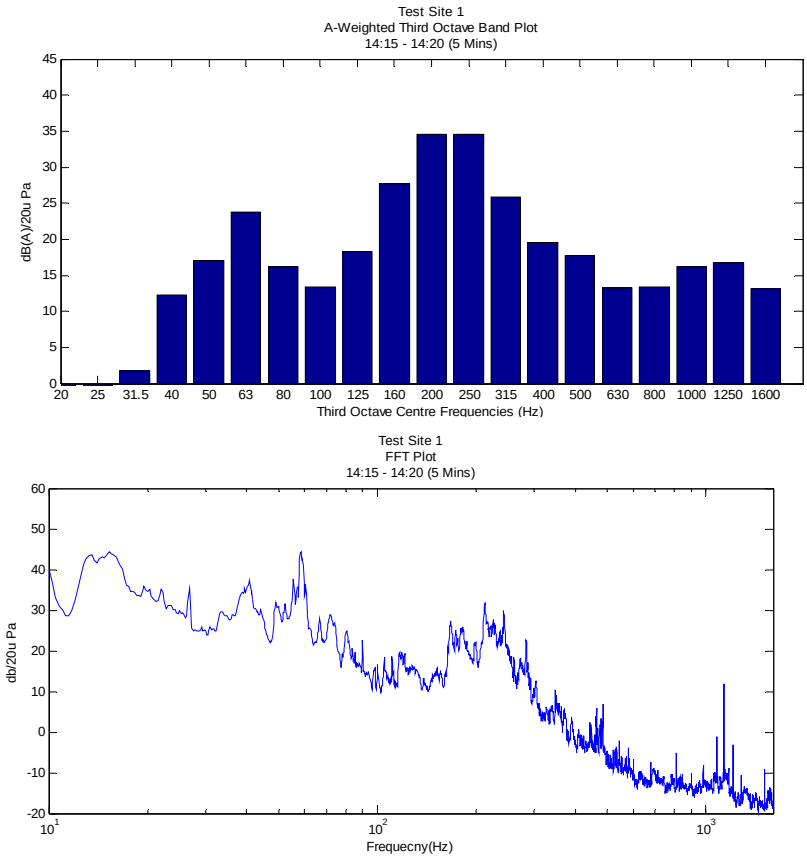

Figure 65 $L_{Aeq,\ 5\ minutes}$ for Case Study 1. Lower; Narrow Band. Upper; A-Weighted Third Octaves.

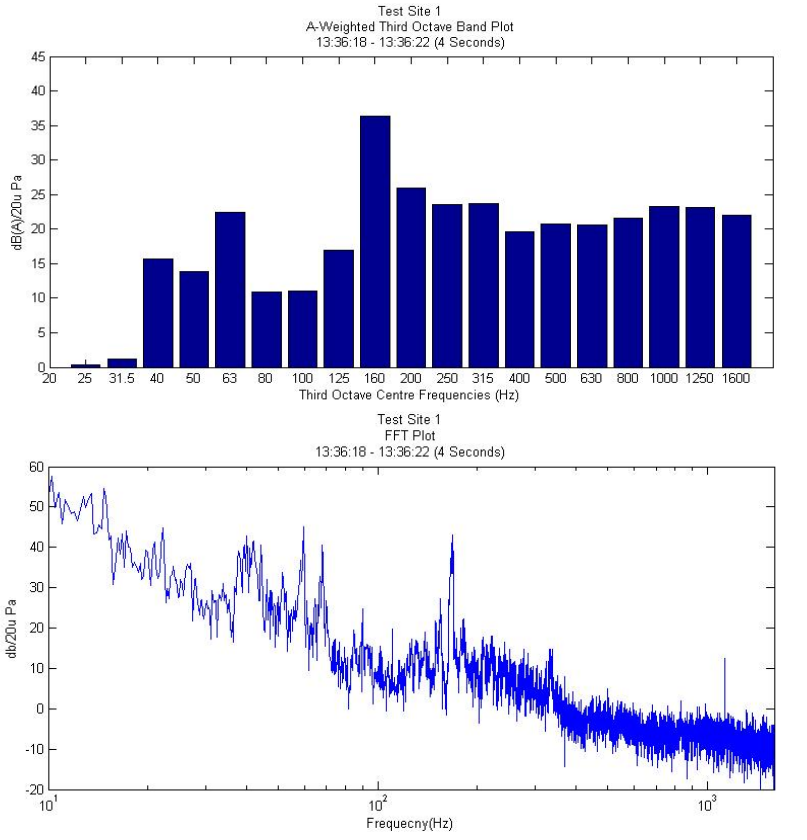

Figure 66. Snapshot example 1. Lower; Narrow Band. Upper; A-Weighted Third Octaves. Rotational speed ~288rpm

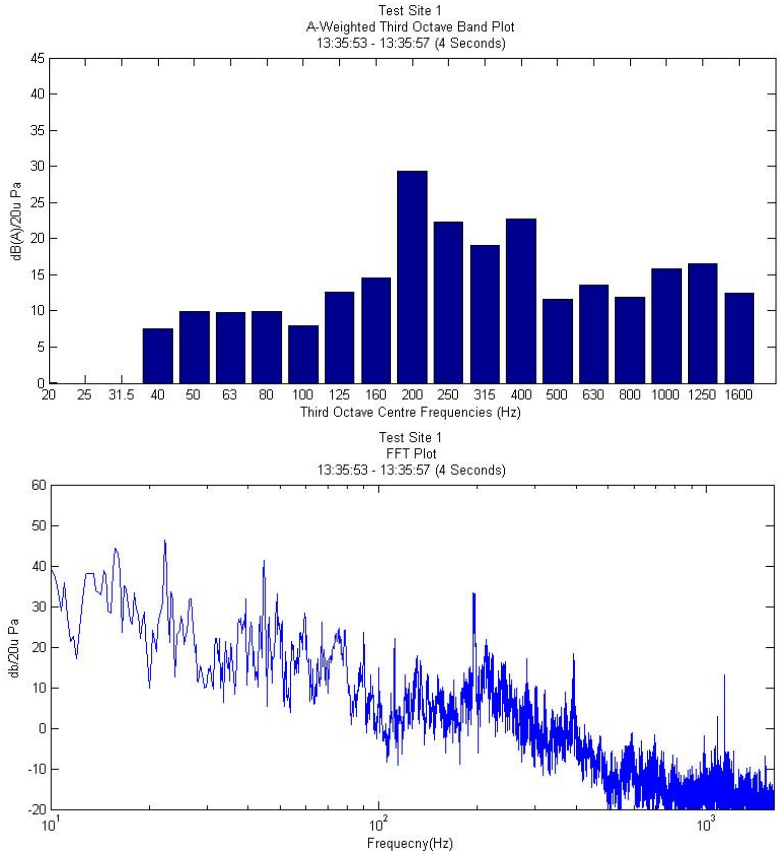

Figure 67 Snapshot example 2. Lower; Narrow Band. Upper; A-Weighted Third Octaves. Rotational Speed ~336rpm

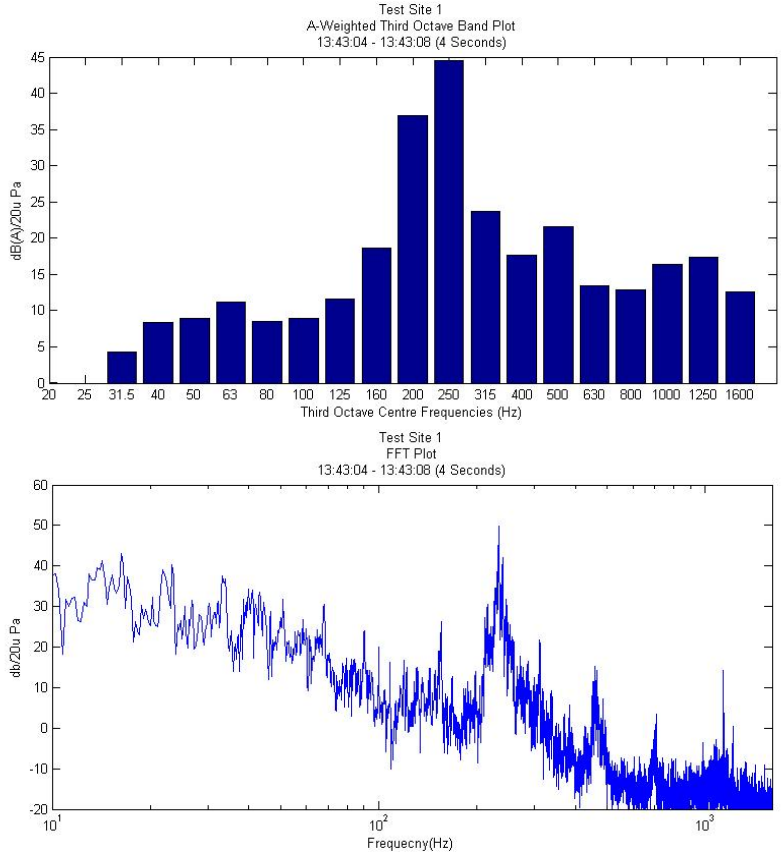

Figure 68. Snapshot example 3. Lower; Narrow Band. Upper; A-Weighted Third Octaves. Rotational Speed ~402rpm

Figure 69 shows the measured internal noise level calculated by the summing the two dominant third octave bands plotted against rotational speed of the turbine. Also shown are the calculated noise levels which will be discussed in section 8.6

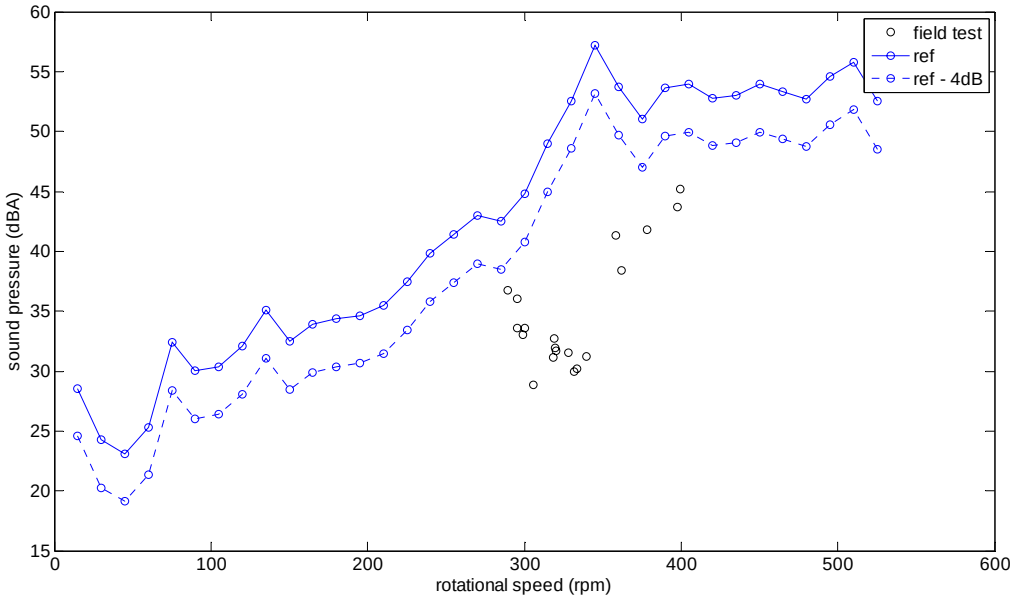

Figure 69 Case study 1: snapshot L_{Aeq} vs rotational speed. Solid line: calculated noise level in reference building. Dotted line: reference building noise level -4 dB

The maximum p.p.v. measured throughout the measurement period was 0.01 mm/s.

8.3 Case study 2

The site details are as follows and as shown in Figure 70

- Three storey flats
- Modern cavity brick construction
- Wall mounted turbine
- Three fixing brackets
- The point of attachment of the turbine is on a stairwell. Therefore no occupancy directly next to turbine. The window seen in the photograph is at the top of the stairwell.
- The turbine is owned by the building owner, however all occupants are tenants.
- Turbine type – MWT1
- Prevailing wind was from a Southerly direction.
- The turbine was operational for majority of time.
- Tests were carried out between 14:00 – 17:00- on 3rd June 2010.

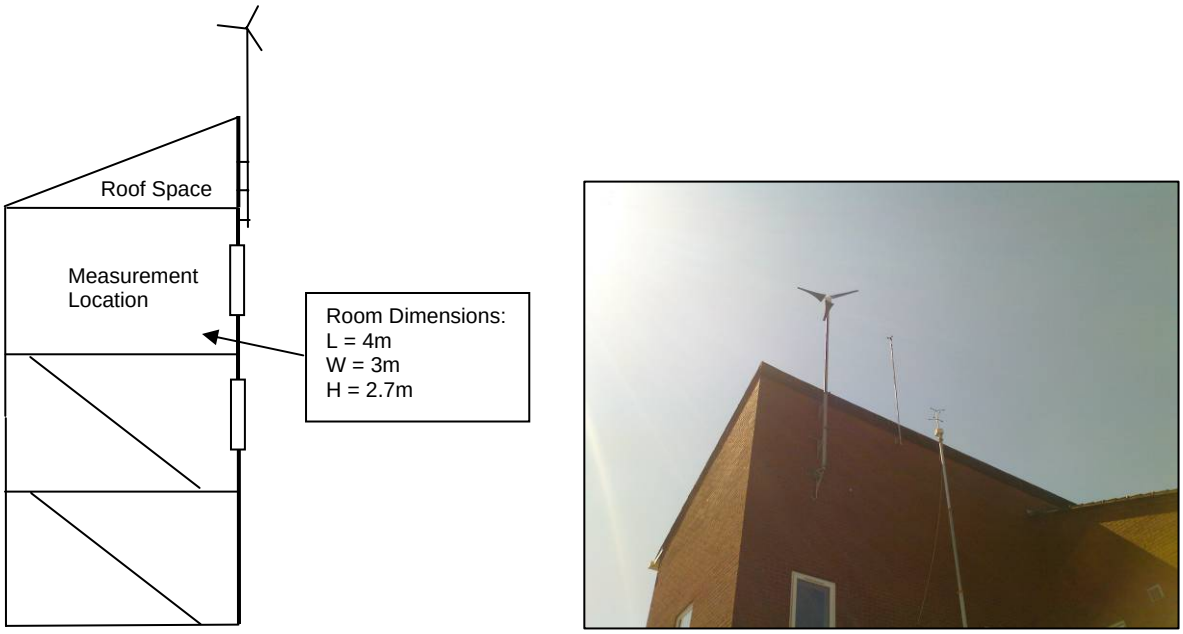

Figure 70 Section through building and photo of Case Study Site 2

8.3.1 Subjective description of sound and vibration

The turbine noise was just audible when little or no background noise was present. The background noise consisted of passing traffic, residents within the flats and a building services fan located approximately 5 metres from the measurement location. The turbine noise could be described as 'humming and whining' and sounding tonal. There were no known complaints from residents with respect to noise from the turbine.

There was no tactile vibration noticed during the measurements and from questioning the building manager there had been no reports of tactile vibration from any residents.

No perceptible rattling occurred during the measurements.

8.3.2 Results

It can be seen in Figure 71 that the turbine noise is dominated by the 160Hz and 200 Hz third octave bands. The FFT plot shows the noise from the turbine, over one minute, is concentrated around 200Hz.

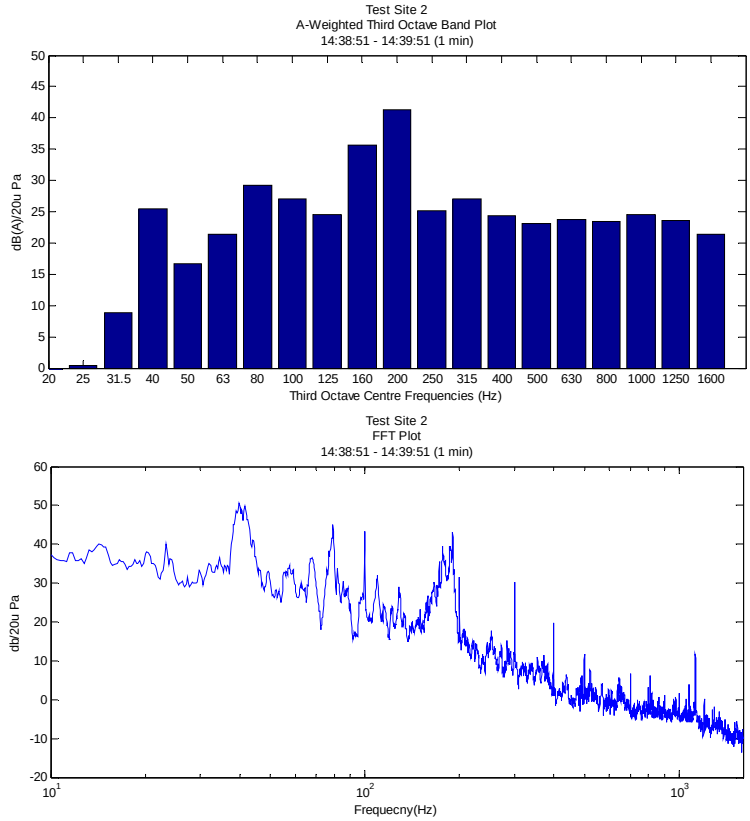

Figure 71 $L_{Aeq,\ 1\ minute}$ for Case Study 2. Lower; Narrow Band. Upper; A-Weighted Third Octaves.

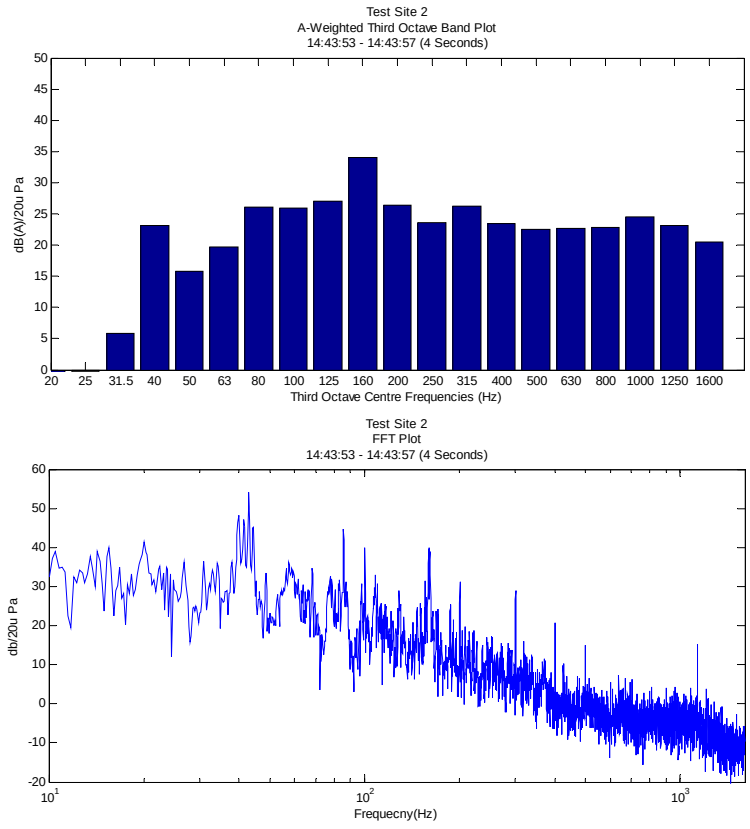

Figure 72 Snapshot example 1. Lower; Narrow Band. Upper; A-Weighted Third Octaves. Rotational speed ~270rpm

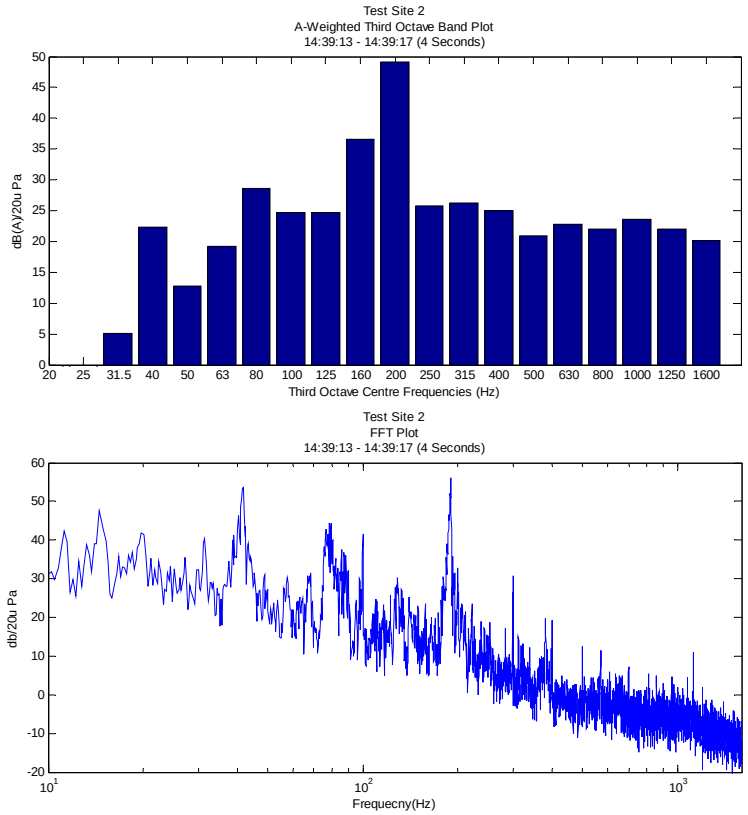

Figure 73 Snapshot example 2. Lower; Narrow Band. Upper; A-Weighted Third Octaves. Rotational Speed ~324rpm

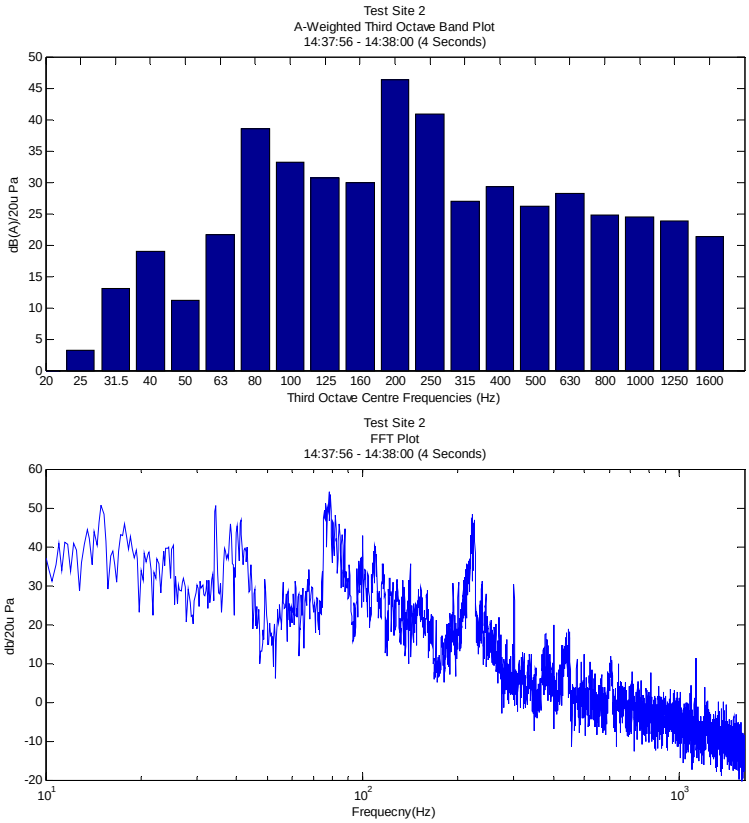

Figure 74 Snapshot example 3. Lower; Narrow Band. Upper; A-Weighted Third Octaves. Rotational Speed ~378rpm

Figure 75 shows the measured internal noise level calculated by the summing of the two dominant third octave bands plotted against rotational speed of the turbine extracted from the frequency analysis of the turbine noise. Also shown are the predicted noise levels which will be discussed in section 8.6.

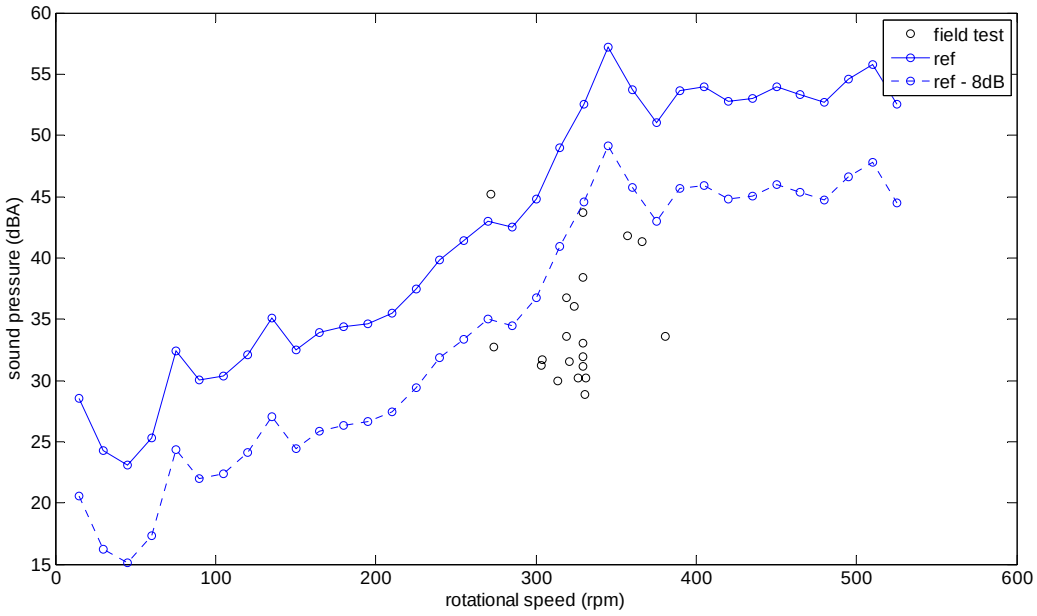

Figure 75 Case study 2: snapshot L_{Aeq} vs rotational speed. Solid line: calculated noise level in reference building. Dotted line: reference building noise level -8 dB

The maximum p.p.v. measured throughout the measurement period is 0.009 mm/s.

8.4 Case study 3

8.4.1 Description of Site 3

The details of this site are as follows:

- Eight storey local authority flats.
- Roof mounted turbine.
- Flat non-penetrating roof mount.
- Turbine type – MWT1
- The turbine was not owned by the occupier of the flat.
- Prevailing wind was from an Easterly direction.
- The turbine was operational for all of the measurement period.
- Tests were carried out between 15:00–17:00 on 10th June 2010.
- The measurements were carried out in an eighth floor flat, directly beneath the turbine.

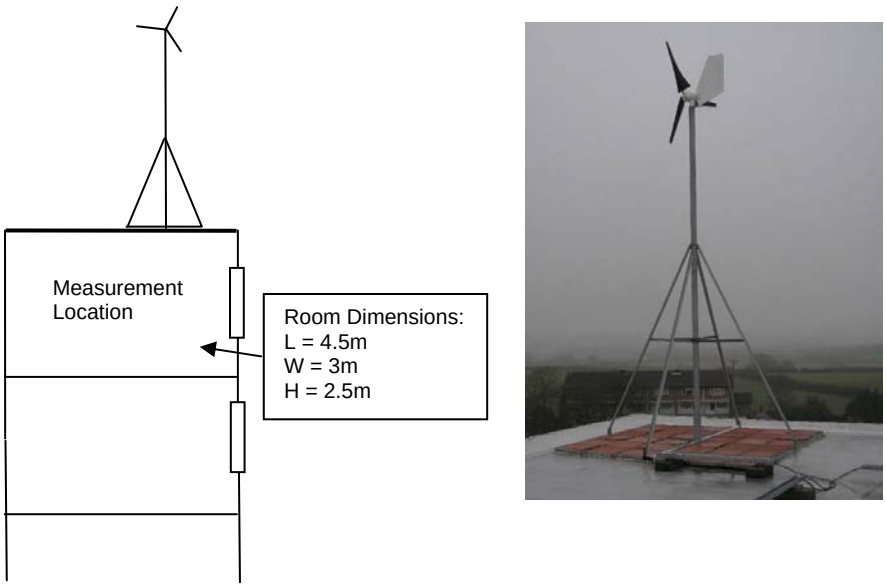

Figure 76 Section through building of Test Site 3 and photo.

8.4.2 Subjective description of noise and vibration

The turbine noise could be heard at all times during the measurement period. The background noise consisted of distant road traffic and residents within the flats. The turbine noise was much more noticeable and subjectively sounded much louder than at any of the other case studies.

The noise was not dominated by the 'Hum and whining' sound, although it could be heard. The noise experienced could be described as 'rumbling wind noise' mixed with the 'hum and whine' noise.

The property, within which the measurements were carried out, was directly beneath the turbine mount, however the residents did not own the turbine and reported being "very annoyed" by the noise experienced. The resident informed us that they had made a complaint with regards to the turbine noise.

There was no tactile vibration or rattling noticed during the measurements and the resident informed us, that they had never experienced tactile vibration or rattling.

8.4.3 Results

An example plot of a one minute L_{Aeq} spectrum is shown in Figure 77.

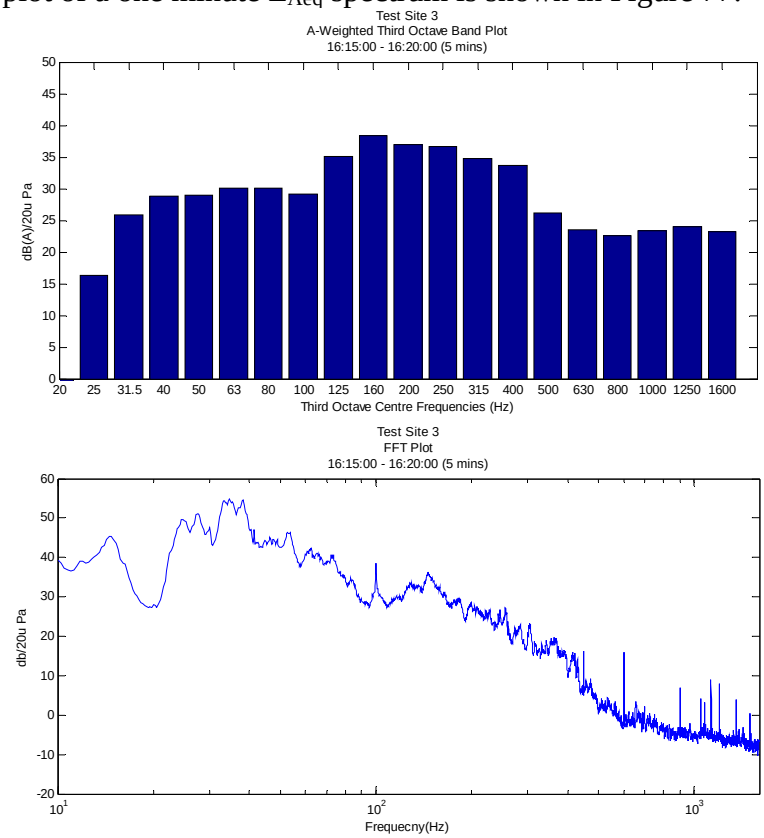

Figure 77 $L_{Aeq,\ 1\ minute}$ for Case Study 2. Lower; Narrow Band. Upper; A-Weighted Third Octaves.

It can be seen in the plots above that the turbine noise is within the 160Hz and 200 Hz third octave bands. However the noise is much more broadband than at the other case studies, which is believed to be due to the mount system. The mount system consisted of an A-frame construction, loaded with paving slabs for stability. During testing of mount systems, it had been noticed that the mount system, including the paving slabs, was rattling and creating new impact sources at the mount base. This is consistent with the broadband noise measured, which we believe to be caused by the many impacts at the base of the mount system itself and not the turbine mounted at the top. There is no definitive spike due to the broadband nature of the noise produced by the combination of the mount system and the paving slabs.

Figure 78 shows the internal dB(A) level of the turbine calculated by the summing of the two dominant third octave bands as a function of rotational speed of the MWT.

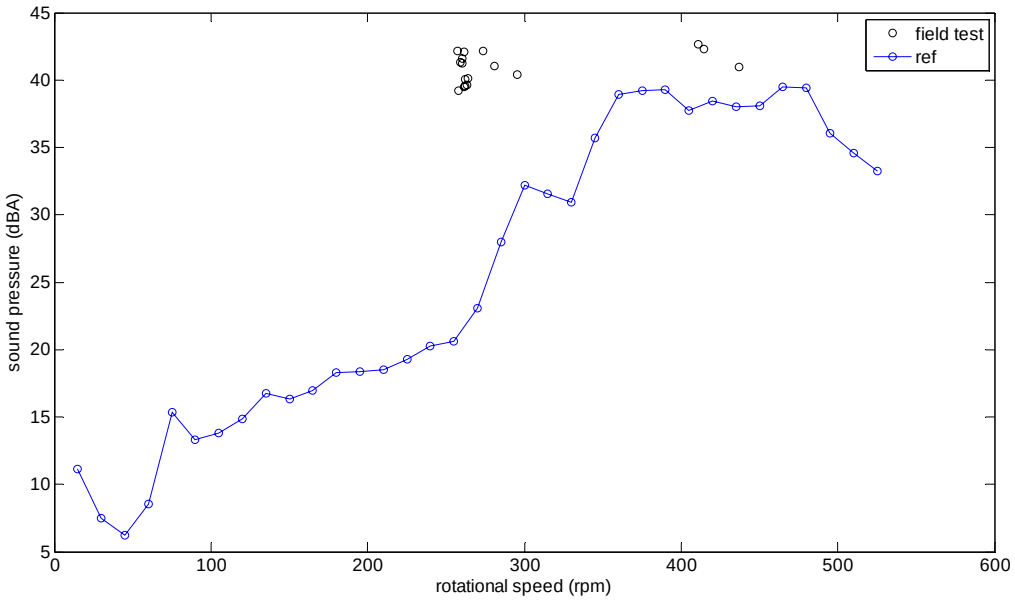

Figure 78 Case study 3: snapshot L_{Aeq} vs rotational speed

We have attempted to extract the rotational speeds of the turbine from the frequency analysis of the measured noise. However, due to the nature of the installation causing what we believe to be many impacts at the turbine base, there may be some error in the rotational speed plotted in Figure 78. Whilst on site the wind in the area was strong and gusty and therefore would be consistent with our extracted rotational speeds of up to 435 rpm. The noise levels are seen to be poorly correlated with rotational speed which again would be consistent with the presence of another source, such as rattling of ballast in the mounting.

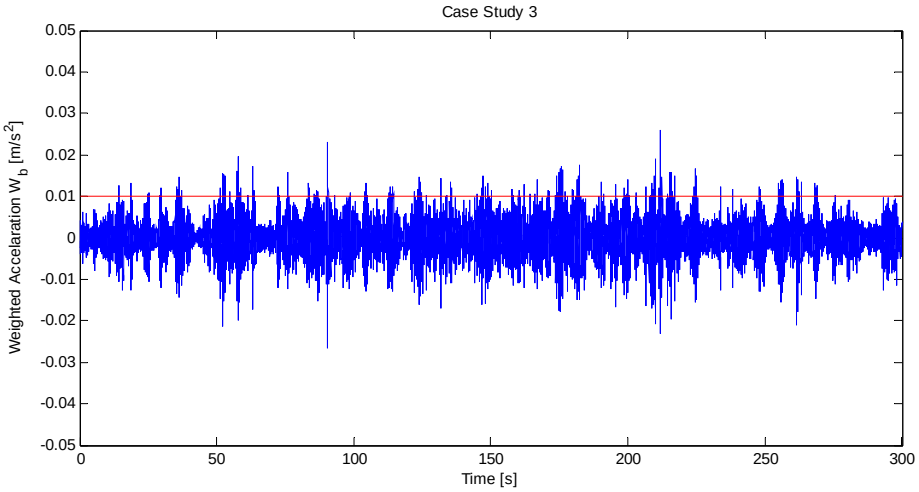

Figure 79: Weighted acceleration shown against the threshold of perception

Figure 79 shows the weighted acceleration on the wall of the flat. Also shown in red is

the value which can be taken as a threshold of vibration. This indicates that vibration would not be expected to be perceptible except for occasional events which could be related either to human activity in the building or possibly to impact from the mounting as described above.

The maximum p.p.v. measured throughout the measurement period was 0.07 mm/s.

8.5 Case study 4

- Site details are as follows:
- Semi-detached house.
- Modern cavity brick construction.
- Turbine on gable end approximately 1m above roof level.
- Two fixing brackets
- The property and turbine are owned by the occupier.
- Turbine type – MWT2
- Prevailing wind was from a Southerly direction.
- The turbine was operational for majority of time.
- Tests were carried out between 15:30 – 17:30 on 1st July 2010.

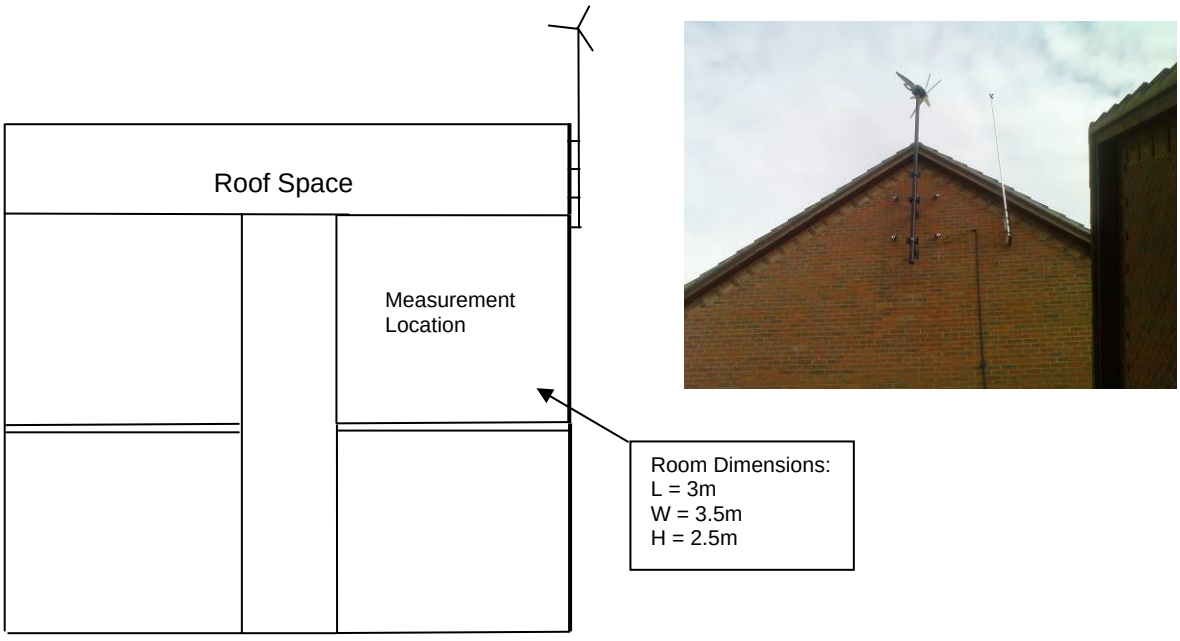

Figure 80 Section through Test Site 4 and photo.

8.5.1 Subjective description of sound and vibration

The turbine noise was just audible above the background noise in rooms along the side of the property of turbine attachment. The background noise consisted of passing road traffic. However, the noise was quieter than experienced at the other case studies.

The MWT2 noise, as with the other case studies, could be described as 'humming and whining' and sounded tonal. However, there was also rumbling and knocking as the turbine speeded up or slowed down. This rumbling/knocking seemed more prominent than at case studies 1 and 2.

Even though the turbine could be heard during operation the resident reported not being annoyed by the noise experienced. The residents' bedroom was on the other side of the house and the occupier informed us that they could not hear the turbine within their bedroom and it did not bother them at any time.

There was no tactile vibration noticed during the measurement period and the resident informed us that they had never experienced any vibration from the turbine operation.

No rattling occurred during the measurement period.

8.5.2 Results

It can be seen in Figure 81 that the measured noise is lower than all the other case study sites. The turbine noise was at a similar level to the background noise, the level of the MWT2 was audible when little background noise was occurring, however a passing car or someone moving around the property would mask it. Therefore, seeing spikes, due to the turbine, in the narrow band plot is more difficult than the other case studies.

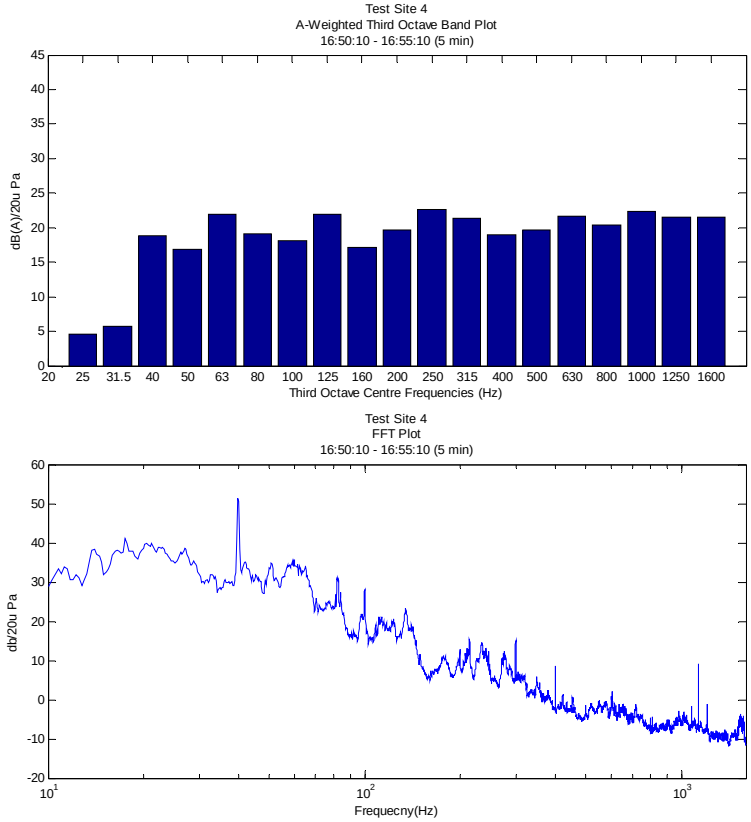

Figure 81. $L_{Aeq,\ 5\ minutes}$ for Case Study 4. Lower; Narrow Band. Upper; A-Weighted Third Octaves.

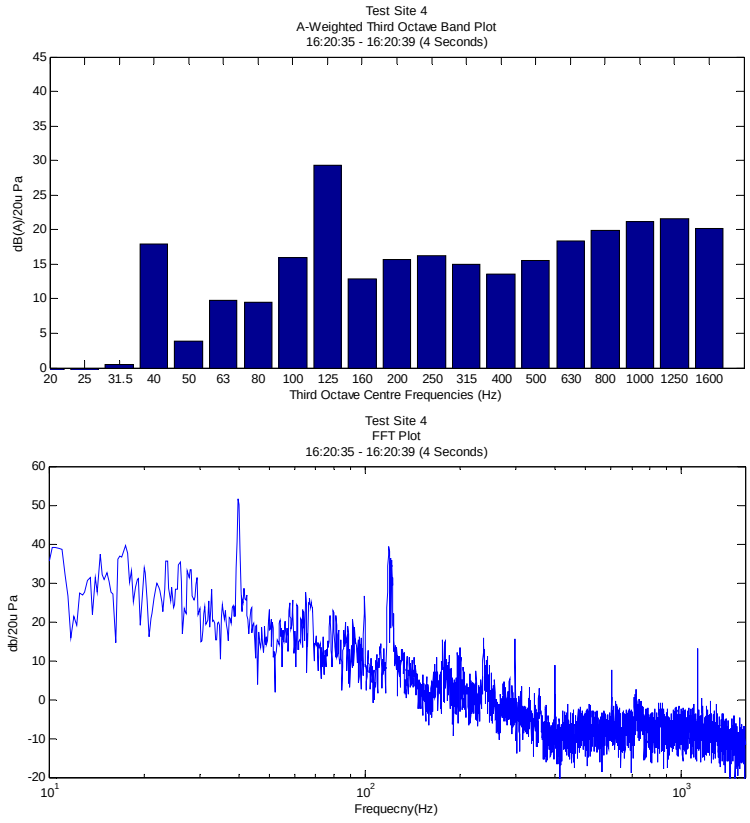

Figure 82. Snapshot example 1. Lower; Narrow Band. Upper; A-Weighted Third Octaves. Rotational Speed ~

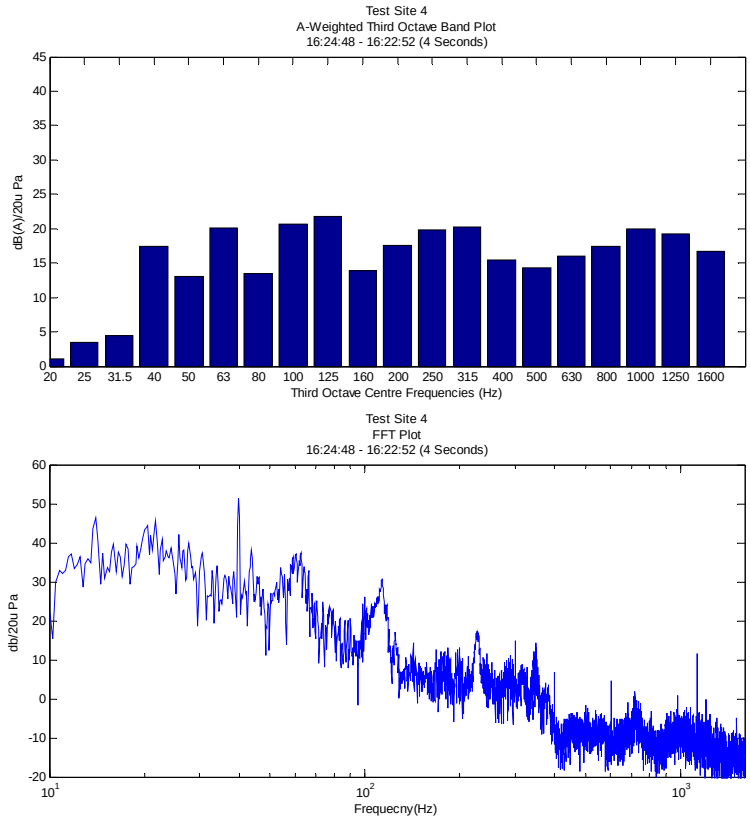

Figure 83. Snapshot example 2. Lower; Narrow Band. Upper; A-Weighted Third Octaves. Rotational Speed ~

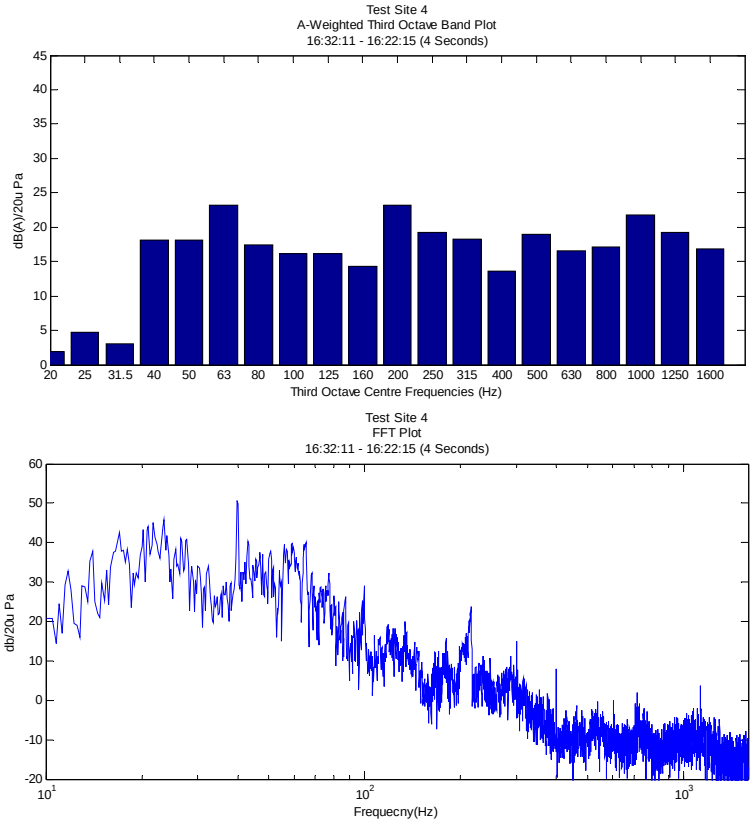

Figure 84. Snapshot example 3. Lower; Narrow Band. Upper; A-Weighted Third Octaves. Rotational Speed ~

Figure 85 shows the rotational speed of the turbine extracted from the frequency analysis of the turbine noise plotted against the measured internal noise level.

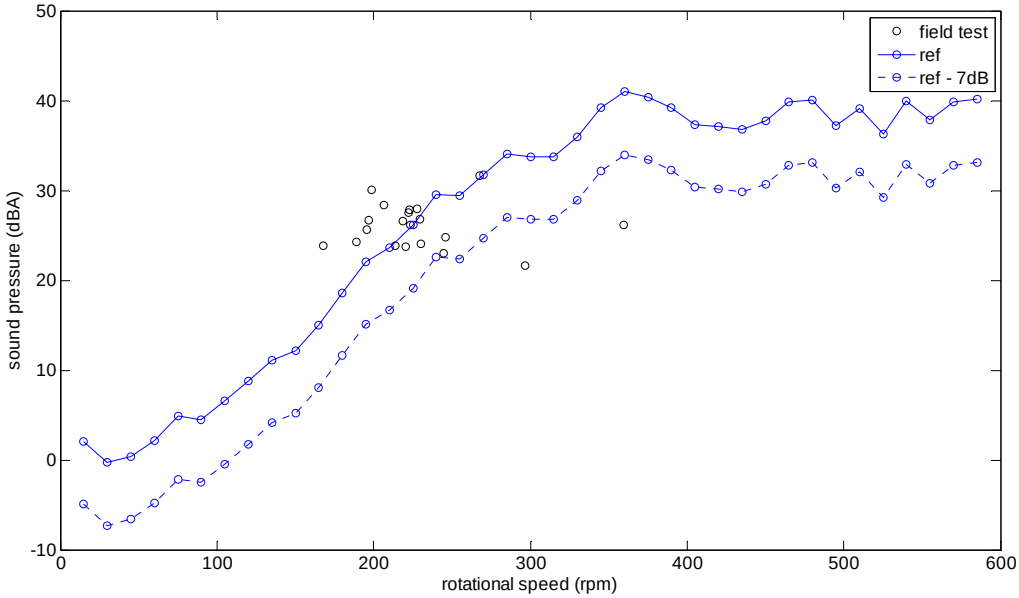

Figure 85 Case study 4: snapshot L_{Aeq} vs rotational speed: Solid line: calculated noise level in reference building. Dotted line: reference building noise level -7 dB

Due to the low level of turbine noise at this site, the noise climate within the property was not dominated by any one or two third octave bands. Therefore, a different procedure has been followed to that used in the previous three case studies. Rather than plot the sum of the dominant bands the overall dB(A) level is plotted against the extracted rotational speed in Figure 85. Table 17 shows details the differences between dB(A) from two turbine dominated third octave bands and the overall dB(A) level for several 5 minute periods.

Table 17: Five minute L_{Aeq} obtained for Case Study 4

Period length (Minutes)	dB(A) – sum of two turbine dominated third octave bands	Overall dB(A) level
5	25	32
5	28	34
2	24	30
5	29	33
5	26	32
5	26	33

The turbine could be heard during these measurements, therefore the table shows that the noise climate within the property during the turbine operation was not dominated by the turbine but the tonal content in the turbine noise was still audible even at this low level.

8.6 Discussion of predicted noise levels

Predicted noise levels in the reference building are compared with measured snapshot measurements in Figure 69, Figure 75, Figure 78 and Figure 85. The reference installation levels have also been corrected to account for construction type, room volume and building layout following the procedure described in section 7.1.

In Case Study 1 (Figure 69) a correction was applied to account for the fact that the attachment point was not directly on the façade of the receiver room but was located further up the gable end (see Figure 64). The correction of -4 dB was obtained from Figure 61. A similar situation occurred in Case Study 4 but no correction was applied in this case because the points of attachment of the MWT partially overlapped the receiver room façade. In Case Studies 2 and 4 (Figure 75 and Figure 78) a -10 dB correction was made for cavity walls according to Table 13 and rooms were also corrected for volume. The correction factors used for the predictions are summarised in Table 18. For Case Study 3 only the reference installation curve is shown (Figure 78). This is because internal noise levels are dominated by impact noise from movement of the ballast in the roof mounting rather than from the MWT and therefore no agreement with prediction is expected.

Table 18:Corrections used in the prediction for Case Studies 1, 2 and 4

	Case Study 1	Case Study 2	Case Study 4
Cavity brick correction	0 dB	-10 dB	-10 dB
Volume	49 m^3	32 m^3	26 m^3
Correction for volume	0 dB	2 dB	3 dB
Correction for second room	-4 dB	0 dB	0 dB
Combined correction	-4 dB	-8 dB	-7 dB

Referring to Figure 75 there is good agreement between the predicted and measured noise levels. It should be remembered that one should not place too much reliance on any individual snapshot measurement because of the short time period over which they are taken. It might be reasonable to take a cluster of snapshot results as indicative of a trend. However, in deriving the blocked forces (in chapter 3) an average of 250 snapshots was taken at each speed so as to include results at different wind speeds and directions. Therefore, the clusters obtained in the field trials are probably obtained over a narrower range of conditions than was the data fed into the predictions. Particularly, variations in wind direction could cause differences of the order of 5 dB according to the studies of mount transmissibility in chapter 5. Figure 69 shows an over-prediction of 5 dB or more, but for a greater range of conditions a better, or worse, agreement could have been obtained.

A strong feature of the predicted noise level is the peak around 340 rpm. This is caused largely by a mast resonance and is therefore strongly dependent on the mast length as can be seen from Figure 42. The mast length used for the calculations was 2.9 m which was estimated to be the mast length from site. Had a shorter mast been assumed then lower sound levels would have been predicted at most rotational speeds and would have produced better agreement with measurement. This indicates that the noise levels for MWT1 are quite sensitive to mast length. As expected, the measured noise levels in Case Study 3, which are predominantly due to impacts rather than the MWT, exceed those predicted to come from the MWT.

Predicted noise levels for MWT2 were lower than for MWT1 which is reflected in the measurements (Figure 78) and is consistent with the size of the units. The agreement is good between the reference installation noise level and the snapshot measurements but is less good when 10 dB is subtracted to account for the cavity wall. Noise levels at this site were relatively low and it is possible that the measurements were affected to some extent by background noise. Therefore, the measured results may be a little on the high side which would tend to improve the agreement with prediction. Also,

we should bear in mind comments from chapter 6 about the variability of cavity wall performance.

Overall, an over-prediction of 5 dB or so has been made for MWT1 and an under-prediction for MWT2 of a similar order of magnitude. Given the complexity of this problem, the lack of prediction methods generally for structure-borne sound and the fact that far greater errors commonly occur, these results are considered to be encouraging. It would however be advisable to exercise caution and build up further experience through measurements.

8.7 Summary of case studies

Table 19 summarises the measured MWT noise and vibration at all sites.

The measured noise levels due to the MWT range from 29dB(A) to 45dB(A). Case study 4 used a different model of MWT (MWT2) and showed similar characteristics but at a lower level. Subjectively, the MWT noise at case study site 4 always sounded 'faint' and unobtrusive and the residents had never been annoyed by the noise, compared to that experienced at case study site 3, which the residents found intrusive and "very annoying".

Table 19: Summary of noise and vibration levels from Case Studies

Case study	MWT	Construction	Mounting	Maximum Measured Level (Leq) (Period)	VDV (8h) $m \cdot s^{-1.75}$	Max measured ppv mm/s	Max rotational speed
1	MWT1	Solid brick	Wall	38 dB(A) (5 mins)	-	0.01	402rpm
2	MWT1	Cavity brick	Wall	45 dB(A) (1 min)	0.0027	0.009	378rpm
3	MWT1	Concrete Roof	Flat Roof	45 dB(A) (5 mins)	0.033	0.02	435rpm
4	MWT2	Cavity brick	Wall	29 dB(A) (5 mins)	0.052	0.01	360rpm

The maximum VDVs measured at all case study sites are below the ranges stated within 'BS 6472-1:2008 Guide to evaluation of human exposure to vibration in buildings' at which adverse comment is expected to occur, and this is consistent with

experience from site.

The maximum peak particle velocity measured at all case study sites are below that stated within ‘BS 7385-2 Evaluation and measurement for vibration in buildings’ with respect to transient vibration cosmetic damage limits. Thus, there does not appear to be a danger of damage being caused to the building by vibration.

9 Conclusions

In Part 1 of the report it was proposed to characterise MWTs as sources of structure-borne sound and vibration using the 'in situ blocked force approach'. In the first four chapters of this report this approach has been tested in the laboratory and in field trials lasting several months at a rural/industrial test site. The conclusion is that it is possible to obtain a reliable intrinsic measure of the source strength of a MWT from measurements of vibration on the mounting of a MWT operating under normal conditions.

It has further proved possible to obtain a curve of the source strength of the MWT as a function of its rotational speed and this is one of the main outcomes of the project. However, expressing source strength directly as a function of wind speed has proved difficult, not because of the noise and vibration aspects but because of difficulty in finding a suitable relationship between rotor speed and wind speed.

One of the possible concerns at the start of the project was that turbulent wind conditions, particularly rapid changes in wind direction might cause additional noise and vibration. This concern has been addressed through an analysis of turbulence both at the rural/industrial test site and an urban roof-top site. Although turbulence is an incompletely understood phenomenon and the standard descriptors are not well suited to this particular problem, the results tend to indicate that turbulence is not the dominant factor in structure-borne sound and vibration. However, audible noise could potentially be produced if the mount system were to spring back after being loaded by a strong gust.

The role of the building in transmitting vibration and radiating sound has been investigated through a series of field studies on six dwellings. It has been shown that transmission into the most exposed room is expected to be lower for cavity walls than for solid brick. However, this situation could be subject to significant variance depending on details of wall ties and junctions. Surprisingly little attenuation was found from the most exposed room to adjacent rooms, particularly for cavity walls. For solid brick walls the attenuation for rooms into the building (away from the façade) would be significant, but little attenuation would be expected for rooms along or up the same façade. This indicates that there would not be much attenuation of sound once it gets into the building structure. Should noise and vibration control be required it would therefore be necessary to achieve this at source (on the MWT itself)

or by modified designs of mounting.

In all four case studies of existing installations the MWT was audible as a whine with a frequency of ~200 Hz. In the roof mounted installation there was an additional rumble believed to be due to movement of ballast in the base of the mounting. The $L_{Aeq,\ 5\ minutes}$ levels were typically between 30 and 50 dB, although at the bottom of this range for MWT2. In only one of the cases did the resident express dissatisfaction.

Tactile vibration did not emerge as an issue in any of the sites, with the possible exception of the roof-mounted installation where occasional peaks might be perceptible. This was thought to be due either to movement in the building or possibly the result of unsteady ballast in the mounting base.

Measured sound levels have been compared with prediction for the four case studies. The agreement is good considering the considerable difficulties encountered in this type of analysis both in terms of the MWT itself and the transmission of sound through the mast and through buildings. Nevertheless, the differences of 5 dB or more between prediction and measurement confirm that caution is required in interpreting the results. The prediction methodology is based on sound principles but many simplifications have been required in order to produce a sufficiently simple method. It will therefore be necessary to build up confidence in the method by trials on real installations.

Micro-wind turbines can be seen to behave significantly differently to larger machines in two main respects. First, the noise levels generated by larger machines generally increase as wind speed increases. However, for MWTs the situation is more complicated and noise levels could go up and down as wind speed, and therefore rotor speed, increases. This is due to structural resonances and is a common characteristic of structure-borne sound. Secondly, the rotor speed of MWTs changes far more rapidly with wind speed with significant changes occurring more or less every second in normal operation. The rotor speed of the larger machines by contrast is relatively stable. The difference is significant subjectively, since whereas the sound from larger machines is generally perceived as a regular ‘swish’, building-mounted MWTs generate a ‘whine’ of varying pitch inside the building. The problem of varying rotor speed also makes it significantly more difficult to relate noise levels to wind speed as discussed earlier.

At this stage the original aims and objectives of the study will be reviewed. The

project aim was:

To provide research into the structure-borne noise and vibration impacts of micro wind turbine installation upon a building (detached and attached), and to develop a methodology to predict these impacts that is sufficiently robust that decisions relating to the amenity of neighbouring attached properties can be predicted.

The first part of the aim, relating to noise and vibration impacts, has been achieved through:

- Reviewing relevant criteria for evaluating the potential impact of noise and vibration on residents;
- Identifying and quantifying the role of the various elements in the transmission of noise and vibration, namely, the MWT itself as the source, the mast as a transmission element and the building in terms of its construction and layout;
- Reporting noise and vibration measurements made inside dwellings of real MWT installations in a form suitable for comparison with relevant criteria (the report is not intended to comment on the acceptability or otherwise of the levels).

The second part of the aim has been achieved through the development and validation of the prediction methodology as detailed in this report. The approach is theoretically sound and based on current best practice and is thus scientifically robust. However, in the context of planning decisions, the 'robustness' does not depend solely on having a firm scientific basis but also on the accuracy of the results. Therefore, validation checks have been conducted at various stages through the project:

- preliminary laboratory tests of the in situ blocked force method;
- on board validation of the blocked force data from site measurements;
- characterisation of the MWT across a range of wind conditions;
- measurements across the range of mast configurations likely to occur in practice;
- supplementary modelling of mast configurations.

Inevitably some sources of uncertainty remain, the largest of which is that relating to the sound transmission properties of the buildings, particularly for cavity brick constructions (see later in the Conclusions). It has also been shown that the sound transmission is sensitive to the mast configuration.

The project objectives and comments are as follows.

1. Develop a methodology to quantify the amount of source vibration from a building mounted micro wind turbine installation, and to predict the level of vibration and structure-borne noise impact within such buildings in the UK;

The first part of this objective has been achieved in the form of the blocked force method which provides a robust and independent characterisation of the source strength of a MWT operating under realistic conditions. Trial measurements have shown this method to give reliable results but that advanced measurements are required over a range of wind conditions in order to generate data of suitable accuracy. This part of the methodology therefore requires specialist measurement skills. The second part has been achieved through the predictions reported in Chapter 8.

2. Test and validate the hypothesis on a statically robust sample size;

In the context of the prediction methodology, the most significant sources of statistical variation are wind conditions, mast and building properties. Wind speed variations have been accounted for by monitoring over an extended period in 'real' wind conditions. This sample size proved sufficient to characterise MWT source strength as a function of rotor speed but not in terms of wind speed as discussed above. Statistical variation in mast properties has been accounted for by testing a range of configurations, supplemented by modelling so that in effect the whole range of possible configurations has been quantified. Regarding building properties, the sample size has been maximised by testing for a number of source and receiver locations, employing a range of different constructions layouts and room sizes. The resulting database, whilst covering a range of possibilities cannot be claimed to provide a full statistical sample of UK constructions even when supplemented by results of standard impact tests as has been done in Chapter 6. Generally, the problem of variable acoustic performance is widely recognised in building acoustics and cannot be removed or even reduced beyond a certain extent by increased sample size. Thus, building performance remains one of the main sources of uncertainty in the prediction methodology with associated 95% confidence intervals up to ±10 dB. This uncertainty may be reduced by making measurements of transfer functions in situ prior to installation of the MWT but this is unlikely to be practical in many cases.

3. Report the developed methodology in a form suitable for widespread adoption by industry and regulators, and report back on the suitability of the method on which to

base policy decisions for a future inclusion for building mounted turbines in the GPDO.

In order to meet the objective of widespread adoption of the methodology it has proved necessary to develop a simplified prediction method (also presented in Part 3 of the report) suitable for use by non-specialists. The simplified method is restricted to masonry constructions which it is believed will, in practice, allow it to be applied to most MWT installations. With the simplified method it will also be necessary to accept uncertainty associated with unknown building properties as described above. The confidence limits and the field trial results suggest an interval of around ±5 dB perhaps more for some cavity constructions. Thus, it has been recommended that confidence be built up by measurements on real installations.

10 Acknowledgements

The authors wish to thank Lyondell-Basell for the use of their site and technical support. The development of the in situ blocked force method was supported by EPSRC (Grant Ref EP/G066582/1) whose support is gratefully acknowledged.

11 References

11.1 Standards

BS EN ISO 3822-1:1999+A1:2008. Acoustics. Laboratory tests on noise emission from appliances and equipment used in water supply installations. Method of measurement.

BS EN 12354-5:2009. Building acoustics. Estimation of acoustic performance of building from the performance of elements. Sounds levels due to the service equipment

ISO 9611:1996, Acoustics — Characterization of sources of structure-borne sound with respect to sound radiation from connected structures — Measurement of velocity at the contact points of machinery when resiliently mounted.

ISO 7626-2:1990 Vibration and shock -- Experimental determination of mechanical mobility -- Part 2: Measurements using single-point translation excitation with an attached vibration exciter

ISO 7626-5:1990 Vibration and shock -- Experimental determination of mechanical mobility -- Part 5: Measurements using impact excitation with an exciter which is not attached to the structure

11.2 Papers

Elliott, A.S. (2009) Characterisation of Structure Borne Sound Sources In-situ. **Ph.D. Thesis**.

Fulford, R.A. & Gibbs, B.M. (1999) Structure-borne sound power and source characterization in multi-point-connected systems, part 2: about mobility functions and free velocities. *Journal of Sound and Vibration*, **220**(2), 203-224.

Gardonio, P. & Brennan, M. (2004) Mobility and impedance methods in structural dynamics. *in Advanced Applications in Acoustics, Noise and Vibration. Edited by F. Fahy and J. Walker*. Spon Press

Hansen, M.O.L. (2008) *Aerodynamics of wind turbines,* Earthscan/James & James.

James, P.A.B., Sissons, M.F., Bradford, J., Myers, L.E., Bahaj, A.S., Anwar, A. & Green, S. (2010) Implications of the UK field trial of building mounted horizontal axis micro-wind turbines. *Energy Policy*, **Article in Press**.

Kaimal, J.C. & Finnigan, J.J. (1994) *Atmospheric Boundary Layer Flows,* Oxford University Press.

Moorhouse, A.T. (2001) On the characteristic power of structure-borne sound sources. *Journal of Sound and Vibration,* **248**(3), 441-459.

Moorhouse, A.T. & Elliott, A.S. (2010) Application of an in-situ measurement method for characterisation of structure-borne sound generated by building mounted wind turbines. In *Proceedings of Internoise 2010*Lisbon.

Moorhouse, A.T., Elliott, A.S. & Evans, T.A. (2009) In situ measurement of the blocked force of structure-borne sound sources. *Journal of Sound and Vibration,*

325(4-5), 679-685.
Randall, R.B. (1987) *Frequency Analysis*, Brüel & Kjær.
Sockel, H. (1994) *Wind-excited vibrations of structures*, Springer Verlag.
Ten Wolde, T. & Gadefelt, G.R. (1987) Development of standard measurement methods for structureborne sound emission. *Noise Control Engineering Journal*, **28**(1), 5-14.
Wagner, S., Bareiss, R. & Guidati, G. (1996) *Wind turbine noise*, Springer Verlag.

11.3 Other References

Encraft (2009) Warwick Wind Trials: Final Report, Encraft http://www.warwickwindtrials.org.uk/resources/Warwick+Wind+Trials+Final+Report+.pdf [20/12/2009]

NOABL. UK windspeed database. http://www.bwea.com/noabl/index.html Accessed 16/07/10

Appendix: details of test sites from chapter 6

Test Site 1

- Two storey detached property.
- Cavity Brick external wall construction, approximately 300mm total thickness with approximately 70mm-80mm Cavity width.

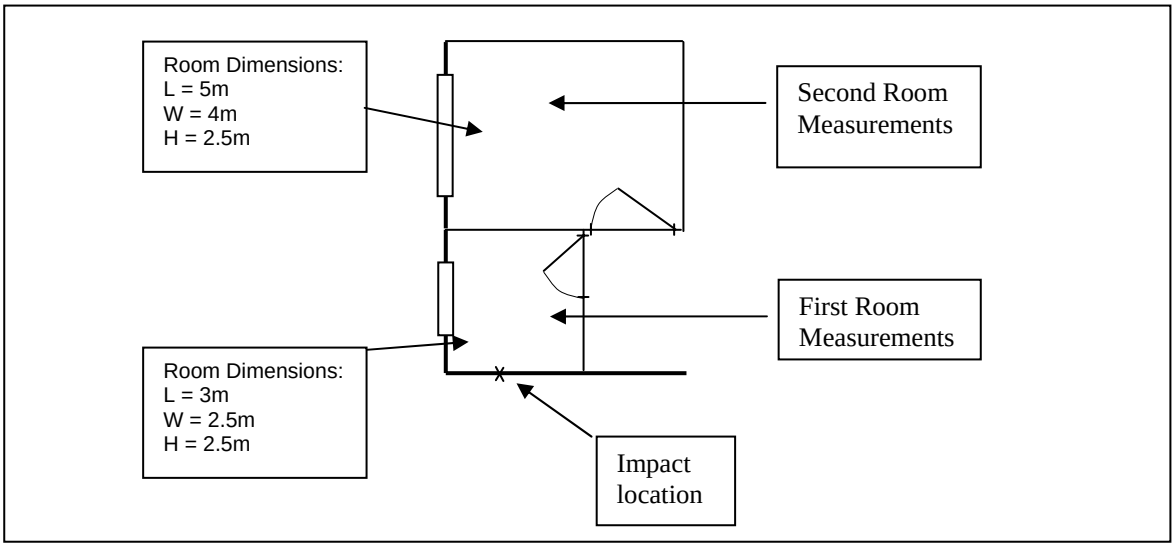

Figure A- 1: Sketch of test location at test site 1. Plan view of first floor.

Test Site 2

- Three storey, shared living space, flats.
- Cavity Brick external wall construction, approximately 300mm total thickness with approximately 70mm-80mm Cavity width.

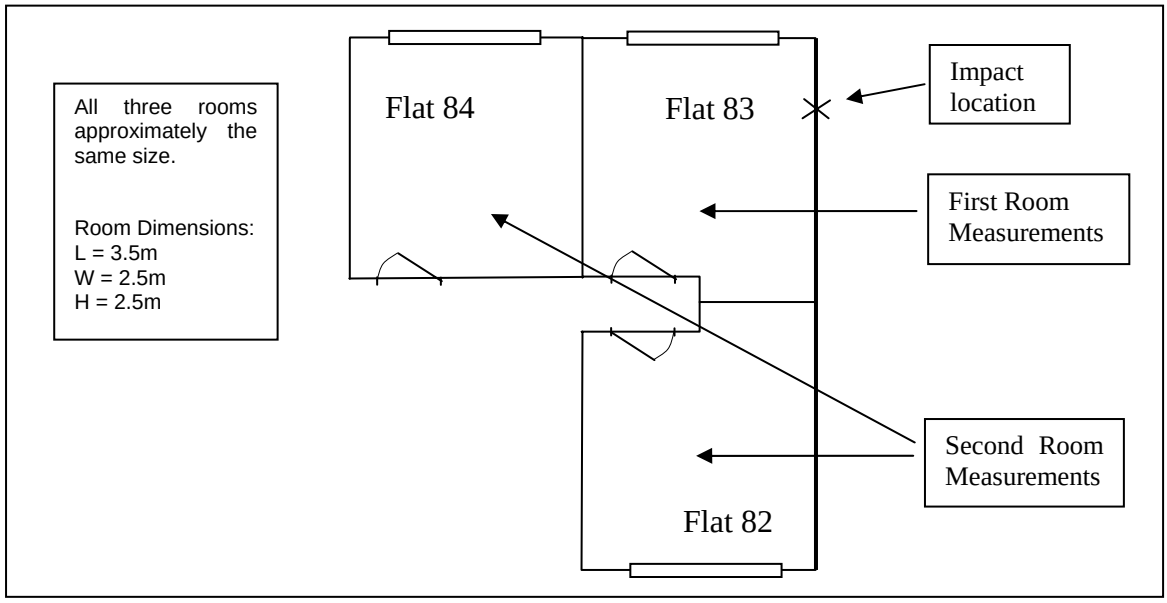

Figure A- 2: Sketch of test location at test site 2. Plan view of first floor.

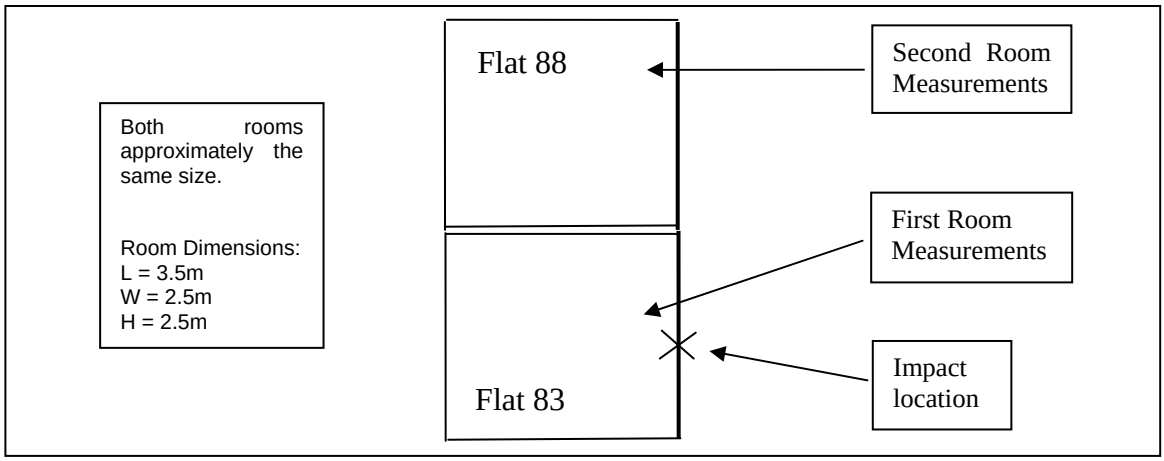

Figure A- 3: Sketch of test location at test site 2. Elevation view of first and second floor.

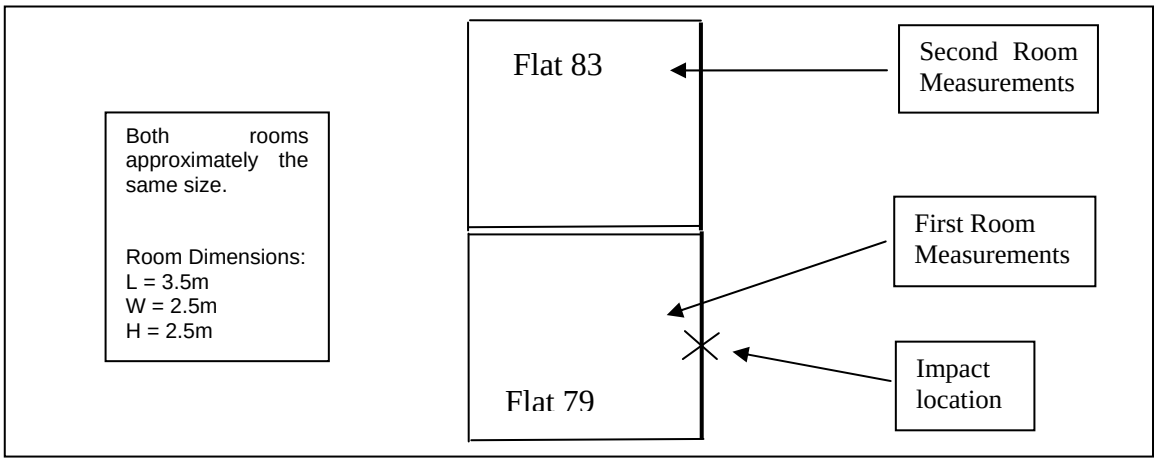

Figure A- 4: Sketch of test location at test site 2. Elevation view of ground and first floor.

Test Site 3

- Three storey, shared living space, flats.
- Cavity Brick external wall construction, approximately 300mm total thickness with approximately 70mm-80mm Cavity width.

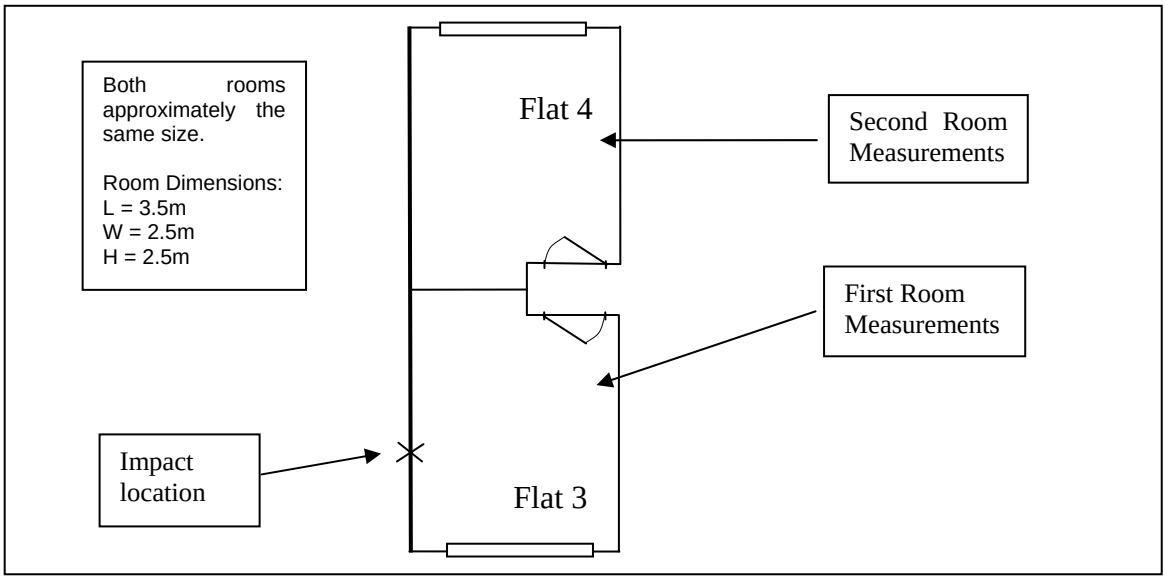

Figure A- 5: Sketch of test location at test site 2. Plan view of first floor.

Test Site 4

- Two storey semi-detached property.
- Solid brick external wall construction.

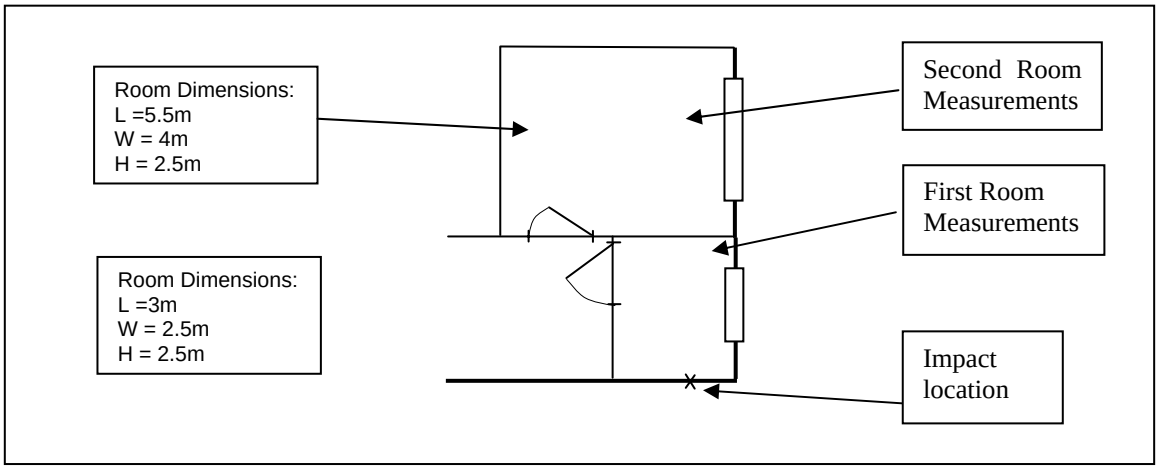

Figure A- 6: Sketch of test location at test site 4. Plan view of first floor.

Test Site 5

- Two storey detached property.
- Solid stone with render external wall construction.

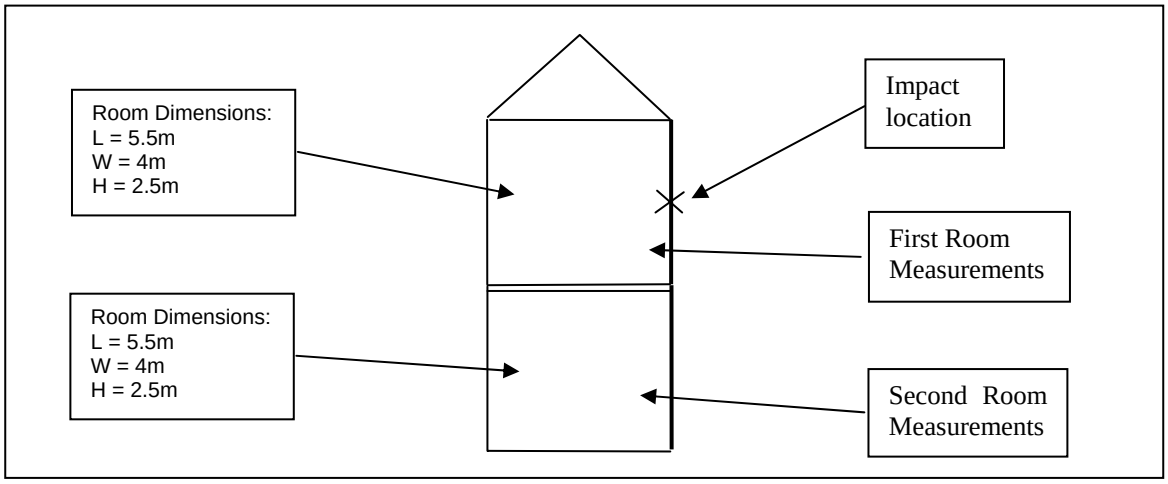

Figure A- 7: Sketch of test location at test site 5. Elevation view of first and second floor.

Test Site 6

- Two storey detached property.
- Solid stone external wall construction.

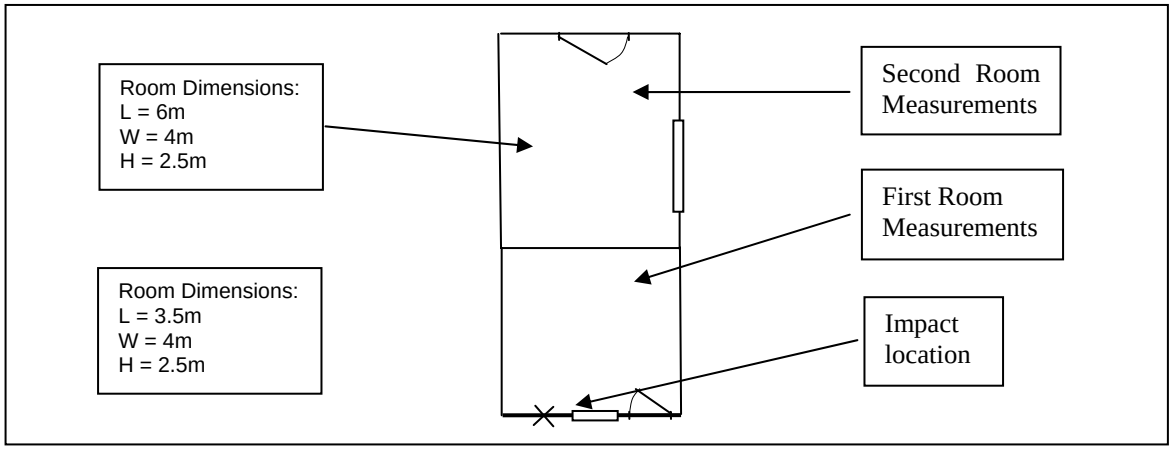

Figure A- 8: Sketch of test location at test site 6. Plan view of ground floor.

University of Salford
Salford
Greater Manchester
M6 6PU
United Kingdom

T +44 (0)161 295 5000
F +44 (0)161 295 5999

www.salford.ac.uk